IMPACT OF MOBILE CRANES ON SHORT SPAN BRIDGES

By

Vishal Gaya

Submitted in partial fulfillment of the requirements for a degree

MSc Eng

IN THE DEPARTMENT OF CIVIL ENGINEERING

FACULTY OF ENGINEERING AND THE BUILT ENVIRONMENT

Supervisor: A/Professor Pilate Moyo

Co-Supervisor: Professor Mark Alexander

December 2011

DECLARATION

I know the meaning of plagiarism and declare that all of the work in the document, save for that which is properly acknowledged, is my own. I also affirm that this work has not been submitted in this, or any other university for examination, or for any other purposes.

Signature……. Date ……

ACKNOWLEDGEMENTS

I would like to express my sincere gratitude to my supervisor A/Prof P. Moyo for his guidance, interest, encouragement and valuable advice throughout this research. My co-supervisor Prof M. Alexander is acknowledged for his interest and encouragement for this project.

I am grateful to the Concrete Material Structural Integrity Research Unit (CoMSIRU) for the opportunity to do my MSc Degree and for the funding which has been provided throughout this research.

The author wishes to acknowledge Mr Mark Gentry from Tandem Cranes for providing a mobile crane and also Mr Harry Viljoen from the Department of Transport and Public Works for making the Berg River Bridge available for the field experiment.

I would like to thank Ms Elly Yelverton and my friends for their support and assistance during the course of the project.

Last but not least, I would like to thank my parents and brother for their continuous support and sacrifices they made throughout the years for me to get this far.

ABSTRACT

The abnormal load management guideline which is currently being used in South Africa is TRH 11. This guideline is based on provisions developed in the 1970s. Design guidelines and traffic loading have changed since then thereby highlighting the need to develop a new abnormal load management system.

TRH 11 considers all the abnormal vehicles as one category. However, literature has shown that even though mobile cranes are regarded as abnormal vehicles, they have different suspension system, axle spacing and use different wheels compared to heavy good vehicles. These characteristics help minimise their impact on road structures.

This thesis presents a study of the impact of mobile crane on short span bridges. Short span bridges span between 5 and 40m are very common in South Africa. A finite element model representing the interaction of a mobile crane with a bridge has been developed using Adina finite element software. Bridges have been modeled based on the criteria specified by the MOT design code of practice. This is because 70% of bridges in South Africa have been designed using this code.

An experimental study to measure the actual dynamic impacts was performed on the Berg River Bridge. The bridge was instrumented with displacement transducers and strain gauges at mid and quarter span respectively. A 36 tonnes mobile crane was used for the field experiment. The impact was measured for different speed scenarios. The acceleration of the bridge under normal traffic loading was also measured. A wooden plank was placed across the lane for one scenario to trigger extensive dynamic vibration and to simulate poor road surface condition.

Data collected from the tests were extracted using ME'Scope Ves and used for comprehensive assessment of the bridge under dynamic loading. Dynamic and static analyses were performed and the impact factor for strain and displacement were calculated. The highest impact factor was 1.16 for a speed of 60 Km/hr. When plotted on the National codes graph, the highest impact falls below the curve representing the South African codes showing that Berg River Bridge is safe under the motion of the mobile crane.

Analysis revealed that high vehicle speed and deterioration in road surface contributes to high impact factors. Experimental findings have also shown that the most important impact forces occur at the bridge approach as the mobile crane crosses the joint irregularities that occur between bridge and the abutments.

Experimental data were used to validate the finite element model of the Berg River Bridge. The model gave almost similar results to the field experiment. Moment and shear impact factor were obtained from the Finite element model.

The model was used to simulate the effects of heavier vehicle weight on the bridge. It was found that as weight increases the impact factor decreases. This decrease is not caused by a decrease in dynamic deflection but an increase of the static deflection.

TABLE OF CONTENTS

LIST OF FIGURES

LIST OF TABLES

1. INTRODUCTION

1.1 Background

Bridges are important components of the transportation system and are among the most expensive investment asset of a country's infrastructure. In South Africa, there are more than 11,000 bridges across the country which has been designed to various codes of practice. There are an increasing number of structures ageing and their health is deteriorating. More than eighty per cent of these bridges have been designed to codes which are no longer used nowadays. These bridges are now subjected to increased stresses due to an increase in the number of heavy vehicles and traffic loading. The increase in traffic loads leads to structural damage of the bridge which in turn leads to a decrease in the lifespan of the road structures.

Most of the bridges in South Africa are short to medium spans ranging from 5m to 40m. They are mainly concrete composite structure made up of precast pre-stressed beams and cast in-situ slab. The use of pre-cast elements is cost and time saving and facilitates the construction of road structures on difficult site conditions.

In the year 2000, the annual cost of overload road damage was estimated to be around R650 million. The accrued backlog for the upgrading, maintenance and repair of about 13,000 bridges was about R37 billion (Sowman and Poree, 2000). A report by the Department of Public Works, the Construction Industry Development Board and the Council for Scientific and Industrial Research of South Africa (2006) suggests that most of the country's infrastructure build in the 1960s-1970s need major refurbishments or in certain cases even to be replaced.

Vehicles are classified in ascending order as normal, abnormal, special and super loads. Abnormal, special and super loads are the ones that have the biggest impact on highway structures. The number of these vehicles is increasing due to the growth in economy and in order to carry more goods in a shorter lapse of time. In the 1980's it was assumed that one out of twenty five vehicles crossing a bridge was an abnormal load vehicle whereas in the year 2000 this statistic changed to one out of fifteen (TRH 11, 2000). In the 1960's, the maximum vehicle length was 20 m whereas nowadays it is very common to have 40 m long trucks. The number of

axles has also increased considerably from 7 to more than 12 to distribute the load. The legal axle weight in South Africa is 12 tons.

The abnormal load management guideline which is used in South Africa is TRH11 which refers to the Guideline for granting of exemption permits for the conveyance of abnormal loads and for other events on public roads. It is based on provisions developed in the 1970s. TRH 11 considers all abnormal loads in one category and does not distinguish between mobile cranes, car carriers, tankers and heavy goods vehicles. Even though these vehicles carry heavier loads nowadays, they do have more wheels per axles, better tyres, more efficient suspension and better braking system and more axles. This helps decrease the impact on highway structures. The current guidelines also assume that there is a maximum of four lanes on highways. However, some recently constructed bridges in South Africa have up to eight lanes. The design guidelines and traffic loading have changed a substantially since the 1970's and there is a need to revise TRH 11.

Most of the abnormal load management systems found in literature refer to impact factors being applied to calculate the maximum allowable load on bridges. However, none of the codes provide details of how the impact factors have been obtained. A further research needs to be carried out to find out about the impact factors and how they affect the dynamics of bridges.

The dynamic interaction between mobile cranes and bridges needs to be investigated. Literature refers to abnormal load vehicles in general but none focus specifically on mobile cranes. Dynamic testing is important since they provide an instantaneous evaluation of the dynamic properties (frequency, damping, stiffness) of the structure. They are also useful in quantifying the extent and rate of degradations of bridges.

1.2 Research motivation

As mentioned in Section 1.1, TRH 11 considers all abnormal vehicles in one category. The construction industry in South Africa has expanded in the last ten years and the use of mobile cranes has increased. Mobile cranes are being preferred to fixed cranes in many projects since they can be moved around, thereby saving the cost of having several fixed cranes on site. In order to reach the construction site, these vehicles have to travel along national, municipal or rural roads and they require special permits if they weigh more than 50 tons. The mobile crane

owners have been complaining about being unfairly penalised by the traffic authorities and are having to use longer routes to reach their destination. Their argument is that mobile crane causes less impact on bridges than other abnormal vehicles due to their different configuration. Mobile cranes have shorter axle spacing, bigger wheels, thicker tyres and use mostly hydro-pneumatic suspensions compared to other abnormal vehicle which are differently configured. This thesis will study the impact caused by mobile crane on bridges.

1.3 Aim of research

The aim of this research is to develop and calibrate a finite element model representing the vehicle-bridge interaction between a 36 tons mobile crane and the Berg River Bridge in the Western Province, South Africa. The impact factors obtained is to be compared with the permitted impact factor from the Codes.

1.4 Scope

The scope of this research consists of:

(i) Conducting a critical review of the abnormal load management system.
(ii) Understand and analyse the different impact caused by abnormal vehicles.
(iii) Developing a finite element model representing a vehicle-bridge interaction that can be used for further investigation.
(iv) Performing field measurement to validate and calibrate the model.
(v) Analyse the impact factors and compare them with the South African Code.

1.5 Limitations

This research has been limited to the impact of mobile cranes on short span bridges. It does not include other types of abnormal vehicles and impact on long span bridges.

1.6 Thesis structure

Chapter 1

Chapter one introduces the topic. It includes the background information and the motivation to carry out this work. The aims and scope of this research also form part of this chapter.

Chapter 2

Chapter two reviews the abnormal load management system which is currently being used in South Africa and other countries. The different loading models and bridge design codes are also investigated.

Chapter 3

Chapter three looks at the different traffic loads which operate in South Africa. The concept of static and dynamic load model is also introduced.

Chapter 4

Chapter four reviews the impact factor acting on bridges and the parameter contributing to them. The different methods of measuring the dynamic effects of a bridge are discussed.

Chapter 5

The different types of suspension systems used by normal and abnormal vehicles are reviewed in chapter five. A comparison between and spring leaf and hydro-pneumatic suspension system which are used by abnormal vehicles has been done.

Chapter 6

The methodology for this thesis is described in Chapter six. The details of the field tests performed and the equipment used are given. The processing of the data obtained from the field experiment is also explained. The construction of a finite element model to represent the vehicle-bridge interaction of the mobile crane and the Berg River Bridge is reported.

Chapter 7

The findings of this research are discussed and analysed in chapter seven. Field results obtained for the different scenarios are compared with those obtained from the finite element. The impact factors obtained for each scenario is compared with the South African code.

Chapter 8

Chapter eight concludes and discusses the validity of the current abnormal load management system. Recommendations for future works are mentioned in this chapter.

2. ABNORMAL LOAD MANAGEMENT SYSTEMS

2.1 TRH 11

TRH11 refers to the Guideline for granting of exemption permits for the conveyance of abnormal loads and for other events on public roads. This guideline was first published in the early 1970's and is based on the following codes; Code of Practice for the design of highway bridges in South Africa (TMH 7), the British Standards BS153and BS5400, the United Kingdom Ministry of Transport (MOT) codes, and the Natal codes. These Codes of practices have been used to design bridges which may be affected by any revision of TRH 11.

The aim of TRH11 is to protect the investment in roads and highway structures as well as for reasons of road safety and traffic management by ensuring that the permissible dimensions and masses of vehicles operating on public roads are respected. Under special circumstances, it may be necessary to accommodate vehicles or loads that are unable to meet the Road Traffic Act. For these cases, the Act empowers road authorities to issue exemption permits under strictly controlled conditions in terms of firm guidelines as set out in the Road guidelines (Road Traffic Act, 1989).

2.1.1 Limitations imposed by bridges and culverts

The philosophy of TRH11 is that by measuring the effective width and the distance between the outer axle groups, the allowable axle load can be calculated. The loading formula for both normal and abnormal load is given below.

Normal loading

The maximum load that an axle group is allowed to carry without having to apply for permits and escorts is calculated using the formula given below.

$$Total\ axle\ load\ of\ group\ of\ consecutive\ axles = 1.8\ [Distance(mm)\ between\ the\ centre\ lines\ of\ the\ extreme\ axles] + 16\ 000\ kg \qquad (2.1)$$

TRH 11 does not provide any information on how the 1.8 and the 16 000 Kg has been obtained.

Abnormal loading

In order to find the maximum load that a bridge can carry, the maximum shear stresses that the vehicle exert on the component members of the critical span have to be found and then compared to the stress for which the bridge has been designed. If the allowable stress is exceeded, structural failure may occur in the bridge. Shear forces and bearing reactions mainly come from those axles which generally lie at or close to the supports. Due to their close proximity to the supports, these axles are less able to spread their effects laterally.

Table 2.1 has been developed for axles or combinations of axles whose gross mass does not exceed 125 000 kg (gross vehicle mass) or 18kN/m². It shows the relationship between effective width, then length between the outer axle group and the allowable load. Each group of axles must not exceed the value given in Table 2.1.

TRH 11 limits the load intensity to 18kN/m² for a single abnormal vehicle based on an effective area. The effective area is assumed to be the area under the effective width and the effective length of the vehicle.

Table 2.1: *Allowable mass on multi-axle groups vehicles (kg) (TRH 11, 1981)*

Distance between outer axles of group (m)	EFFECTIVE WIDTH (EW) (m)						Tracking required
	3.5	3.6	3.7	→	4.6	4.7	
1.2	30050	30900	31800		38650	38650	30900
1.5	31600	32500	33400		41500	42400	33900
1.8	33100	34050	35000		43500	44450	36300
↓							
5.7	52900	54400	55950		69550	69550	55650
6	54450	56000	57350		70000	70000	56000

The formula which has been used to develop the Table 2.1 is given as;

$$Allowable\ load\ (kg) = EW(6.850 + 0.00145 \times distance\ between\ outer\ axles\ of\ group)$$

Where EW is the effective width i.e. $EW = \text{vehicle width (Wv)} + 1.2\text{m}$. The distance between the outer axle groups are in mm.

TRH11 does not provide any detail on the procedure used to obtain the 6.850 and 0.00145 factors which is included in the allowable load equation.

Wherever the allowable loads exceed the maximum tracking load from the last column, vehicles will have to be escorted and structures will be temporarily closed to other road users. When vehicles or combination of vehicles weighing more than 125 000 kg are crossing a bridge, stress and moment calculation will have to be done to check if the structure is able to support that load.

2.1.2 Remarks

TRH 11 needs to be revised since there have been a lot of developments in the transportation industry and the code of practice for the design of bridges & culverts since 1981. Vehicles are able to carry heavier loads and the number of axles and wheels per axles have also increased.

It is not clear how impact factors are applied or if they are applied in this guideline. The effects of shear, bending moments and reactions, mixed traffic conditions and transverse distribution are also not considered. TRH11 assumes that the all abnormal vehicles will have the same impact on bridges. However this may not be correct since for example, mobile cranes and trucks have different types of suspension system and axles configuration and will have different impact on bridges.

Therefore there is a need to evaluate the applicability of TRH 11 in the present and future road traffic environment.

2.2 Summary report for the assessment of abnormal load vehicles on road bridges

In 1991, there was attempt to introduce a new guideline for the management of abnormal load in South Africa. It was developed by Duncan but has never been implemented (CSIR, 1991). It has the similar philosophy as TRH 11. However, the approach is more rigorous since it does not only consider the effect of axle groups but also the effect of the whole vehicle on the bridge. Duncan also takes into account the effect of mixed traffic loadings and impact factors due to speed, moment and reaction forces.

This report gives a full account of the criteria and assumptions used for assessing the mass effects of abnormal load vehicles (ALVs) on bridge structures. These include items such as the effective width of vehicles, associated traffic models, critical effects, impact factors, assessment parameters, structural overloading, transverse bending moments and span length. The study produced the following table which relates the length of the axle group, the vehicle width and the allowable load for a particular speed.

Table 2.2: *Maximum permissible loads (Kg) on multi axle groups and abnormal load vehicle*

Length of axle group (m)	VEHICLE WIDTH Wv (m)								
	2.3	2.4	2.5	2.6	→	3.1	3.2	3.3	3.4	3.5
1.2	26610	27410	28210	29010		31050	31420	31970	32150	32520
1.4	27370	28190	29010	29840		31940	32310	32690	33070	33440
1.6	28130	28970	29810	30660		32820	33200	33590	33980	34370
1.8	28880	29750	30620	31480		33700	34100	34490	34890	35290
↓										
4.0	37190	38310	39430	40540		43400	43910	444420	44930	45440
5.0	40970	42200	43430	44660		47810	48370	48930	49500	50060
↓										
30.0	92670	95450	98230	101010		108120	109400	110670	111950	113220

The above table has been developed for vehicles travelling at a speed of 30km/hr or less. Two other tables have been developed for vehicles travelling at crawl speed (5-10km/h) and between 10 km/h and 20 km/h. At speed higher than 30km/hr, it is not safe for abnormal vehicles (ALV) to travel on road structures as the impact caused to the bridge is high.

The formula used to develop this table is

$$MG = R \times Mg \times Fw \tag{2.3}$$

Where MG = Allowable load

R = Permissible load reduction factor

Mg = Permissible axle group load

Fw = Vehicle width factor

The formulae have been derived from the comparisons of the effects of various ALV combinations with the capacity of bridges built to carry normal and abnormal design loadings.

2.2.1 Permissible load reduction factor (R)

When vehicles travel above crawl speed, the loading must be reduced because of the impact forces. The empirical percentage-impact/ speed relationship from the Table 2.3 shows that as vehicles travel faster, impact increases (CSIR, 1991).

Table 2.3: *Empirical percentage-impact/ speed relationship for solo ALV movements*

ALV speed S (km/h)	Percentage impact PØ
34	20
30	15
25	10
20	5
18	4
16	3
13	2
9	1

ALV speed S (km/h)	Percentage impact PØ
80	50
66	49
63	48
57	45
50	40
46	35
42	30
38	25

The speed at which abnormal load vehicles cross bridges must therefore be carefully monitored in order to avoid structural damage. The equation used to calculate the permissible load reduction factor (R) is given below (CSIR, 1991).

$$R = 1/\emptyset' \quad (2.4)$$

$$\emptyset' = 1 + P\emptyset\frac{\emptyset-1}{50} \quad (2.5)$$

Where $\emptyset'$ is the impact factor

R= 0.8 for maximum speed < 30 km/hr

R=0.8797 for maximum speed <25 km/hr

R=0.90 for basic crawl speed

2.2.2 Permissible axle group load (Mg)

This loading was initially obtained by placing stationary abnormal load vehicles models in the optimum position on decks free from other traffic. This represents a crawl speed with no impact

forces involved. The total axle group load was plotted against the length of the extreme axle group to obtain Equations 2.6 and 2.7 (CSIR, 1991).

$$Mg = 30.5 + 5.2188\,Lg \qquad for \quad Lg \leq 16m \tag{2.6}$$

$$Mg = 98 + Lg \qquad for \quad 16m < Lg < 30m \tag{2.7}$$

2.2.3 Vehicle width factor (Fw)

Vehicles having a width of less than 2.65 m are considered as narrow vehicles and those having a width of more than 2.65 m are referred to as wide vehicles.

$$Fw = 0.28(1 + 0.9704\,Wv) \qquad for \quad 2.30 \leq Wv \leq 2.65m \tag{2.8}$$

$$Fw = 0.67(1 + 0.1858Wv) \qquad for \quad 2.65 \leq Wv \leq 3.50m \tag{2.9}$$

These equations yield values of 0.9049, 1.0 and 1.1058 respectively for 2.30, 2.65 and 3.50m wide vehicles (CSIR, 1991).

2.2.4 Mixed traffic loading

This research has produced two tables, one for rural and one for urban mixed traffic for narrow vehicles travelling at a speed of 30 km/h. Mixed traffic means that other vehicles are allowed to allowed to use the bridge at the same time. The permissible road reduction factors are taken as R = 0.725 and R = 0.650 for rural and urban traffic respectively. It is important to note that the mass allowed on very short axle groups in urban areas is almost identical to that given by the bridge formula plus 25% (CSIR, 1991).

2.2.5 Computer program, ASSESS

This program was developed from the above study and is able to evaluate the movement of ALV across bridges. Vehicles may have up to 40 axles and be either narrow or wide. It also assumes that bridges have two 3.7 m wide lanes and may consist of up to three spans. Assessments are based on the comparison of effects due to the ALV and the original bridge design loadings (i.e. moment and shear comparison). The program also caters for change in the impact factors, associated traffic levels and vehicle overloading. This program is more suited for engineers as the output requires an engineering background to understand.

2.2.6 Conclusions

The summary report for the assessment of abnormal load vehicles on road bridges is more detailed than TRH11 and it takes into account dynamic loads. However, the impact factors need to be revised since it is quite conservative when compared to impact factors from other countries as show in Figure 2.1.

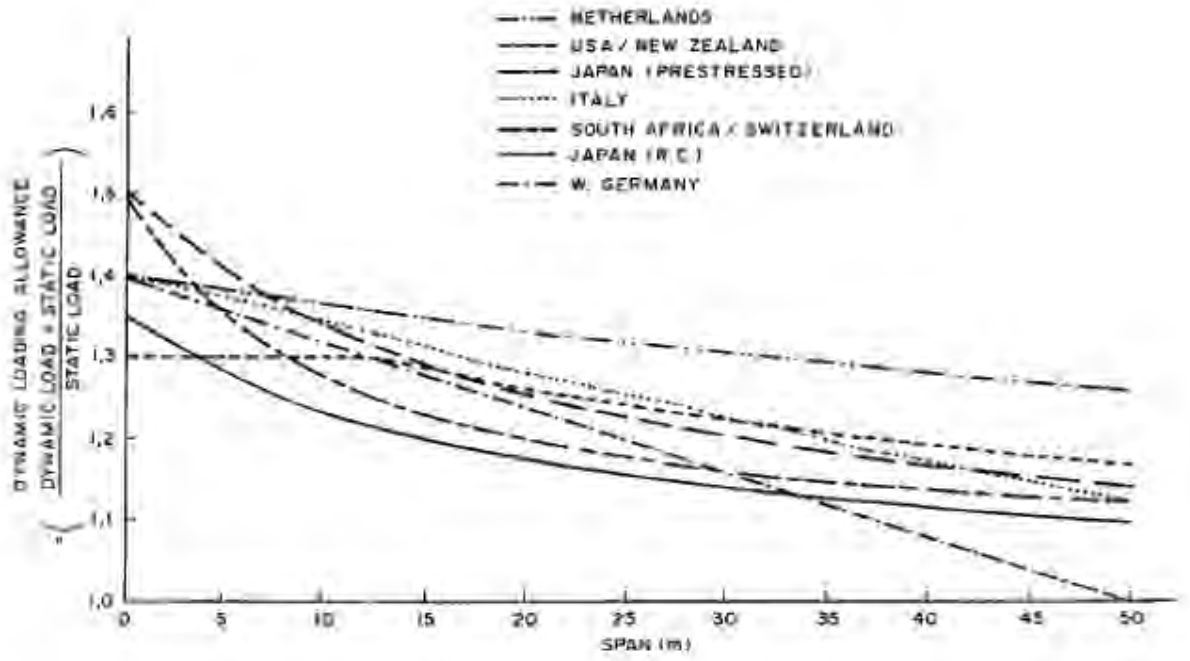

Figure 2.1: *Variation of dynamic loading allowance with span for different countries (CSIR, 1991)*

All vehicles have been assumed to have the same suspension system in this report. However, in real life even though trucks and mobile cranes are considered as abnormal vehicles, they have completely different axle configurations and suspension systems.

Therefore a further research is required to investigate the dynamics effects of mobile cranes on bridges since they are being widely used in South Africa nowadays.

2.3 Abnormal load management software

Commercial softwares have been developed to facilitate the management of abnormal loads. They simplify the calculation and comparison of the allowable load to the permitted load provided that the right data are imputed. One such software is OPTAX.

OPTAX is able to determine the optimum axle weight and spacing of a proposed vehicle travelling over a simply supported span, such that the maximum bending moments and shear forces caused by several trains of vehicle did not exceed those due to a control vehicle (test vehicle) for any span (BES Division, 1983). The program can vary the span length, the spacing between the vehicles and the number of vehicles. An impact factor of 1.8 is automatically applied to all OPTAX calculations. The use and availability of this software is however unknown.

Another software which is used to manage abnormal loads is ABLOADS. It has been developed in association with the Kent County Council. ABLOADS is capable of checking the loading capacity of complex bridges provided that vehicle axle weights and spacings are known.

2.4 Hong Kong legal limitations

In Hong Kong the legal limits (Normal Loading) are prescribed in the 'Transport Planning and Design Manual".

2.4.1 Axle spacing

The distance between two consecutive axles is limited to between 1.02m and 1.85m. The minimum spacing between axles not in the same group is limited to either 2.1m or 4.2m. The maximum length of a heavy vehicle is limited to 18.9m.

2.4.2 Axle weight

The allowable axle loads for two closely spaced axles are given in Table 2.4. Two closely spaced axles mean that the axles are spaced at a distance of no more than 2.5m and no less than 1.02m.

Table 2.4: *Maximum allowable weights for 2 closely spaced axles in Hong Kong*

Distance between 2 closely spaced axles (m)	Permitted total axle weight (t)
<1.02	5.5
≥ 1.02	8.0
≥ 1.05	8.5
≥ 1.20	9.0
≥ 1.50	9.5
≥ 1.85	10.0

The maximum gross vehicle weight in Hong Kong is limited to 42 tonnes. Vehicles exceeding this load are considered to be abnormal or super load and require special permits to operate.

The load management system in Hong Kong is different to TRH11. In South Africa, vehicles are able to carry up to 50 tonnes without having to apply for a permit. This is mainly because bridges in Hong Kong have been constructed using different codes and hence the load allowance is different.

2.4.3 Hong Kong loading model

The model has been developed from data obtained from a Weigh-in-Motion (WIM) system. The Weigh-in-Motion technology has the ability to weigh vehicles as they travel on highways. The development of the Hong Kong bridge live load model is based on the average extreme daily moments and shear forces which occur at mid-span of simply supported bridges. The bridges are spanned between 5 and 40m. They vehicles weighed were classified as (a) short vehicles (vehicles less than 12m); (b) medium combined vehicles (vehicles between 12 and 15m); and (c) long combined vehicles (vehicles length greater than 15m). Figure 2.3 and Figure 2.3 respectively show the average extreme daily shear and moment caused by the three types of vehicles. HKA refers to the average shear and moment caused by all the vehicles (Chan, 2002).

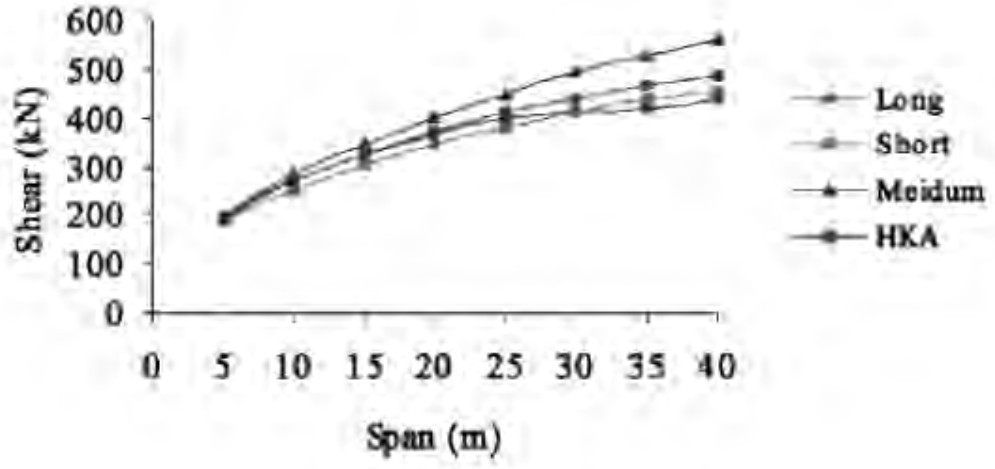

Figure 2.2: *Average extreme daily shears in simply supported spans due to short, medium and long combined vehicles (Chan, 2002)*

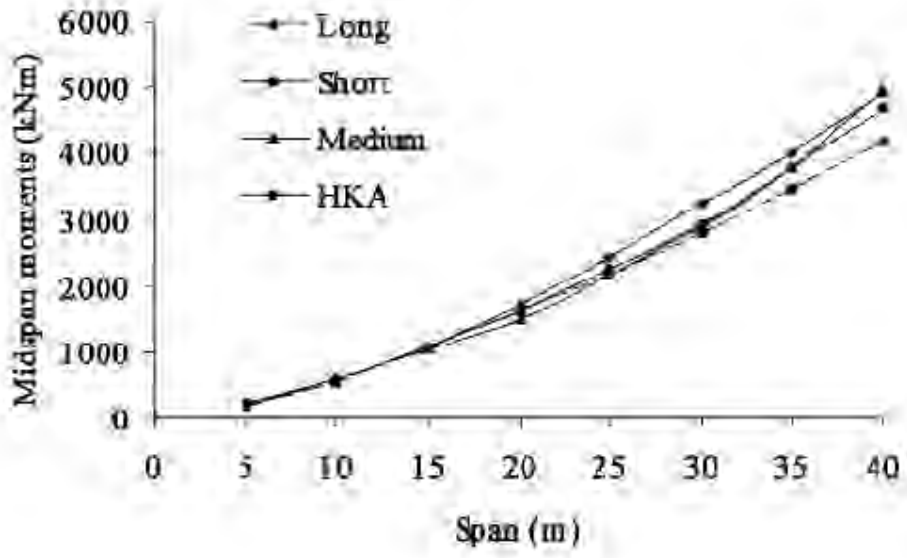

Figure 2.3: *Average extreme daily moments in simply supported spans due to short, medium and long combined vehicles (Chan, 2002)*

The Weigh-in-Motion data was used to find the relationship between the gross weight (W/t) of the vehicle and the equivalent base length (B_m/m). This relationship is shown in Figure 2.4.

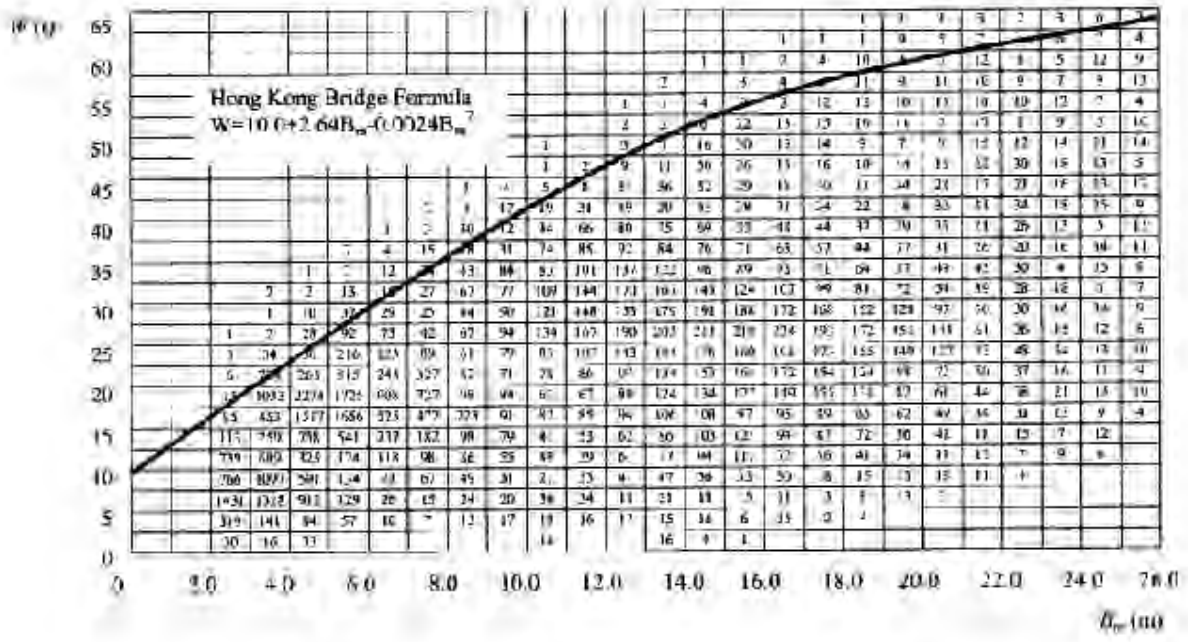

Figure 2.4: *W/B_m plot using Hong Kong WIM data (Chan, 2002)*

The fitted curve is assumed to represent 98% of the data. The equation of the best fit curve is given by:

$$W = 10 + 2.64Bm - 0.0024Bm^2 \quad (2.11)$$

This equation is very similar to the Ontario Bridge formula which is given by:

$$W = 20 + 2.07Bm - 0.0071Bm^2 \quad (2.12)$$

The moment caused by a load uniformly distributed over a finite length B_m can be expressed by the following formula:

$$M = \eta\left(1 - \frac{Bm}{2L}\right)W \quad (2.13)$$

Where η = maximum influence line ordinate

Bm= Loaded length (m)

W= gross Load (tonne)

L= Span length (m)

2.5 Truck weight limit formula for US highways

The bridge formula which is used to calculate the allowable load for trucks on US highways is given by Equation 2.10.

$$W = 500\left(\frac{N}{N-1}l + 12N + 36\right) \leq 80\,000\ lb\ (36\,363\ Kg) \quad (2.10)$$

Where $W =$ Maximum allowable weight of any group of axles; $N =$ Number of axles in the group; and $l =$ Extreme axle spacing of the group.

The philosophy of this formula is that the actual stresses cannot be more than 5% greater than the allowable design stress for bridges designed for HS20 trucks and not higher than 30% for bridges designed for H15 trucks (James & Zhang, 1991). Trucks that pull trailers are designated as HS for example HS20 refers to a 20 tons semi-trailer truck. Figure 2.5 shows the layout of an HS20 truck. However this formula is not reliable since the 80 000lb weight is arbitrary. It has been

proven that if the 80 000lb weight limit is removed, the formula would not safely limit longer and heavier vehicle. (James, Noel, Furr, & Bonilla, 1986)

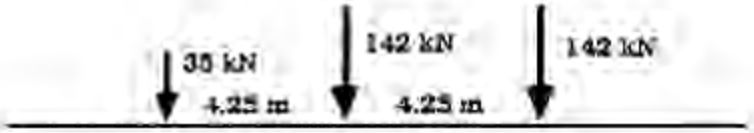

Figure 2.5: *Standard HS20 truck*

New formulas have been proposed to safely limit truck weights and allow an increase in the vehicle weight without overstressing the bridge.

$$W = 1{,}000(L + 34ft) \quad L \leq 56ft \tag{2.11}$$

$$W = 1{,}000\left(\frac{L}{2} + 62ft\right) \quad L > 55ft \tag{2.12}$$

The above formulas work well for both single and multi-span bridges. It has been developed by taking into account the axles spacing, vehicle length and also the shear and moment effects. Like TRH11, it does not take into account the impact factors and the type of vehicles. Therefore a further research is essential to find out how the dynamic impact factors will affect the above formulas.

2.6 Live load models in South Africa

In South Africa, live load models for bridges have varied over the years. The very first documented load model consisted of sixteen oxen and a loaded wagon (Ullman, 1987). The main load models used since that time are:

- Public Works Department (PWD) Standard Bridge loading which consisted of a steam tractor and four wagons, or a road roller, with an impact allowance of 50% (1912-1935).
- United Kingdom Ministry of Transport (MOT) Standard Train which consisted of a steam traction engine with three trailers as shown in Figure 2.6 (1925-1956). The trains of vehicle was based on the heaviest commonly occurring vehicles, except that the actual axle weights were increased by 50% to allow for impact.

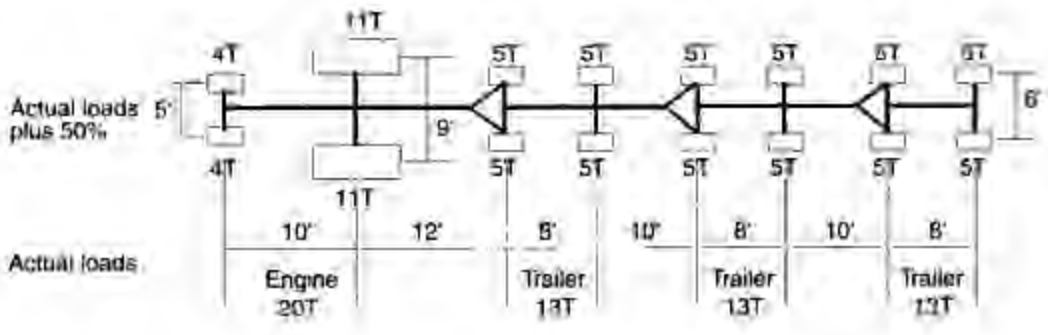

Figure 2.6: *Standard Load for Highway Bridges (MOT, 1922)*

- United Kingdom Ministry of Transport Equivalent Loading Curve which was based on the MOT standard train but made allowances for a lower concentration of loading and a reduction in the impact allowance on longer spans. The design load consists of a uniformly distributed load (UDL) in conjunction with a knife edge load (KEL). The UDL was derived from the Standard Loading Train by taking the weights of all the axles of the train on a particular loaded length and converting them to a uniformly distributed load. The weight of the locomotive axle was taken as the KEL. (Cape 1947-1960, Transvaal 1956-1987, Natal 1935-1976)
- BS 153: Part 3A, British Standards Institute, (1954) that considered of a loading curve similar to the MoT curve except for an increase in design load for spans less than 6m and a decrease for spans greater than 22.9m. The principle of notional lanes and the abnormal vehicle type was also were also introduced in this code. This code is discussed in more details later in this chapter. (Cape 1961-1987)
- TMH 7 Part 2 (1978-present) "Code of Practice for the design of Highway Bridges and Culverts in South Africa". This code was first published in Natal before being published by the Department of Transport for use throughout South Africa in 1981. This code is discussed in more details in the section 2.7.

Table 2.5: *Number of bridges designed to the various abnormal vehicles codes of practice from 1910 to 1989 in South Africa (Duncan, 1991)*

Design Loading	Number of structures	Percentage
MOT HB32	3135	54.3
BS153 HB30	1604	27.8
HB36	36	0.6
HB45	304	5.3
BS 5400 HB36	44	0.8
HB45	105	1.8
TMH 7 NB24	89	1.5
NB 30	128	2.2
NB 36	324	5.6
Total	5769	100.0

Table 2.5 shows the summary of abnormal vehicle design load usage from 1910-1989 for bridges of span greater than 6m

Table 2.6 shows the approximate number of bridges designed to various codes of practice between 1910 and 1990 in South Africa (Duncan).

Table 2.6: *Inventory of bridges designed to various codes of practices (Chan, 2002)*

Design Code	Number of bridges	Percentage
PWD	492	4.4
PRE	253	2.3
MOT	7719	68.8
BS153	1460	13.0
BS 5400	130	1.2
TMH7	763	6.8
Other	405	3.6
Total	11222	100.0

2.7 Code of practice for the design of highway bridges and culverts in South Africa

This code of practice is also known as TMH 7 (Technical Methods for Highways). It is based on the principles of limit state design with reference made to BS 5400 and the National building Code of Canada. Limit state design is the logical and practical procedure that has been evolved to achieve acceptable probabilities so that the structure being designed will remain fit for the required purpose during some reference period with its intended life taken into consideration (TMH 7, 1981). The limit states which are commonly used for the design of bridges are the ultimate limit state (ULS) and the serviceability limit state (SLS). This code of practice assumes that the bridges in South Africa have been designed for a lifetime of 100 years provided they are regularly inspected and maintained.

2.7.1 Ultimate limit state (ULS)

Ultimate limit state design is concerned with the collapse and failure of individual elements within a structure. The ultimate limit states which are applicable to this code are:

a. Loss of equilibrium of a part or the whole of the structure considered as a rigid body.
b. Rupture of critical sections of the structure, excessive deformation or resonant vibration.
c. Transformation of the structure into a mechanism.

d. Deterioration due to fatigue to a point where failure occurs.
e. A state of instability which relates to the collapse in strength of only part of a section.

2.7.2 Serviceability limit state (SLS)

Serviceability limit state is usually associated with the durability of a structure. It is mostly concerned with traffic situations which occur more frequently than the very rare situation which has to be allowed at ULS. The SLS applicable to this code are:

a. Deformation
b. Local damage or cracking
c. Vibration

While the two limit state deals with entirely different aspects, there is some correlation between them. By meeting the requirements of the ULS, that the requirements of the serviceability state are also satisfied (BS 5400, 1978).

2.8 BS 153: Normal loading model

This loading model takes into account both bending moments and shear. For simplicity of design, and bearing in mind that traffic loads are never the same, it is considered that the use of one loading model (Uniformly distributed load + Knife edge load) for both bending moment and shear calculation is justified for short span bridges. For longer loaded structures, it is assumed that the axle loads are uniformly distributed along the length (BS 153, 1954).

The normal loading curve was developed by comparing the effects of two different trains of vehicles for spans of up to 75 ft and spans of 75-500 ft respectively. A 4-axle 22-ton vehicle was chosen as the main vehicle in the train since it provided a particularly heavy loading. Shear forces and bending moments were calculated and compared for transverse and longitudinal members. For spans between 20 and 75 ft, the comparisons were very similar to those derived from the Equivalent Loading Curve (BS 153, 1923). Between 75 and 500 ft span, the comparison of the loading effects was based on a single line of vehicles and a uniformly distributed load (UDL) and knife edge load (KEL) was derived. From 500 ft to 3000 ft span, the UDL was calculated assuming an average weight of traffic per linear foot of lane; this represented a train of vehicles with a car in between each truck. It was assumed that this loading occurs in only one lane and was unlikely to occur simultaneously in two adjacent lanes. An impact allowance has

been added to the derivation and this amount to a 25 per cent increase in load of any one axle of one vehicle, or any single pair of adjacent wheels of two vehicles travelling side by side (BS 153, 1954). The normal loading curve is shown in Figure 2.7.

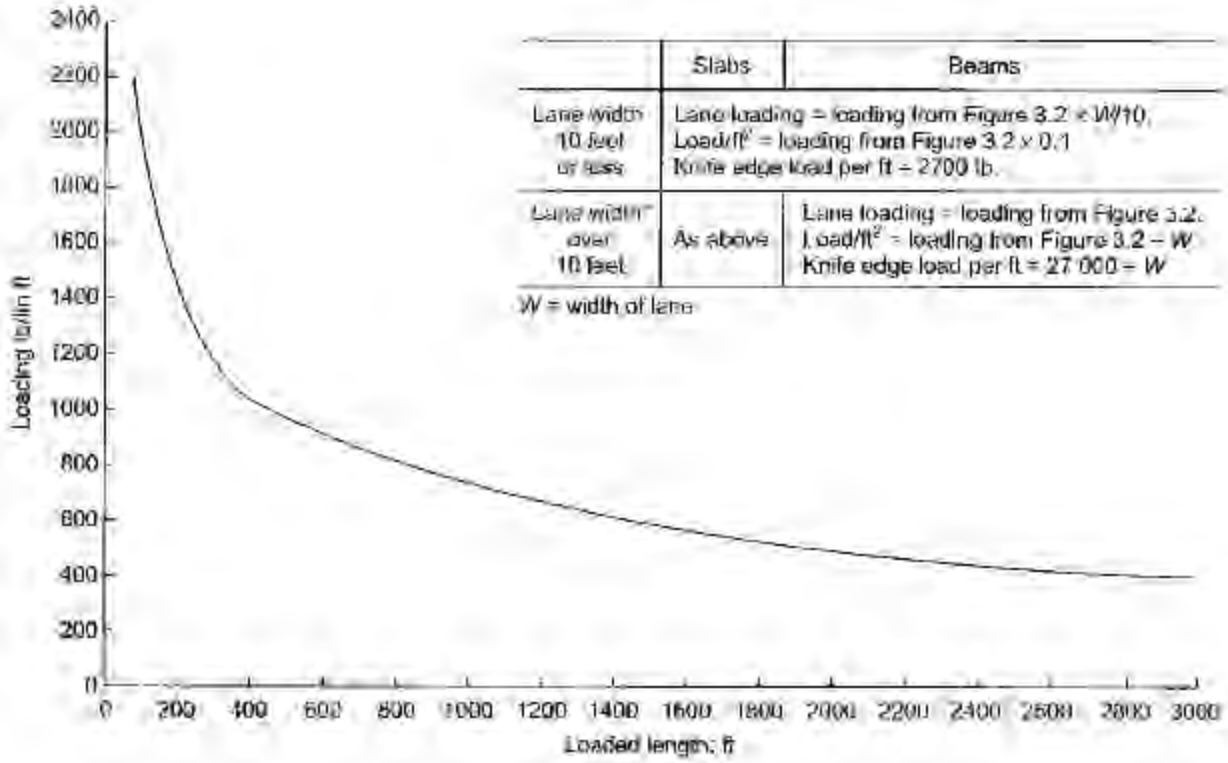

	Slabs	Beams
Lane width 10 feet or less	Lane loading = loading from Figure 3.2 × W/10 Load/ft² = loading from Figure 3.2 × 0.1 Knife edge load per ft = 2700 lb	
Lane width over 10 feet	As above	Lane loading = loading from Figure 3.2. Load/ft² = loading from Figure 3.2 – W Knife edge load per ft = 27 000 – W

W = width of lane

Figure 2.7: *Loading curve for normal (HA) highway loading (BS 153, 1954)*

3. HIGHWAY LOADS

3.1 Traffic loads

Highway structures are designed for normal, abnormal and super loadings. Normal traffic design loading codes consider the effects of light and heavy vehicles that may occur on road bridges. This type of loading is commonly referred to as HA or NA loads. Abnormal vehicle design loadings are intended to for heavy indivisible loads with a gross mass exceeding 50 tonnes (CSIR, 1991). These loads generally form a basis for designing transverse members, including cross beams and deck slabs. The term HB or NB is used to describe these loadings. Highway loads are divided as follows:

- Legal: up to 50 tonnes
- Abnormal: 50 to 180 tonnes
- Special: 180 to 250 tonnes
- Super: over 250 tonnes

Figure 3.1 shows the relationship between the average load per metre of notional lane and the effective loaded length for normal traffic loadings in South Africa.

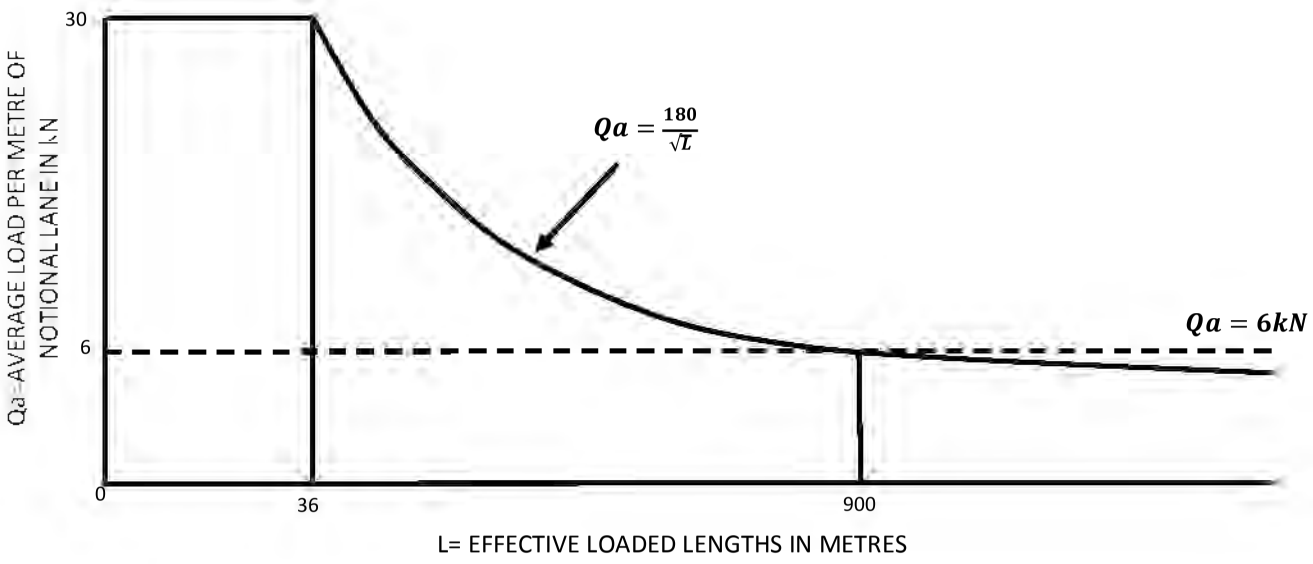

Figure 3.1: *Loading curve for HA loading (TMH 7, 1981)*

For loaded length up to 36 m, the load per metre of notional lane is 30 kN. For loaded length in excess of 36 m, the average load per metre is derived from the formula:

$$Qa = \frac{180}{\sqrt{L}} \quad (2.1)$$

Where L = the effective loaded length in metres

And Qa = average load per metre of notional lane in kN.

For a loaded length greater than 900 m, an additional loading case with Qa = 6 kN/m is uniformly distributed on all loaded parts, shall be considered.

A nominal axle load of $\frac{120}{\sqrt{n}}\ kN$ per notional lane has to be added to Qa for HA loading where *n* is the loading sequence number for the relevant lane, i.e. n =1 for the first lane with loaded axle load, n = 2 for the second lane (TMH 7, 1981). Only one axle load is applied to a single lane and it must act transversely with the longitudinal direction of the lane. The loading sequence 'n' for the different lanes causing the most severe effect is selected. Whenever the transverse distribution in a lane has no significant effect on the element being considered, the axle load is applied as a knife edge load which is uniformly distributed over the full width of the lane (TMH 7, 1981).

For this research we will concentrate mainly on abnormal and some special loads up to 200 tonnes. Super loads have special routes on which they can operate. These roads are closed to other roads users when being used by super vehicles. Abnormal vehicles are mostly car carriers, mobile cranes, container trucks and trucks carrying heavy metal structures, precast elements and petroleum products. Figure 3.2 and 3.3 below give the layout of a mobile crane and a truck respectively.

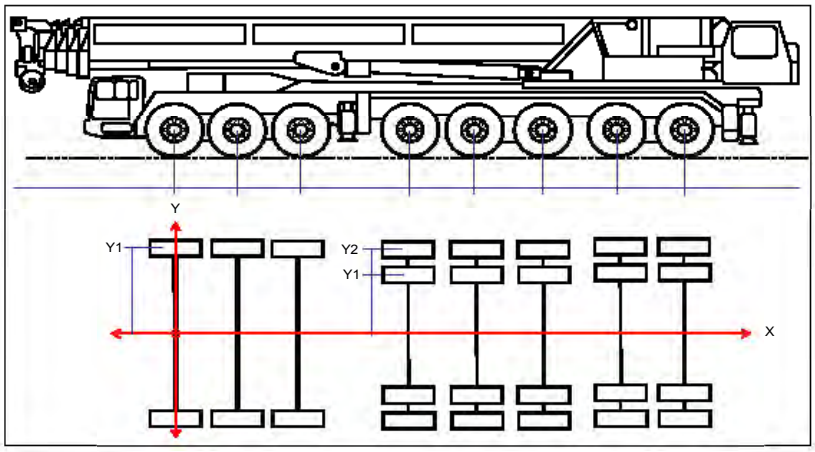

Figure 3.2: *Generic axle and load configuration of a mobile crane*

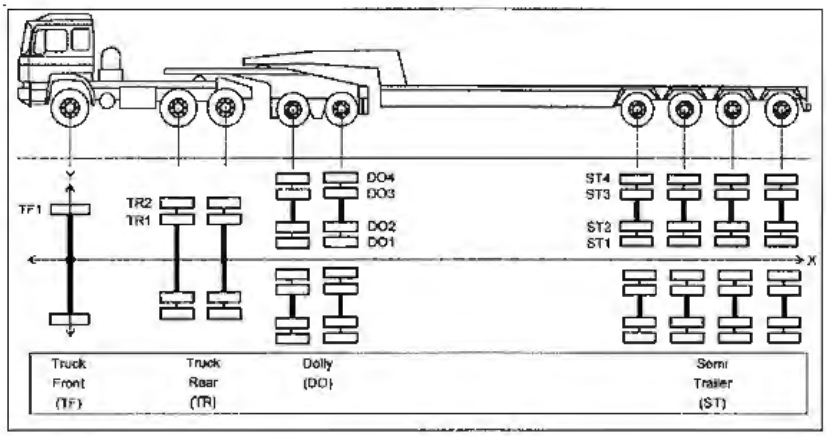

Figure 3.3: *Generic axle and load configuration of a typical abnormal load vehicle*

The mobile crane in Figure 3.1 has eight axles and three axle groups. The X-axis gives the distance between the between the axles and axle groups while the Y-axis gives the vehicle width. Whenever Y2 is greater than Y1, Y2 is taken as the vehicle width. Figure 3.2 shows a truck having nine axles and four axle groups. The truck rear, the dolly and the semi trailer all have dual tyres. These vehicles are only allowed to operate provided they stick to the speed and load limit imposed to them.

3.2 Load combinations on bridges

The primary loads which act on bridges are dead loads, earth pressure, traffic loads (live load) and wind load. The secondary loads are centrifugal, braking, accidental skidding and vehicles collisions with bridge parapets and support. The different load combinations which can be used for bridge design are given below.

Combination 1: Dead loads, earth pressure and traffic loads (TMH 7, 1981).

Combination 2: Combination 1 plus wind loading (TMH 7, 1981).

Combination 3: Combination 2 plus temperature loading (TMH 7, 1981).

Combination 4: Dead loads plus secondary live loads (BS 5400, 1978).

Combination 4: Dead loads plus those due to friction at bearings (BS 5400, 1978).

TMH 7 and BS 5400 uses partial factors compared to previous codes which were based on permissible stress. The use of partial factors improves the safety margin. Safety factors are applied to the dead, wind and live loads. Dead load generally has a lower factor of safety since dead load can be calculated more accurately using weight of steel and concrete.

3.3 Dead load (D)

Dead load is the gravity load due to the self weight of the structural and non-structural elements which are permanently connected to the bridge (A.S. Nowak & M. Szerszen, 1998). The components of D which are usually considered are:

D1 = weight of factory-made elements (steel and precast concrete members)

D2 = weight of cast-in-situ concrete members

D3 = weight of wearing surface (asphalt)

D4 = miscellaneous weight (e.g. railing, luminaries)

3.4 Live load (L)

Live load covers a range of forces produced by vehicles moving on the bridge. The effect of live load depends on many parameters including the span length, truck weight, axle loads, axle configuration, position of vehicle on the bridge (transverse and longitudinal), number of vehicles on the bridge, girder spacing and stiffness of structural members (slab and girders) (A.S. Nowak & M. Szerszen, 1998).

3.5 Dynamic load

Dynamic load effect is considered as an equivalent static load which is added to the live load. Dynamic load is dependant on three major parameters: road surface roughness, bridge dynamics (frequency of vibration) and vehicle dynamics (suspension system). Simulation of this type of

loading requires the generation of a road profile which is done by using Fourier transform of the power spectral density function. The beam also needs to be modelled as a prismatic beam (A.S. Nowak & M. Szerszen, 1998).

3.6 Assessment of Short Span Bridges

The assessment procedures were developed by Flint and Neill partnership in association with the Transport Research Laboratory (TRL) and Imperial College, London. The first step was to produce a probabilistic live model based on a large sample of vehicle weight and length recorded on a motorway site. These data were supplemented by measurements of the wheel forces on road surfaces from moving vehicles in order to model the dynamic effects of vehicles running on different types of roads (Flint and Neill partnership, 1996). The two sets of data were then used to develop a static and dynamic load model.

In the second stage, a set of reliability analyses were carried out on short span bridges for six different traffic scenarios namely high, medium and low traffic flows and poor and good road surfaces. From the analyses the values of the reliability for the worst case (i.e. high traffic flow and poor road surfaces) were selected. They were then used as target values to find suitably modified partial load factors which were applied to other scenarios to give similar reliability (Flint and Neill partnership, 1996).

In the third stage, the reduced partial factors together with comparisons of characteristic load effects were used to derive load reduction factors to the less onerous traffic scenarios (Flint and Neill partnership, 1996)

3.7 Static load models

3.7.1 Vehicle data

The vehicle data was collected over a two week period on the M6 in England (Ricketts N. J. and Page J, 1997). Data was obtained from a weigh-in-motion system which was installed in one carriageway of the M6. This system could record information for each vehicle passing over detectors including speed, axle spacings and axle weights. From the recorded data, it was possible to find the overall length of the vehicle, the headway between vehicles and their axle and gross weights. Details of about 255 000 were recorded together with the date and time of each vehicle (Ricketts, N. J. and Page J, 1997).

The equipment used was unreliable at speed lower than 35 mph. Data was therefore not available for times that the M6 was congested. The video camera at the site also allowed filtering out any vehicles which were considered to be abnormal or special.

3.7.2 Traffic modelling

The vehicles in the data were run in the order in which they were recorded over three different influence lines to obtain histograms of the individual and joint lane load effects. The three influence lines represented the mid span bending moments in a simply supported beam, the end shears in a simply supported beam and the bending moments over the central supports of a two span bridge. Traffic simulations for each influence line shape were done for several loaded length from 2.5 to 50 m and the magnitude of each single loading event was defined as the peak load effect (Ricketts, N. J. and Page J, 1997).

The histograms containing the load effects for the two weeks of traffic was then raised to the power of the daily traffic flow to give the cumulative distribution function of the daily maxima. From this distribution, the parameters for the best fit Extremal Type 1 distribution were obtained representing the distribution of the maximum load events for the two weeks period. This information was then used to derive the parameters for any desired return period for various load effects concerning loaded lengths, influence shape lines and traffic lanes.

3.8 Dynamic load model

3.8.1 Data collection

Tests were carried out on 28 selected bridges using specially instrumented vehicles. Four articulated vehicles and one rigid vehicle were used and the dynamic wheel/road surface loads on each wheel were continuously recorded. The vehicles were run over road surfaces classified as good, medium and bad and also over three planks with different profiles placed on a smooth road surface. Apart from the wheel load test, high speed surface recording vehicles were also used to measure the road surface profiles (Ricketts, N. J. and Page J, 1997).

Two of the bridges were then selected and instrumented so as to measure their dynamic responses to the test vehicles. Displacements were measured at both bridges and at one of them, the strain in the beam were also measured. The vehicle instrumentation was recorded at the same

time as the measurements from the bridges themselves as the test vehicles drove over the two bridges at 10 and 40 mph (Ricketts, N. J. and Page J, 1997).

3.8.2 Dynamic effect model

The wheel load data recorded from the 28 bridges were used in the dynamic response analysis of a number of simple bridge models which were assumed to represent a range of different types of construction. These analyses were then used to prepare a histogram of all the dynamic amplification factors calculated for vehicle wheel forces.

In order to confirm the adequacy of the theoretical calculations, some of the vehicles were run over two specially instrumented bridges. Both bridges consisted of three spans with the road surface quality on one described as good and the other one as bad. The test vehicles were run across the bridge at 10 and 40 mph. These test confirmed that the dynamic amplification factor derived from the theoretical analyses were realistic. They also confirmed that the dynamic response of a bridge to a moving load could be determined by a static analysis using the measured but varying wheel load (Ricketts, N. J. and Page J, 1997).

3.9 Probabilistic load model

The probabilistic load model was developed to be used in the reliability analysis. It is composed of the three following elements:

a. A model based on Load Model 1 in Eurocode 1 Part 3 to give a set of static load effect.
b. A statistically defined factor which enables the required probability distribution of the load effects to be derived from the static load model.
c. A statistically defined factor to enable the static load effects to be enhanced to take account of the dynamic effects.

The statistical and the dynamic model derived from the previous sections are used to represent different traffic flows and road surfaces for the various spans being considered. Separate statistical load models were derived from simply supported bridge to cover the cases listed below:

a. Extreme lane 1 effects due to the passage of a single very heavy vehicle.
b. Joint extreme multi-lane effects due to the coincident passage of heavy vehicles.
c. Heavily compressed stationary traffic closely spaced laterally.

3.10 Reliability analysis

For this analysis, simply supported reinforced concrete slab bridges and beams and slab bridges with spans up to 20 m were investigated. The bridges were designed using the load specified in the assessment of highway bridges and structures manual (Department of Transport, 1993) and the relevant strength were obtained from BS 5400. Optimum sets of partial factors were obtained for the six scenarios of traffic and road conditions. The live load factor was then adjusted to obtain a uniform reliability (Ricketts, N. J. and Page J, 1997).

In the case of slab bridges, there was little variation in the live load factor for the different traffic flows but the partial factors required for the poor road surfaces were on average 7.5% greater than those for the good surfaces. For beams and slab bridges with spans greater than 20 m, the live load partial factor for the good surface cases were generally lower than those for the poor surfaces. However there was about a 6% increase in the partial factors required for the low traffic flow cases.

These findings were used to modify the load reduction factors K which is obtained from the characteristic load effect comparison. K is defined as the ratio between the characteristic effect obtained using the relevant probabilistic load model and the effect obtained using the HA loading (BS 5400, 1978) for a 2.74 m lane width. The K factors were then multiplied by a constant normalising factor to make sure that it complies with the Highway Agency guidelines (Highway Agency, 1997).

4. IMPACT FACTORS ON BRIDGES

The impact load factor is defined as the ratio of the maximum response under a moving load, divided by the maximum response for the same, static load. In other words, it is the amplification of the static load. Dynamic amplification can have a significant effect on the stresses in a bridge, especially when its natural frequency is excited by vehicles travelling at speeds which induce a resonance effect. (Li, OBrien, & Gonzalez, 2006)

The main parameters which contribute to the dynamic impact factors are the bridge span length, number of lanes, radius of curvature, surface roughness, vehicle braking, suspension system and speed, positioning and weight of the vehicle(s) on the bridge. The fundamental frequency and damping of a bridge also contributes to the impact factors. These parameters can be expressed in terms of dynamic impact factors for longitudinal moment, reaction and deflection of the bridge.

4.1 Effects of the natural frequency on the dynamic impact factor

Impact formulas have been developed by codes and guidelines from several countries. The dynamic load allowance (DLA) is usually given in terms of the span length of the natural frequency of the bridge. The natural frequencies of bridges generally vary from 1 Hz to as high as 15 Hz. Most abnormal vehicles apply dynamic loads in the 1.5 to 4.5 Hz frequency range (Green, Cebon, & Cole, 1995). Engineers should therefore avoid designing bridges having a frequency of less than 5 Hz to prevent matching of the vehicle's and bridge frequency. The Ontario Highway Bridge design code and the Swiss design code have adopted this concept. A penalty is imposed on designers if the two natural frequencies coincide.

Figure 4.1 shows the variation of the DLA for different national codes. All DLAs are plotted against the natural frequency, including those originally calculated in terms of span length. The relationship which has been used to relate the frequency, f_o, to span length L_{max} is as follows:

$$f^0 = 82Lmax^{-0.9} \tag{4.1}$$

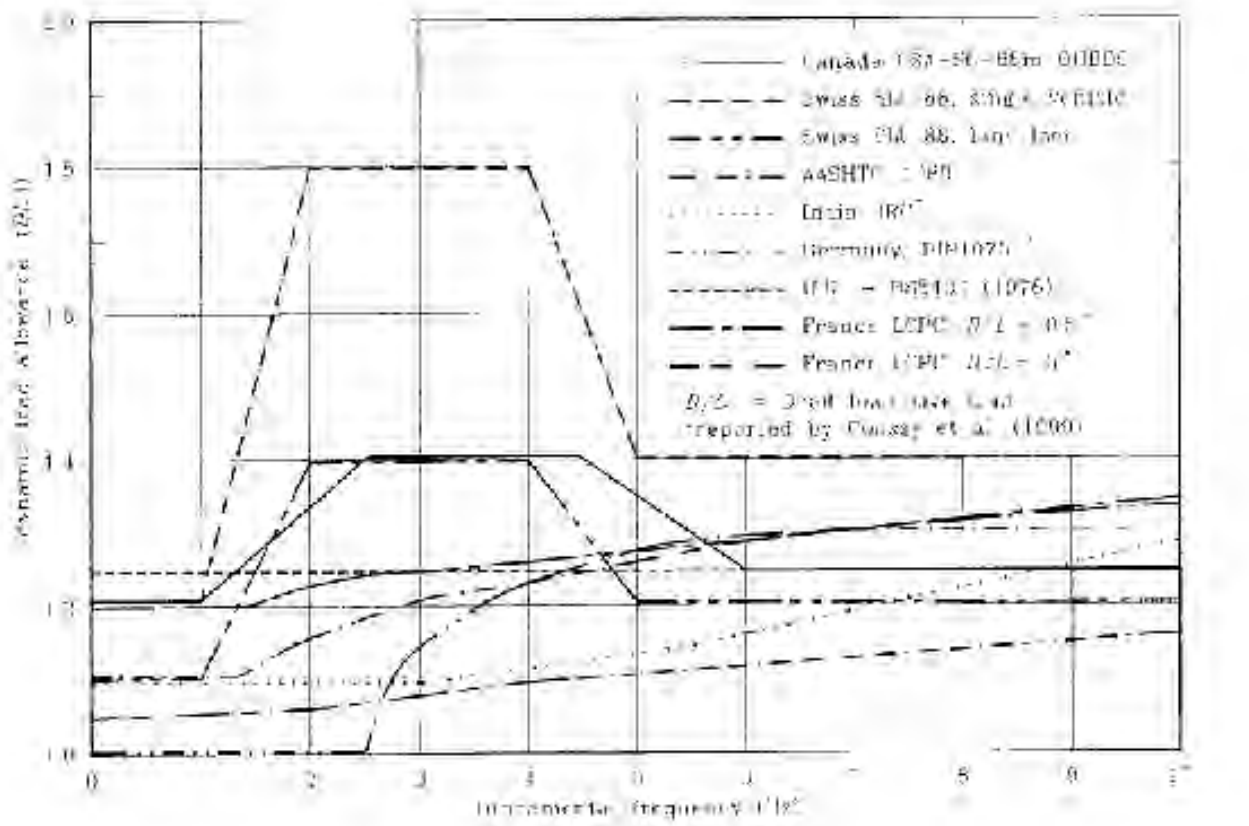

Figure 4.1: *Dynamic load allowance (DLA) versus fundamental frequency for different national codes (Paultre, Chaallal, & Proulx, 1992)*

4.2 Influence of surface roughness on the dynamic impact factor

The roughness of the road has a major influence on the dynamic amplification factor. The road surface is classified using the International Roughness Index (IRI) as 'poor', 'average' and 'good' profiles.

Several studies have modeled deterioration of the road surface by placing a wooden plank on the road and having vehicles running over it. The deterioration may be due to potholes, delaminations or a threshold between the bridge approach and the deck. The plank helps excite the dominant flexural modes corresponding to low frequencies (Kwasniewski et al, 2006). Table 4.1 show the effect of speed and road surface conditions on the impact factors.

Table 4.1: *Resultant Impact Factors for Tested Bridges (Kwasniewski et al, 2006)*

Factor	Speed (Km/hr)	One truck (%)	Two trucks (%)
No Plank	48	2.5	20.0
	80	82.3	50.5
Plank	48	79.2	-
	80	164.0	-

The difference in elevation between the asphalt and the concrete bridge is very common for several bridges and this lead to an increase in the dynamic interaction between the truck wheels and the bridge deck. Since increased speed causes high dynamic effects, reduction in speed is a viable option for abnormal vehicles to ensure safety.

The most obvious way of reducing the bride response is to minimise the effects of surface roughness. Good maintenance of the bridge surface helps decrease the excessively large dynamic wheel loads (Green, Cebon, & Cole, 1995).

4.3 Effect of the wheel distribution factor on the dynamic impact factor

The wheel-load distribution factor (DF) represents the distribution of the vehicular load among the load-carrying components of the bridge. The DF can be calculated from the equation (Nowak, Kim, & Stankiewicz, 2000):

$$DF_i = \frac{n\epsilon_i}{\sum_{j=1}^{6}(\frac{EI_j}{EI_i})\epsilon_j} \tag{4.2}$$

Where ϵ_i and ϵ_j are the measured strains of the ith and jth girders respectively; $EI_i and\ EI_j$ are the bending stiffness of the ith and jth respectively; and n is the number of wheel loads in the transverse directions.

The DF's only show how how the wheel loads are distributed transversely among the girders when an abnormal vehicle is located at a specific position. Figure 4.2 shows the wheel distribution factor for a six bridge girder at four different truck locations(Kwasniewski et al, 2006).

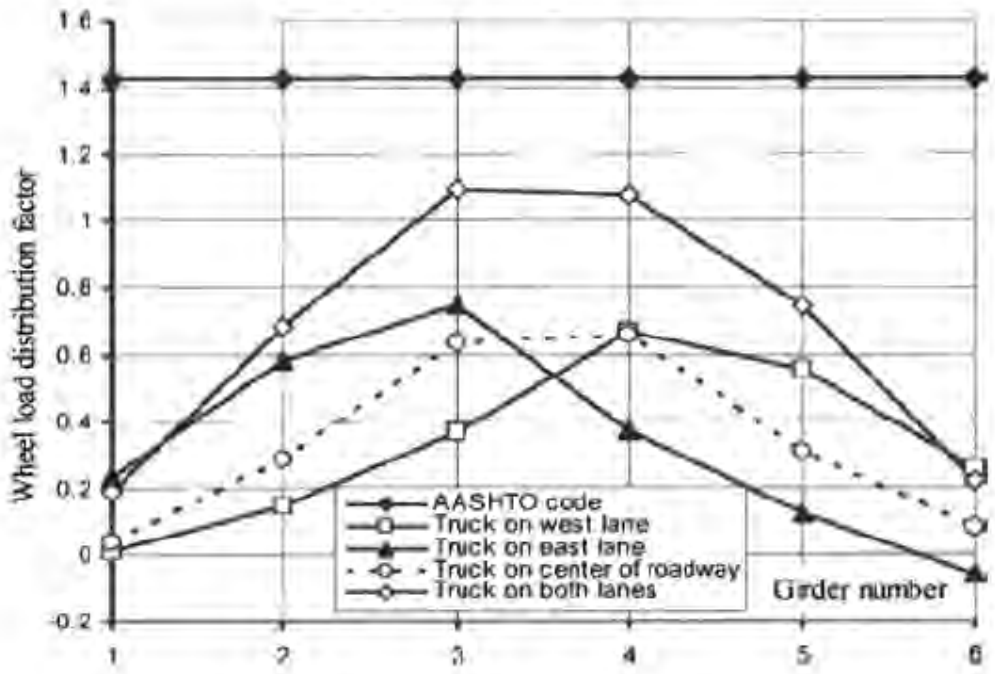

Figure 4.2: *Wheel distribution factor for a six bridge girder at four different truck locations (Kwasniewski et al, 2006)*

4.4 American Association of State Highway and Transportation (AASHTO) method

All moving vehicles generate additional dynamic effects on bridges. The design code defines the dynamic load as an additional static live load. In the AASHTO (1994) design code, the standard impact factors are specified as a function of span length only. The following formula has been established:

$$Im = \frac{50}{L+125}.100\% \quad (4.3)$$

Where L= Length in feet of the loaded portion of the span;

Im= Impact factor which cannot be greater than 30%

The impact factor Im (AASHTO, 2002) can also defined as a ratio of the dynamic increment (R_D – Rs) in structure response to the static response. This results in the following relationship:

$$Im = \frac{RD-Rs}{Rs}.100\% \quad (4.4)$$

Where R_D = dynamic response; and Rs = static response

4.5 The Swiss Method

In the Swiss Method, the impact factor applied to the actual load effects is calculated using the following formula (Anderson, 2006):

$$I_f = I_b f_m f_s (1+\in) \quad (4.5)$$

Where: I_f = final impact factor

I_b = impact factor for the bridge

f_m = reduction factor for the vehicle mass

f_s = speed reduction factor for the vehicle

$\in$= coeficient of variation

The impact factor for the bridge depends on the nature of the bridge under construction. For a simply supported bridge having a span of L/m (Anderson, 2006):

$$I_b = \frac{3}{L} \quad (4.6)$$

For a simply continuous bridge with *n* span, each having a length of L/m, the bridge impact factor is given by:

$$I_b = \frac{4.5}{L\times\sqrt{n}} \quad (4.7)$$

A heavier vehicle will have a smaller impact effect than a lighter vehicle. This is because a heavier vehicle is less likely to 'bounce' and 'bouncing' of vehicles contribute to high impact factors. A mass reduction factor f_m is therefore used. For vehicles having a weight of less than 16 tonnes f_m is taken as 1. Otherwise, it is given by the following formula (Anderson, 2006):

$$f_m = 0.819(10^{0.436-0.0254T} + 0.15) \quad (4.8)$$

Where T = the weight in tonnes

The faster the heavy vehicle is travelling, the higher will be its impact. Also the 'bouncing' of the vehicle will be higher. The equation below relates the vehicle speed V (in km/h) and the impact factor.

$$f_s = \left(\frac{V}{80}\right)^{0.75} \quad (4.9)$$

4.6 The New Zealand Method

In this method, the impact factor, *I*, is applied to the total live load such that:

$$I = 1 + \frac{15}{L+38} \quad (4.10)$$

Where L is the length of the span.

The impact factor cannot be greater than 1.3 (Ministry of Work and Development, 1976).

4.7 The Italian Method

The impact factor for spans less than 100m is given by the following equation:

$$k = 1 + \frac{(100-L)^2}{100(250-L)} \quad (4.11)$$

Where k = the impact factor; L= distance between the bearings for the main bridge members and the effective span for the slabs and beams (Ministry of Public Works, Italy 1962)

4.8 AASHTO Impact factors for horizontally curved steel box bridges

The dynamic impact factor of horizontally curved steel box bridges is presented as a function of the span length, the radius of curvature and the first fundamental frequency of the bridge (D.R.Scheling, 1992). This study assumes that a vehicle can idealised as two forces acting on a radial line, acting normal to the bridge's deck and travelling at a constant speed on two circumferential path, 6 feet apart. This approach ignores the mass of the vehicle. The following formulas have been developed for the impact factors for moment on horizontally curved bridges.

$$I_{mr} = 0.32 \qquad for\ R \leq 800ft \quad (4.12)$$

$$I_{mr} = \frac{0.34-R}{40000} \quad for\ 800ft < R \leq 4000ft \quad (4.13)$$

$$I_{mr} = 0.24 \qquad for\ 4000ft < R \leq 12000 \quad (4.14)$$

I_{mr} refers to the dynamic factor for moment as a function of the radius of curvature R in feet. The results of the impact analysis for moment, torque, shear, reaction and deflection are given as

function of the fundamental natural frequency. The linear functions that define the upper bound values of impact for each parameter are summarised as follows (D.R.Scheling, 1992):

$$I_{mf} = 0.225 + 0.0314f_1 \quad (4.15)$$

$$I_{Tf} = 0.225 + 0.0157f_1 \quad (4.16)$$

$$I_{Sf} = 0.165 + 0.0157f_1 \quad (4.17)$$

$$I_{Rf} = 0.200 + 0.0239f_1 \quad (4.18)$$

$$I_{Df} = 0.240 + 0.0063f_1 \quad (4.19)$$

Where $I_{mf,}I_{Tf,}I_{Sf,}I_{Rf,}I_{Df}$ refer to the dynamic impact factors as functions of the fundamental frequency f_1 for moment, torque, shear, reaction and deflection respectively.

4.9 OHBDC Impact factors for horizontally curved steel box bridges

The Ontario Highway Bridge Design Code (OHBDC) for dynamic load allowance is not specifically applicable to curved box-girder bridges, but it is relevant because impact is a function of the fundamental frequency of the bridge (D.R.Scheling, 1992). The equations for the moment impact factor (I_{mf}) for different fundamental natural frequencies (f_1) are as follows:

$$I_{mf} = 0.250 \qquad for\ 0 < f_1 \leq 1.0\ \text{Hz} \quad (4.20)$$

$$I_{mf} = \frac{0.150+f_1}{10} \quad for\ 1.0 < f_1 \leq 2.5\ \text{Hz} \quad (4.21)$$

$$I_{mf} = 0.400 \qquad for\ 2.5 < f_1 \leq 4.5\ \text{Hz} \quad (4.22)$$

$$I_{mf} = \frac{0.850-f_1}{10} \quad for\ 4.5 < f_1 \leq 6.0\ \text{Hz} \quad (4.23)$$

$$I_{mf} = 0.250 \qquad for\ 6.0 < f_1 \quad (4.24)$$

4.10 Impact factors for composite concrete-steel cellular straight bridges

Composite concrete-steel cellular bridges are widely used on highways throughout the world. Their main features are that they are lighter, have shallower depth of cross section, have significant longitudinal bending stiffness and have torsional stiffness to resist eccentric load when compared to open section bridges (X.Zhang, 2003).

In this study, abnormal vehicles were idealized as a pair of concentrated forces, with no mass, travelling across the bridge. Expressions for the dynamic impact factors for moment, reaction and deflection have developed in terms of the fundamental frequency of the bridge. These expressions are compared to those from Ontario Highway Bridge Design Code and the Canadian Highway Bridge Design Code in Figure 4.3, 4.4 and 4.5. These equations represent the upper bound envelopes drawn to define the results.

The equation for the moment (I_M) and deflection impact factor are as follows:

$$I_M = 0.15 - \frac{f}{60} \quad for\ f < 2Hz \qquad I_M = 0.12 \quad for\ f \geq 2Hz \tag{4.25}$$

$$I_D = 0.20 - \frac{f}{30} \quad for\ f < 3Hz \qquad I_D = 0.10 \quad for\ f \geq 3Hz \tag{4.26}$$

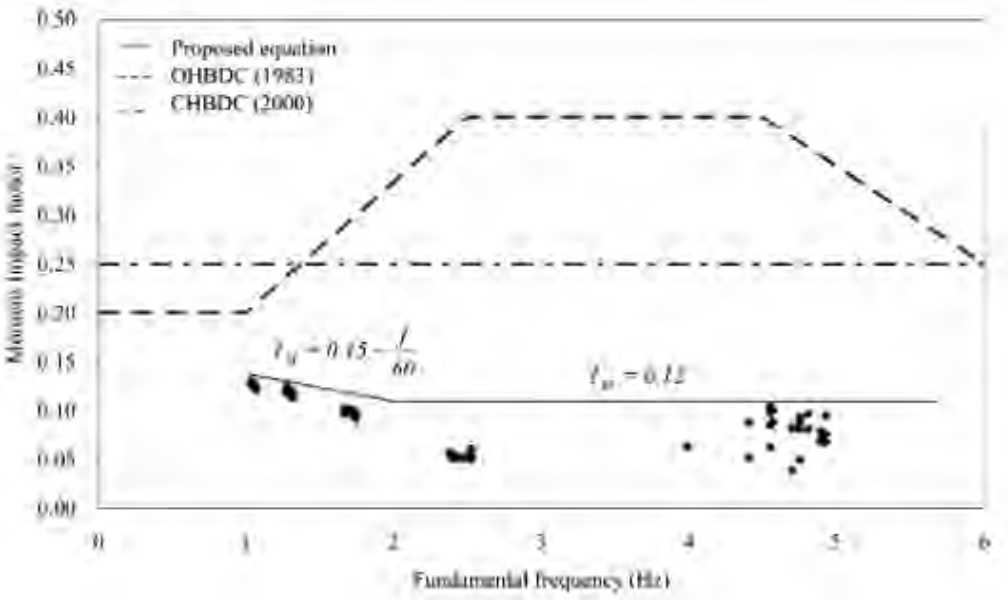

Figure 4.3: *Moment impact factor versus fundamental frequency (X.Zhang, 2003)*

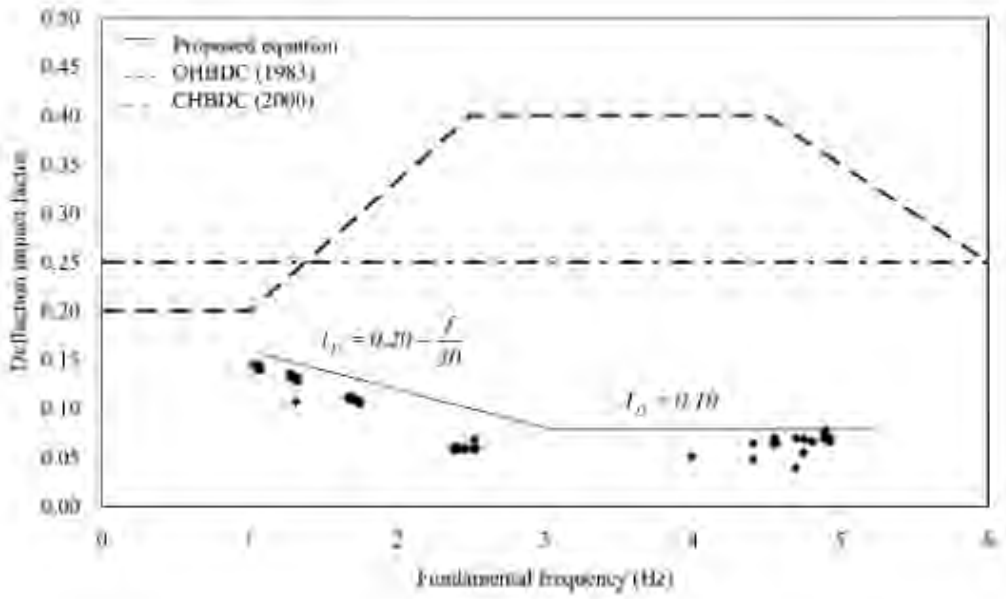

Figure 4.4: *Deflection impact factor versus frequency (X.Zhang, 2003)*

Figure 4.3 and 4.4 show that the impact factors for both moment and deflection from the study are significantly smaller than those from the codes. This may be due to the high torsional stiffness and excellent load distribution characteristics associated with cellular structures. It can be said that the impact factors established by the codes are very conservative.

The equation for the Reaction impact factor is as follows:

$$I_R = 0.60 \ for\ f < 1.5\ Hz \quad I_R = 0.80 - \frac{f}{7} \ for\ 1.5 < f < 3.5Hz \quad I_R = 0.35 \ for\ f \geq 2Hz \qquad (4.27)$$

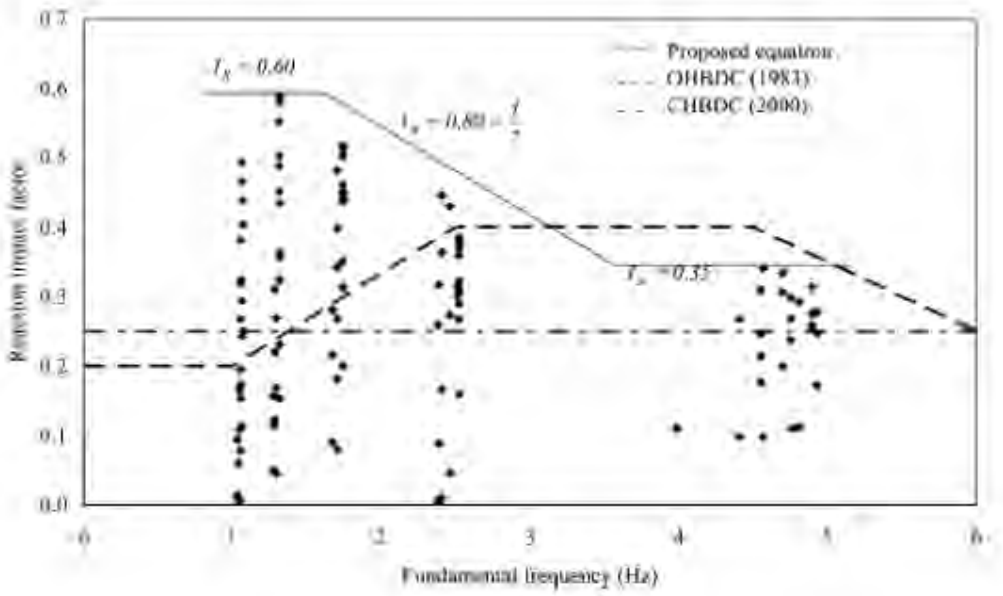

Figure 4.5: *Reaction impact factor versus fundamental frequency (X.Zhang, 2003)*

The impact factors are also expressed in terms of the bridge span. The formulas are given below:

$$I_M = 0.12 + \frac{L}{4000} \quad for\ L > 60m \qquad I_M = 0.12 \quad for\ L \leq 60m \tag{4.28}$$

$$I_D = 0.10 + \frac{L}{1810} \quad for\ L > 40m \qquad I_D = 0.12 \quad for\ L \leq 40m \tag{4.29}$$

$$I_R = 0.30 + \frac{L}{270} \quad for\ L < 80m \qquad I_R = 1 - \frac{L}{200} \quad for\ L \leq 60m \tag{4.30}$$

4.11 Impact factors for horizontally curved composite box girder bridges

These types of bridges are very popular nowadays, especially in urban areas where multilevel interchange structures are used. Horizontally curved composite box girder bridges are light weight, have shallow depth, and significant longitudinal bending stiffness. The cross section of such bridges is favored for its considerable torsional stiffness to resist the applied loads (X.Zhang, 2003). This study follows the same principle as the one described in Section 4.10 except that the impact factors are given in terms of the span to radius of curvature ratio$\left(\frac{L}{R}\right)$.

$$I_M = 0.22 - \frac{0.03L}{R} \tag{4.31}$$

$$I_D = 0.15 \tag{4.32}$$

$$I_R = 0.68 - \frac{0.18L}{R} \tag{4.33}$$

Impact factors of curved bridges are influenced by the vehicle's speed. An increase in the truck speed increases the impact factors. Since the design speed increases with a decrease in bridge curvature, impact factors for bridge with low curvature are higher than those with high curvature (X.Zhang, 2003).

4.12 Methods of measuring the dynamic effects of bridges

4.12.1 Field measurements

Several experimental procedures are used to measure the dynamic load allowance. The techniques which are most frequently used are impact tests, use of eccentric or reactional mass exciters, use of normal traffic, wind generated (ambient) vibrations, sudden release of static load or imposed displacement and vibrations generated by braking vehicles. (Paultre, Chaallal, & Proulx, 1992).

Common data recorded from site are displacements, strains and accelerations. Displacement and strains are usually measured using LVDTs and strain gauges respectively while acceleration is measured using accelerometers.

Figure 4.6, 4.7 & 4.8 show the displacement, strain and acceleration data recorded for two trucks crossing a bridge at 80 km/h (Kwasniewski et al, 2006).

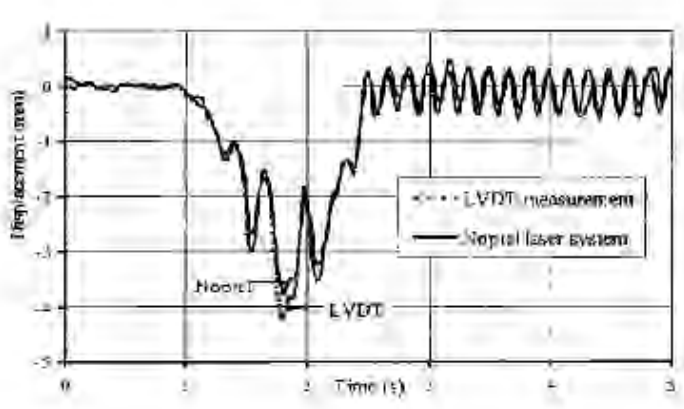

Figure 4.6: *Time history of displacement for two trucks crossing a bridge at 80 km/h (Kwasniewski et al, 2006)*

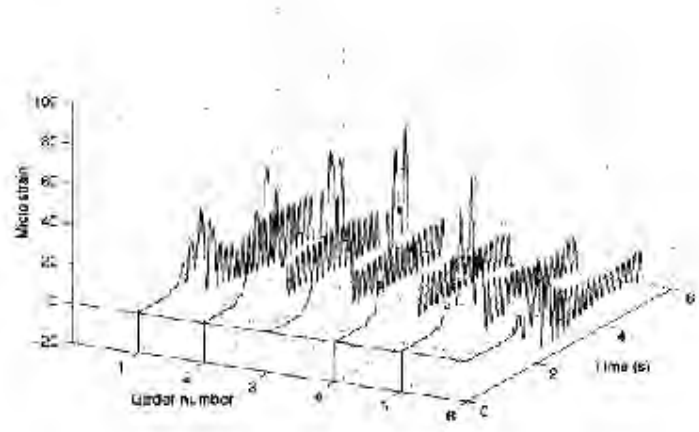

Figure 4.7: *Example of strain readings at the bottom of the girders (Kwasniewski et al, 2006)*

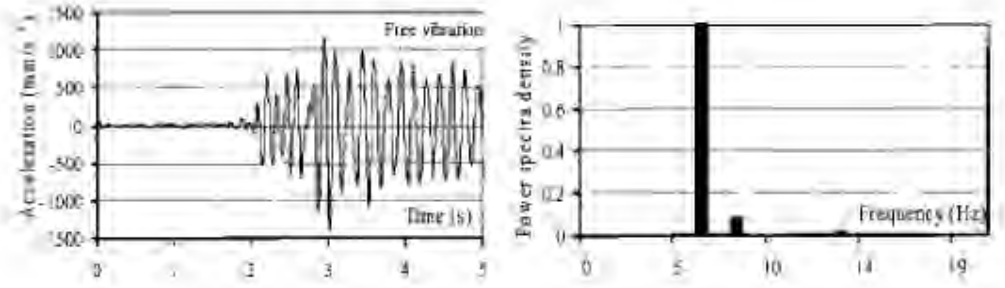

Figure 4.8: *Acceleration history and power spectra density (Kwasniewski et al, 2006)*

Kwasniewski et al, 2006 also confirmed that the static strains corresponding to two trucks match well with the sum of readings for loadings of a single truck.

4.12.2 Finite element modelling

The main purpose of a finite element (FE) analysis is to help in the interpretation of experimental results and to determine the sources of high impact factors. The common FE packages used for bridge analysis are ABAQUS, ADINA, Nastran and LS-DYNA. Both the bridge and the vehicle can be modelled using these softwares. A typical finite element model of a bridge and truck is shown in Figure 4.9.

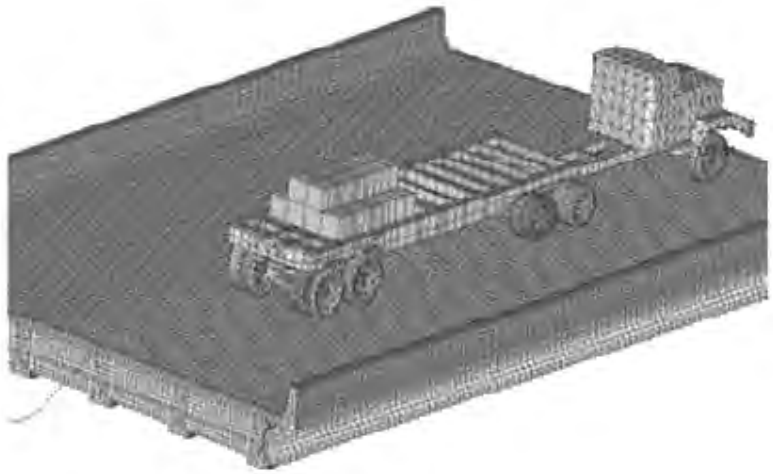

Figure 4.9: *Finite-element models of tested truck and bridge system (Kwasniewski et al, 2006)*

The dynamic test results are obtained from the accelerometers and are used to calibrate the finite element model. The natural frequencies are recognised as the abscissas corresponding to the peak values of the power spectra density and they are calculated using the discrete Fourier transform (Kwasniewski et al, 2006). The FE model can be compared with the test reslts for deflection, moment and reaction forces.

In several dynamic impact studies, vehicles have been modelled as a pair of concentrated forces moving along a deck with no mass. This is because the weight ratio of the design vehicle and that of the bridge is less or equal to 0.3 (X.Zhang, 2003). The vehicle is assumed to move smoothly with no slippage at constant velocity and being in constant contact with the bridge at all times.

The dynamic interaction of the wheels and suspension system with the bridge can also be modelled. Figure 4.10 show two different models of the interaction.

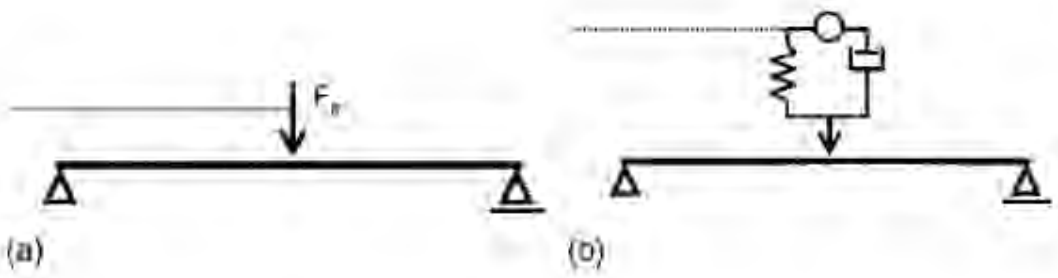

Figure 4.10: *Interaction models of truck wheels and bridge deck surface: (a) pure dynamic motion of concentrated force over perfectly straight bridge beam; (b) model includes mass, spring, and damper (Kwasniewski et al, 2006)*

The first model has a negligible dynamic effect on the bridge response since even the highest practical vehicle velocities are much lower than the theoretical values of critical velocities that can cause extensive vibrations (Kwasniewski et al, 2006).

Figure 4.10 (b) models the vehicle suspension system and is commonly used to describe the dynamic response of individual truck axles or wheels.

Even though FE modelling is less expensive and allow for faster introduction of new design improvements and maintenance decisions, actual field tests are still the most reliable source of information. They are the only way of validating the finite element model.

4.13 Chapter summary

The impact factors have been developed for abnormal vehicles in general. None of the literature focuses on the impact mobile cranes on bridges. As mentioned in Chapter 4, even though mobile cranes form part of abnormal vehicles, they have different suspension systems and axle configurations. Therefore a study of the impact caused by the suspension system is required to fill in the gaps.

Dynamic testing is important since they provide an evaluation of the dynamic properties (frequency, damping, stiffness) of the structure. They are also useful in quantifying the extent and rate of degradations of bridges. The main parameters which contribute to the dynamic impact factors are span length, number of lanes, radius of curvature, surface roughness, suspension system and speed, positioning and weight of the vehicle(s) on the bridge. These parameters can be expressed in terms of dynamic impact factors for longitudinal moment,

reaction and deflection of the bridge. The impact factors are also different for the different types of bridges investigated.

Finite element modelling is very useful way of simulating the effect of abnormal vehicles on bridges. The bridge and the vehicle can be modeled as a finite element mesh and a pair of concentrated forces respectively. The suspension system of the vehicle can also be modeled by a mass, spring and damper.

5. SUSPENSION SYSTEMS

As mentioned in Chapter 4, suspension systems are one of the parameter which influences the impact on bridges. A suspension system usually consists of springs, shock absorbers and linkages that connect a vehicle to its wheel. The main purpose of a suspension system is to absorb part of the shock when the vehicle hit a bump, allowing the tires and axle to move independently and ensuring that the vehicle occupants are comfortable and reasonably well isolated from road noises and vibrations. Springs that are too hard and too soft cause the suspension to become ineffective. Therefore tuning of the suspension system is critical. Suspensions springs are always used in combination with a damper. The energy that has been temporarily stored in the spring is converted into heat by the damper thereby decaying the amplitude of oscillation.

If a truck's axle is attached directly to the frame, without any type of suspension springs, the driver would feel every crack in the road since nothing would be in place to absorb the impact. In fact, he would not be able to control the vehicle because its tires would bounce off the ground whenever it hits a bump (Wickell, 2002).

The European Community drop test defines a "road friendly" suspension as one which has a natural frequency of less than f = 2Hz and a damping coefficient greater than ς = 20%. The suspension systems which are commonly used are as follows:

5.1 Leaf spring

A leaf spring suspension system is made up of arched pieces of steel that are made to flex when the truck hit a bump or when a load is applied to the vehicle but with an ability to return to its original shape. One end of the leaf spring is attached to the frame and the other end to a shackle that can move, allowing the spring's overall length to vary as its arch flexes (Wickell, 2002).

Figure 5.1*: Leaf spring suspension system (http://en.wikipedia.org/wiki/Leaf_spring)*

For heavy vehicles, a leaf spring is made from several leaves stacked on top of each other often with progressively longer leaves as shown in figure 5.1. This type of suspension systems is generally used for trucks, 4x4 and military vehicles.

5.2 MacPherson

MacPherson suspension is mostly used in small cars due to its simplicity and low manufacturing cost. It uses the axis of a telescopic damper as the upper steering pivot.

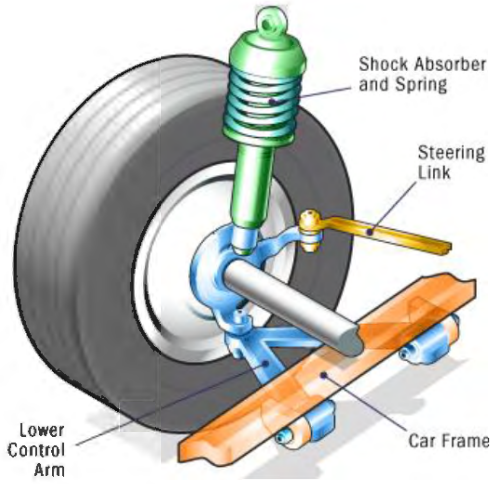

Figure 5.2: *MacPherson suspension system (http://auto.howstuffworks.com/car-suspension4.htm)*

This suspension system has a few drawbacks which makes it difficult to implement in trucks. It does not allow vertical movement of the wheel without some degree of either camber angle change, sideways movement or both (Setright L.J.K, 1974). It also tends to transmit noise and vibration from the road to the vehicle's body making it uncomfortable to drive.

5.3 Air suspension

Air suspension is a type of vehicle suspension which is powered by the engine or an electric air pump. The pump pressurises the air, using compressed air as a spring. It is a recent technology and provides a softer ride compared to vehicles having coil springs or leaf suspension system.

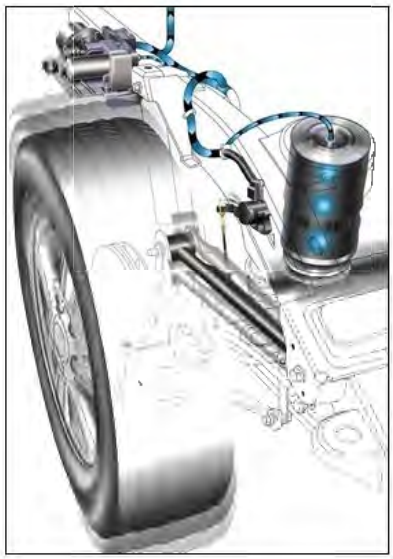

Figure 5.3: *Air suspension system (www.autobasicslibrary.blogsome.com)*

This type of suspension system is expensive but it is efficient when used on heavy vehicles due to its self levelling characteristic when travelling on different road conditions. It can be modelled by the following deflection equation:

$$Fair = Fstat\left[1 - \frac{Ax}{V^0}\right]^{1.38} \quad (6.1)$$

Where *F*air = force in spring; *F*stat = static suspension force; A= cross sectional area of spring; V_0= static volume of spring; x= deflection of spring (Green, Cebon, & Cole, 1995).

5.4 Hydro-pneumatic

Hydro-pneumatic suspension systems represent a new generation in suspension design. A hydro-pneumatic suspension system includes hydraulic struts selectively interconnected to obviate the need for shock absorbers and springs used in conventional abnormal load vehicles. The spring of such a system is represented by suspension cylinders with varying oil level. The suspension cylinder also performs as a damper in a hydro-pneumatic system. Whenever there is a change in operating conditions, the degradations in the suspension is detected by an electronic controller

which in turns adjust the spring stiffness to re-improve the ride. The system hydraulic supply is capable of raising and lowering the vehicle for off and on road conditions (Wolfgang, 2010).

Hydro-pneumatic suspensions have the ability to adjust their suspension stiffness (spring rate) by varying the force on the suspension cylinder and allowing oil to flow in and out. This leads to a change in hydraulic pressure and therefore a change in position of the piston rod. An increase in spring rate makes the ride smoother due to reduced vibrations. This type of suspension is dependent on the actual operating temperatures. Higher temperatures cause the spring to soften while lower temperatures make it stiffer. The following equations lead to the relationship between the natural frequency of the suspension system and the static spring load:

$$\omega = \sqrt{(\frac{c}{m_F})} \tag{6.2}$$

$$\omega = 2\pi f \tag{6.3}$$

$$F_{F1} = m_F g \tag{6.4}$$

$$c = n\frac{F_{F1}{}^2}{P_0 V_0} \tag{6.5}$$

$$f = \frac{1}{2\pi}\sqrt{\frac{nF_{F1}g}{P_0 V_0}} \tag{6.6}$$

Where: m_F- static spring load, *f*-suspension frequency, P_0- accumulator precharge pressure, V_0- accumulator volume and *c*- stiffness

Equation 6.4 shows that the stiffness is dependent on the static spring load and also the pressure and volume of the accumulator. The natural frequency of the suspension changes proportionally with the square root of the static spring load (Wolfgang, 2010). Hydro-pneumatic suspensions are able to absorb excitation frequencies from below 1 Hz to sometimes over 10 Hz.

Figure 5.4*: Hydro-pneumatic suspension system*

Hydro-pneumatic suspension systems are used especially in applications where:

a. A level control needs to work frequently and needs to react quickly. All the vehicle's suspensions are independent of each other which make it efficient when used on rough terrains. Figure 5.5 shows a separate hydro-pneumatic spring for an axle.

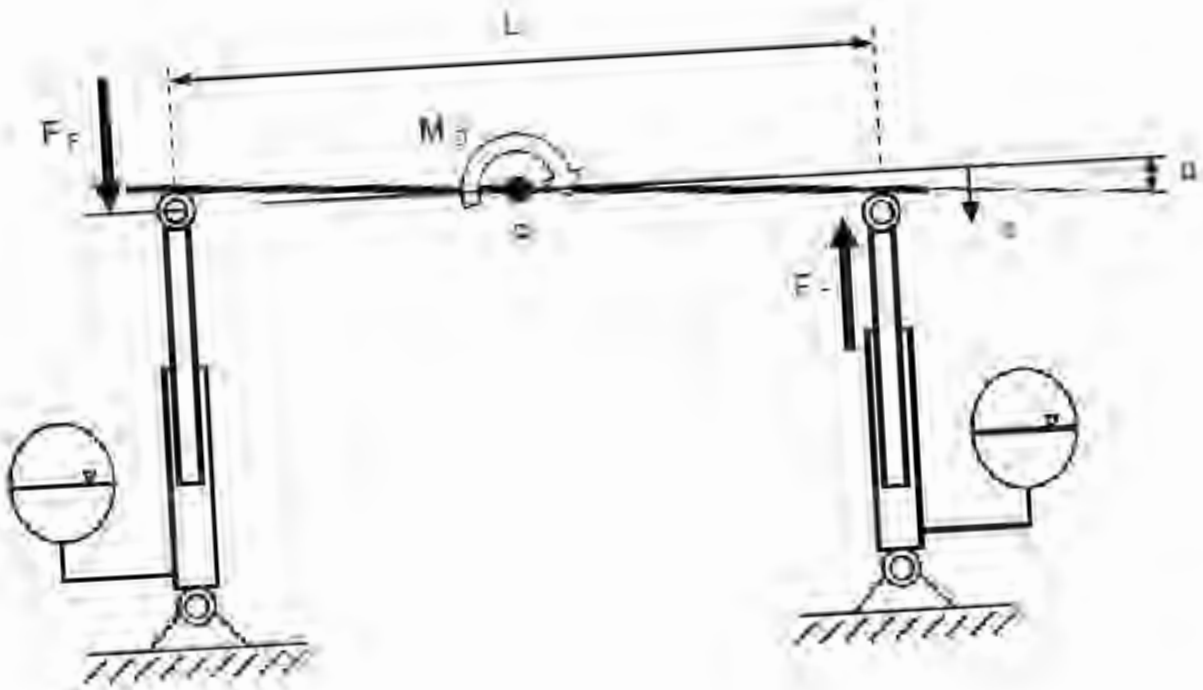

Figure 5.5: *Independant hydro-pneumatic springs (Wolfgang, 2010)*

b. Little space is available for suspension elements.
c. The spring rate needs to be adjustable.

This type of suspension system is commonly used for construction machinery/trucks, mobile cranes, tanks, agricultural vehicles, mining and heavy load trucks.

Figure 5.6 shows the relationship between the axle stiffness, the suspended axle load and the vertical natural frequency of the front axle of a TLS tractor. The graph indicates that a vertical natural frequency of about 2 Hz is achieved for most of the range of the suspended axle load.

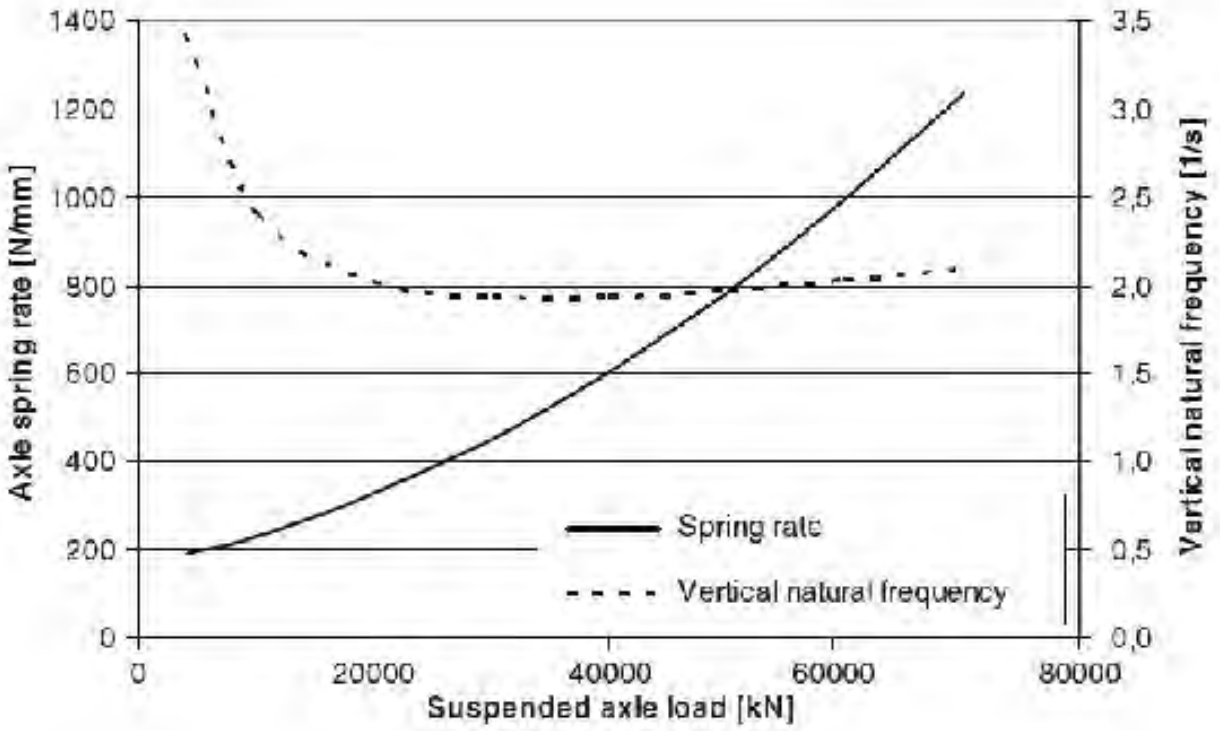

Figure 5.6: *Axle spring rate and vertical natural frequency of a TLS I (Wolfgang, 2010)*

5.5 Effects of the different suspension system

The most obvious difference between the suspensions is their response under loading. While the spring rate of the mechanical spring (coil and leaf spring) is constant, the spring rate for the hydro-pneumatic and air suspension is more or less progressive as shown in Figure 5.7.

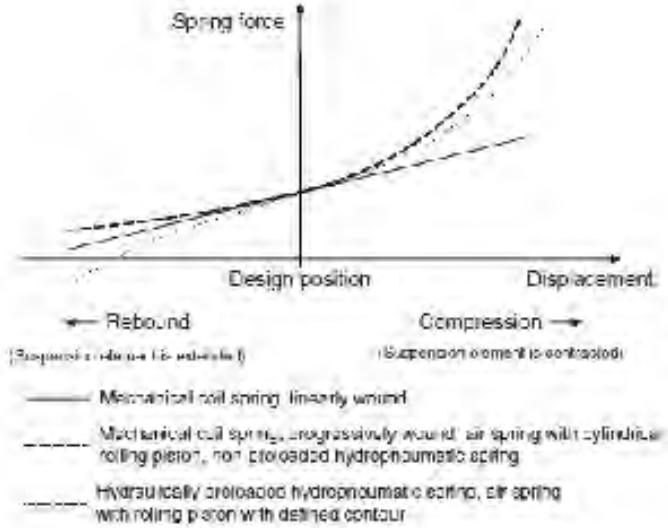

Figure 5.7: *Force-displacement-curves for mechanical and gas-sprung systems (Wolfgang, 2010)*

Heywood (2007) investigated the bridge response under three different types of suspension systems. These were:

a. A hydro-pneumatically suspended crane
b. An air-suspended six axle articulated vehicle and
c. A steel-suspended six axle articulated vehicle (mechanical system)

It was found that the dynamic effects induced by the hydro-pneumatically suspended crane are about 1/3 of those caused by conventional mechanically sprung commercial vehicle. In these suspensions, hydraulic rams act as suspension and equalising elements and by varying the oil content and gas pressure in the accumulators, the suspension characteristics can be varied to suit the road condition (Heywood, 1997). It is also reported that hydro-pneumatic suspensions could be expected to perform on a par, if not better, than air suspended vehicles for most bridges.

The air suspensions provide a relatively low stiffness and therefore a relatively low bounce frequency for a given axle load. They also offer a smooth and progressive deflection compared to steel suspensions (leaf and coil springs) which causes a sudden deflection under load (Directorate for Science, 1998). Steel suspension systems have high natural frequency at low loads and a low frequency at high loads.

Green and Cebon (1995) investigated the impact caused by air suspensions and leaf-sprung vehicles on three bridges in England. Their study showed that the vehicle with the air suspension causes the least dynamic bridge response. This is mainly because the air suspension system has a lower natural frequency than the leaf suspension thereby applying smaller dynamic load to the bridge. The air suspensions are also better damped than the leaf-spring suspensions and hence absorb energy from the bridge vibration (Green, Cebon, & Cole, 1995).

5.6 Chapter Summary

Hydro-pneumatic suspensions usually operate independent of each other and therefore they may have different spring rates and damping depending on the terrain they are travelling on. Based on the theoretical analysis, there is tentative evidence suggesting that vehicles having air and hydro-pneumatic suspensions should be allowed to carry more load than vehicles having leaf spring

suspensions. However, more theoretical and experimental work is needed before this suggestion can be extended to apply to all bridges and heavy vehicles.

6. METHODOLOGY

6.1 Introduction

The most economical way of investigating the vehicle-bridge interaction is to use finite element modeling. The Finite Element Model which has been used for this thesis is ADINA. This research focuses on the interaction of a mobile crane with a bridge. The dynamic impact caused during this interaction has been analysed and compared with field measurements which has been performed at a later stage.

In Chapter 6, a review of the parameters influencing the impact factors have discussed. The main parameters are the span length of the bridge, number of lanes, radius of curvature, surface roughness, vehicle braking, suspension system and speed, positioning and weight of the vehicle(s) on the bridge. Previous studies have been done and calibrated for abnormal vehicles. Even though mobile cranes are considered as abnormal vehicles, they have different axle's configurations and suspension systems when compared to trucks. This research studies the impact caused by the hydro-pneumatic suspension of a mobile crane under different loading, speed, bridge span length and surface roughness.

Most of the bridges in South Africa are short span bridges. The research simulates the interaction of mobile cranes with bridges spanning between 5 and 40m. Bridges have been modeled based on the criteria specified by the MOT design code of practice. This is because 70% of bridges in South Africa have been designed using this code.

Field testing involved measuring strains, displacements and natural frequency of the Berg River Bridge under the effect of a mobile crane for different scenarios. All results were captured and analysed using the commercial softwares Lab VIEW and ME'Scope Ves respectively.

Validation of the strains and displacement were then done by comparing the experimental results to the Finite Element Model results.

6.2 Vehicle-bridge interaction model

The vehicle-bridge interaction system has been modeled in Adina as a mass-spring-damper system crossing a beam. The case of a single vehicle crossing a simply supported bridge is modeled as a point force crossing a simply supported beam at a constant velocity. It is assumed

that the wheels of the mobile crane remain in contact with the bridge at all times. The vehicle bridge interaction is modeled using the Bernoulli-Euler differential equation.

$$EJ\frac{\partial^4 \upsilon(x,t)}{\partial x^4} + \mu\frac{\partial^2 \upsilon(x,t)}{\partial t^2} + 2\mu\omega_b\frac{\partial \upsilon(x,t)}{\partial t} = \delta(x-ct)P \quad (6.1)$$

Where E= elastic modulus; t= time at which the force arrive on the beam; $\upsilon(x,t)$= beam vertical deflection at point *x* and time t, measured from the equilibrium position when the beam is loaded with its self weight only; J= second moment of area; μ= mass per meter; ω_b= circular frequency of damping of the beam; P= concentrated force of constant magnitude; $\delta(x)$= Dirac function; and c=constant velocity of the load (Li, OBrien, & Gonzalez, 2006).

Adina is a Finite Element software which is commonly used for applications where reliability is of critical importance. The analysis can be linear or highly non linear, including effects of material nonlinearities, large deformations and contact conditions (http://www.adina.com/index.shtml). Previous studies have confirmed that Adina is capable of simulating such the vehicle-bridge interaction model.

6.3 Bridge model

For this research, short span bridges have been modeled as beam elements. The bridges have single, double and triple span decks having lengths of 10m, 15m, 20m, 30m and 40m.

A number of three dimensional beam elements have been defined in Adina to make the mesh finer. These elements were then meshed to define a beam. The mesh size used is 1m. Table 6.1 gives the number of beam elements and element length for the respective bridge spans.

Table 6.1: Number of beam elements and element length defined for the respective beam length

Beam Length (m)	Number of beam Elements	Element Length (m)
10	10	1
15	15	1
20	20	1
25	25	1
30	30	1
40	40	1

The beams are simply supported on a pin and roller support. For the two and three spans bridges, the beam is continuous over the middle supports. The pin support is fixed for the x,y and z translation and the x-rotation. The roller support is fixed for the y and z translations and x-rotation.

Figure 6.1 shows a 10m single span bridge having 10 elements and which is simply supported at P1 and roller supported at P11. P12 is a reference point which is used to define the directions.

Figure 6.1: *10m single span bridge modelled in Adina*

The beam has been defined as an isotropic linear elastic material having an elastic modulus of $35x10^9$ N/m² and a density of 2400 Kg/m³. The moment of inertia (J) of the beam cross section is 1.3901m^4. These values have been used in previous studies done by E. Obrien.

6.4 Vehicle model

6.4.1 Mobile crane data

The mobile crane has been modeled using data obtained from the Liebherr mobile cranes website (http://www.liebherr.com). Liebherr is a German manufacturer and their cranes are widely used in South Africa and the rest of the world. They manufacture mobile cranes having an operational weight between 24 and 96 tonnes.

The axle weight limit in South Africa is 12 tonnes per axles. Vehicles having a gross weight greater than 50 tonnes are categorized as abnormal vehicles and require a permit to operate. Five models of cranes having the following details have been modeled in Adina:

Model 1

LTM1090-4.1 crane has 4-axles and an operational weight of 48 tonnes. It has a lifting capacity of about 90 tonnes. Its maximum travelling speed is 80km/hr. Table 6.2 gives the maximum weight that each axle can carry.

Table 6.2: *Maximum axle weight for LTM1090-4.1mobile crane*

Axle	1	2	3	4	**Total**
Weight (T)	12	12	12	12	48

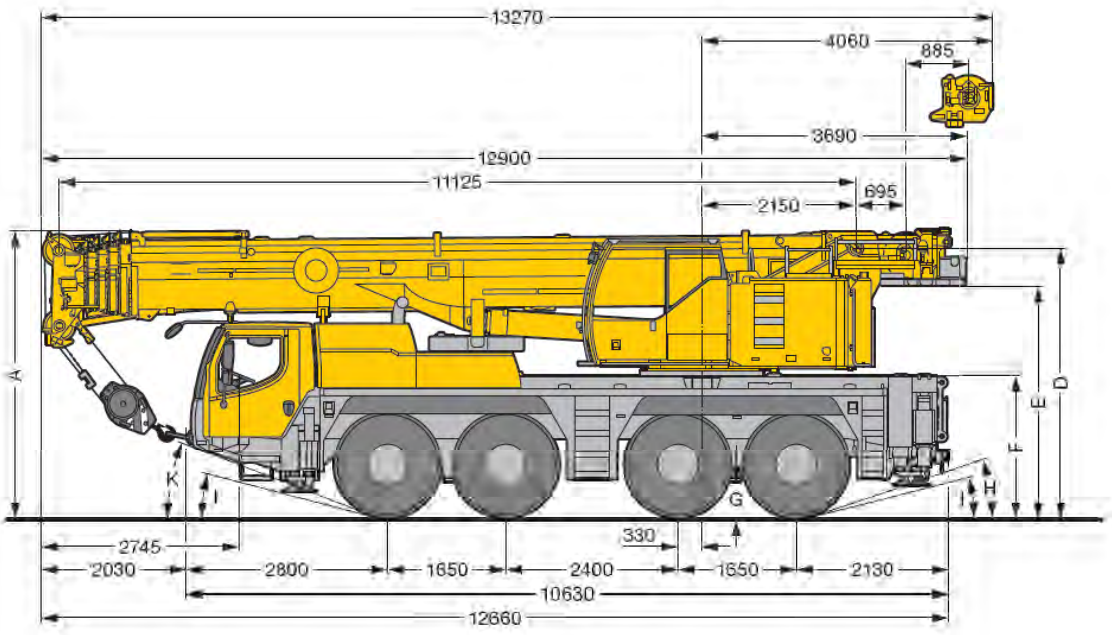

Figure 6.2: *Axle spacing for the LTM1090-4.1 mobile crane*

Model 2

The LTM 1130-5.1 crane has 5 axles and has an operational weight of 60 tonnes. It has a length of 14.4 m and its maximum operational speed is 80km/hr. This type of crane can lift up to 130 tonnes provided it has a counterweight of 42 tonnes. Table 6.3 gives the maximum weight that each axle can carry.

Table 6.3: *Maximum axle weight for LTM 1130-5.1mobile crane*

Axle	1	2	3	4	5	Total
Weight (T)	12	12	12	12	12	60

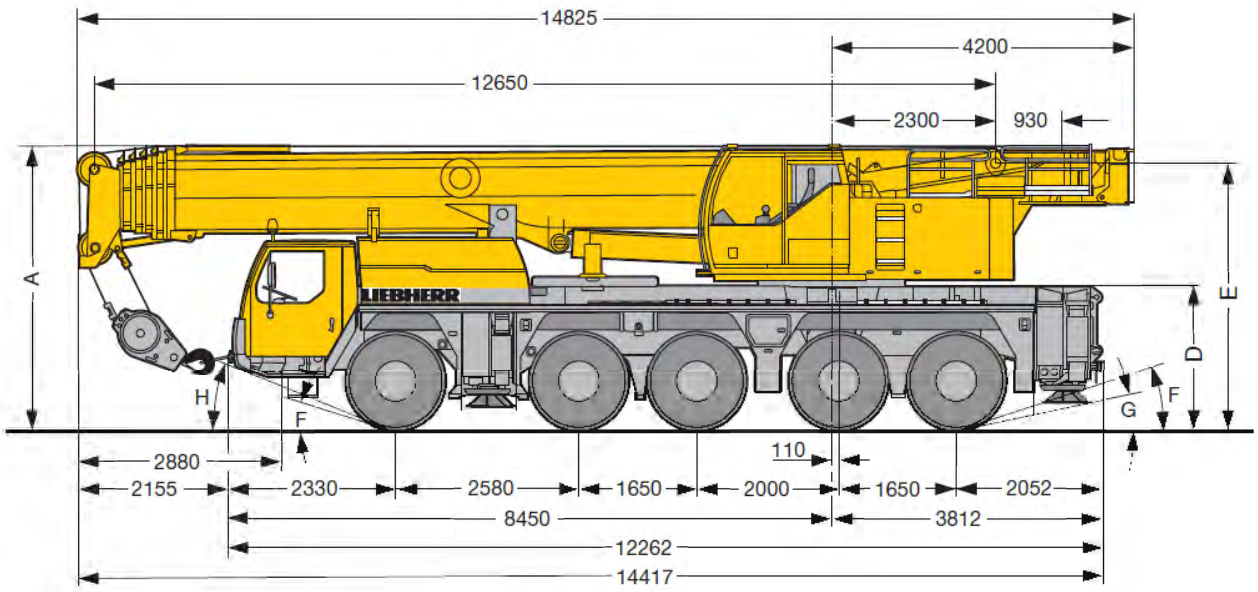

Figure 6.3: *Axle spacing for LTM 1130-5.1 mobile crane*

Model 3

The LTM 1150-6.1 crane has 6 axles and has an operational weight of 72 tonnes. It has a length of 16.08 m and its maximum operational speed is 80km/hr. This type of crane can lift up to 160 tonnes provided it has a counterweight of 46.8 tonnes. Table 6.4 gives the maximum weight that each axle can carry.

Table 6.4: *Maximum axle weight for LTM 1150-6.1mobile crane*

Axle	1	2	3	4	5	6	Total
Weight (T)	12	12	12	12	12	12	72

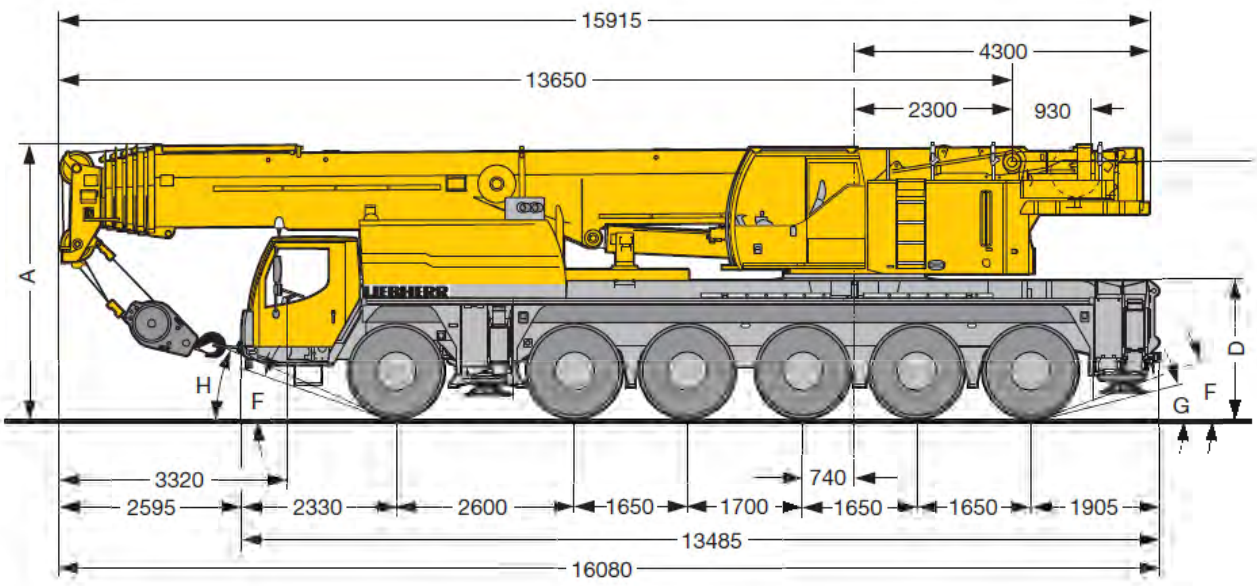

Figure 6.4: *Axle spacing for LTM1150-6.1 mobile crane*

Model 4

The LTM 1400-7.1 crane has 7 axles and has an operational weight of 84 tonnes. It has a length of 18.45 m and its maximum operational speed is 80km/hr. This type of crane can lift up to 400 tonnes provided it has a counterweight of 140 tonnes. Table 6.5 gives the maximum weight that each axle can carry.

Table 6.5: *Maximum axle weight for LTM 1400-5.1mobile crane*

Axle	1	2	3	4	5	6	7	**Total**
Weight (T)	12	12	12	12	12	12	12	84

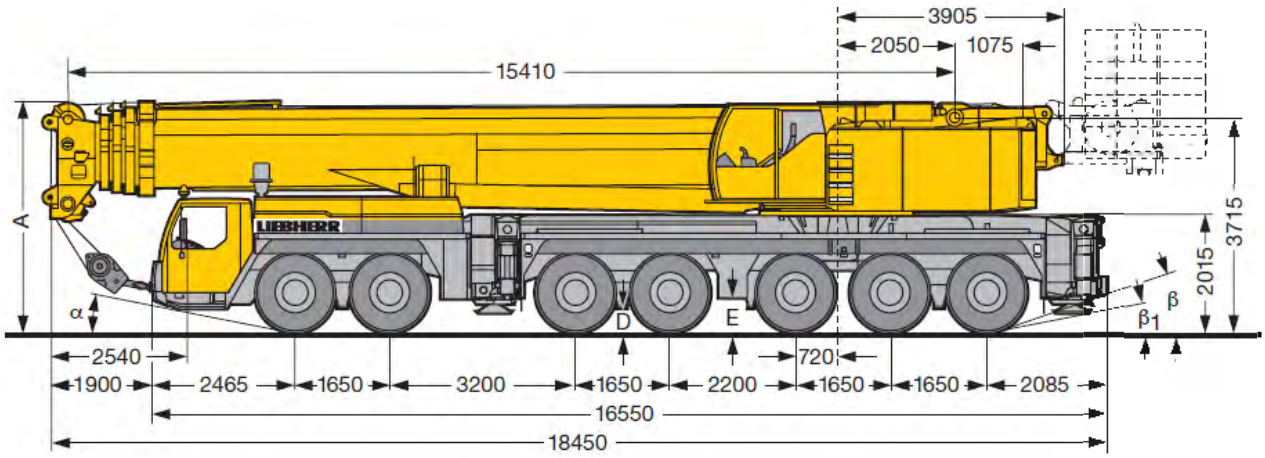

Figure 6.5: *Axle spacing for LTM 1400-5.1 mobile crane*

Model 5

The LTM 1500-8.1 crane has 8 axles and has an operational weight of 96 tonnes. It has a length of 20.48 m and its maximum operational speed is 80km/hr. This type of crane can lift up to 500 tonnes provided it has a counterweight of 165 tonnes. Table 6.6 gives the maximum weight that each axle can carry.

Table 6.6: *Maximum axle weight for LTM 1500-8.1mobile crane*

Axle	1	2	3	4	5	6	7	8	**Total**
Weight (T)	12	12	12	12	12	12	12	12	96

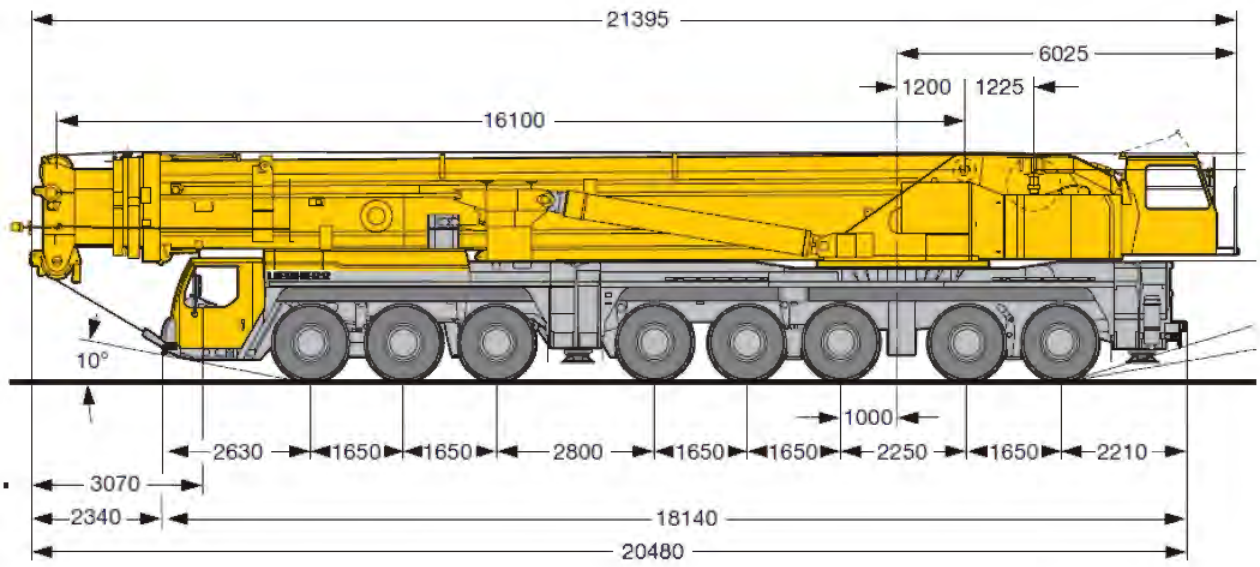

Figure 6.6: *Axle spacing forLTM 1500-8.1 mobile crane*

Model 6

The LTM 11200-9.1 crane has 9 axles and an operational weight of 108 tonnes. It has a length of 24.98 m and its maximum operational speed is 75km/hr. This type of crane can lift up to 1200 tonnes provided it has a counterweight of 202 tonnes. Table 6.7 gives the maximum weight that each axle can carry.

Table 6.7: *Maximum axle weight for LTM 11200-9.1mobile crane*

Axle	1	2	3	4	5	6	7	8	9	**Total**
Weight (T)	12	12	12	12	12	12	12	12	12	108

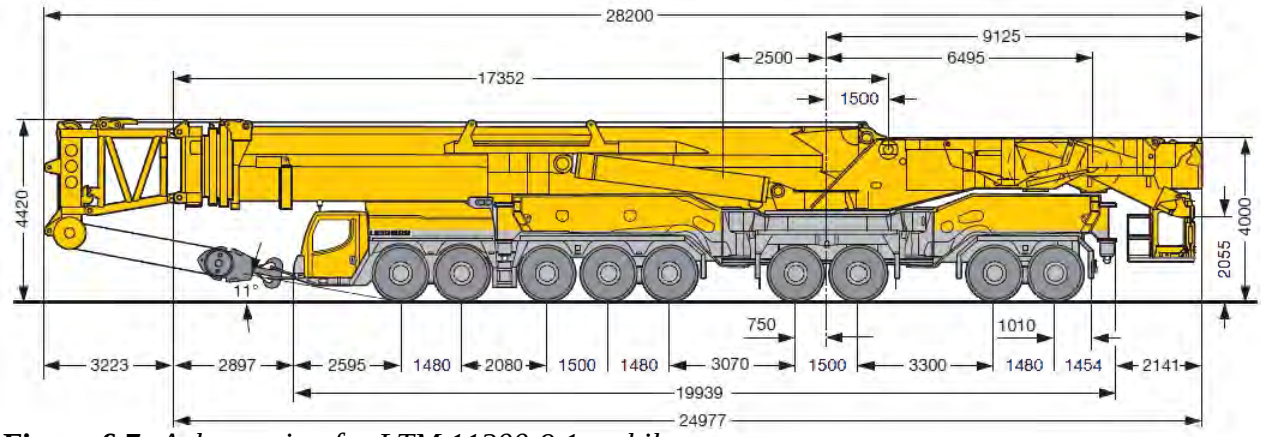

Figure 6.7: *Axle spacing for LTM 11200-9.1 mobile crane*

6.4.2 Finite element model

Each axle of the mobile crane has been modeled as a single degree of freedom system (SDOF) in Adina. Figure 6.8 shows the modeled system.

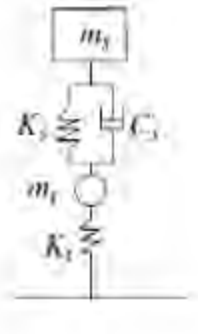

Figure 6.8: *Single degree of freedom system representing the axle of a mobile crane*

Where *ms*= Axle weight; K*s*= Suspension stiffness; C*s*= damping coefficient of suspension system; *mt*= tire weight; K*t*= Tyre stiffness

The motion of the mobile crane has been represented by the following equation:

$$Ma+Cv+Kx = F \quad (6.2)$$

Where M= mass of vehicle; C= damping of the vehicle; K= stiffness of the vehicle; a= acceleration of the vehicle; v= velocity of the moving vehicle; x= displacement of the SDOF system.

6.4.3 Axle weight

The weight of each axle has been represented by a point load which moves along the beam elements. Each axle has been defined using a different load number. The direction in which the load acts has been specified.

The motion of the axles is defined by the load arrival time function in Adina. The time at which an axle arrives at any point defined on the beam is calculated manually and input in the finite element software.

The time function defines how the load varies with time. For this study, a triangular load has been chosen with a time step 1000. The motion of each axle is represented by a triangular load in Figure 6.10. The first axle of the mobile crane enters the bridge at point 1. As the load approaches point 2, the dynamic effect due to the load increases and as it moves away from point

2, the effect decreases. This cycle repeats itself for each beam element until the vehicle leaves the bridge.

Figure 6.9: *Triangular load moving along the beam*

Overlapping of the triangular occurs because the minimum distance between the axles is 1.65m and the beam element length is 1m.

6.4.4 Stiffness and damping of the hydro-pneumatic suspension

The spring rate and damping of the suspension system is modeled using the spring element group in Adina. A spring element joins each node on the beam and a birth and death time is defined for each element. An element is born when the 1st axle arrives at a node and dies when the last element leaves the node. The stiffness and damping is defined for each element.

The stiffness of the system consists of the suspension spring rate and the tyres stiffness. Equation 10.3 has been used to calculate the effective stiffness.

$$\frac{1}{k_{eff}} = \frac{1}{k_s} + \frac{1}{k_t} \qquad (6.3)$$

Where k_{eff}= Effective stiffness; k_s = Suspension stiffness; k_t=Tyre stiffness

Values for the suspension spring rate and damping and tyre stiffness have been obtained from studies done by Eugene OBrian (Li, OBrien, & Gonzalez, 2006).

The vehicle speed has been modeled using the load arrival time function. The speed at which an axle reaches a node can be varied by changing the load arrival time. The mobile cranes listed in Section 71.1 have been modeled travelling on the bridge at speed of 10km/hr (crawl speed), 30km/hr, 50km/hr and 80km/hr. The maximum speed at which the mobile cranes can travel is 80km/hr (http://www.liebherr.com).

6.5 Surface roughness

The surface roughness of bridges depends on the quality of asphalt and concrete used and also on the frequency of maintenance.

In the finite element model, the surface roughness has been modeled by varying the suspension stiffness and damping of the mobile crane. It has been assumed that the spring rate and damping will be different when the vehicle is travelling on a rough terrain compared to smoother surface.

6.6 Impact factors

The impact factor for this research is defined as the maximum response of the bridge while the mobile crane is travelling on it divided by the maximum response when the vehicle is static on the bridge. Equation 7.4 is used to calculate the impact factor.

$$Im = \frac{R_D - R_S}{Rs}.100\% \quad (6.4)$$

Where R_D = dynamic response; and R_s = static response

The dynamic and static responses for the shear, deflection and moment have been obtained from analysis done in Adina.

6.7 Field Measurements

The main objective of this research was to perform dynamic testing on a bridge while a mobile crane is travelling on it under various speeds and scenarios. Strain measurements and displacements were measured using strain gauges and LVDTs respectively. The experimental results obtained were then analysed and compared to the Finite Element Model.

The Western Province Department of Transport and Public works was contacted since they are the one who manage the bridges in the Cape Town. The bridges that were requested had to be located in an area where there is not much traffic during the day since closure of the structure would be needed. Three bridges were kindly provided and two of them namely B5031 across the Sand River and B5032 across Bot River were located along the R304 road going towards Malmesbury. The third bridge was the Berg River Bridge which spans along the Berg River close to Wellington. All the three bridges have been designed to carry abnormal loads.

Figure 6.10: *Bridge (B5031) across Sand River*

Figure 6.11: *Bridge (B5032) across Bot River*

A site visit was done to inspect the accessibility to the bottom of the bridges since the transducer devices had to be fixed under the deck or beams. There was no vehicular access to the bottom of Bridge 5031 and 5032 which would make it difficult to carry the field testing equipment. These

two rivers were also at full flow which would make it difficult and dangerous to fix the strain gauges and LVDTs. Therefore B5031 and B5032 were not considered.

One of the spans of the Berg River Bridge was accessible and the mid-span height between the beams and the ground was about 2.5m. Therefore a small ladder could be used to fix the transducers to beams. There is no river under this span and hence the data collecting system could be easily set up. A description of this bridge is given in Section 7.7.1.

6.7.1 Berg River Bridge

The Berg River Bridge is located on the R44 road going towards Wellington in Western Cape Province, South Africa. The bridge is busy throughout the day and is used by both normal and abnormal vehicles. It was constructed in 1974 and is a twelve-span bridge carrying two opposite lanes traffic. One of the spans crosses the Berg River.

The total length of the bridge is 336m with each span measuring 28m long and 13.4m wide. Figure 6.12 shows the span which has been used for the dynamic tests.

Figure 6.12: *Berg River Bridge*

Each span consists of eight simply supported beams which are 1.7 apart. The mid-span height of the tested span is 3.5m. An initial survey of the structure indicated that it was in good condition to undergo dynamic tests. There were no visible cracks on the structure.

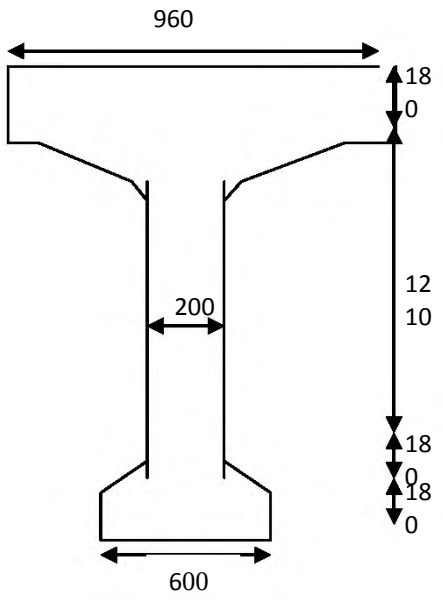

Figure 6.13: *Beam cross section*

6.7.2 Mobile Crane

A 36 tonnes 3-axles Grove GMK 3055 crane was kindly provided by Tandem Cranes for the purpose of this research. Tandem Crane Hire is a crane hire company and is very active in the Western Cape Province South Africa.

Figure 6.14*: 3-axles Mobile crane*

Each axle supports 12 tonnes which is the legal axle load in South Africa. The maximum lifting capacity of the crane is 63 tonnes. The crane can travel at a maximum of 80 km/hr. The length and width of the crane are 10.895m and 2.550m respectively.

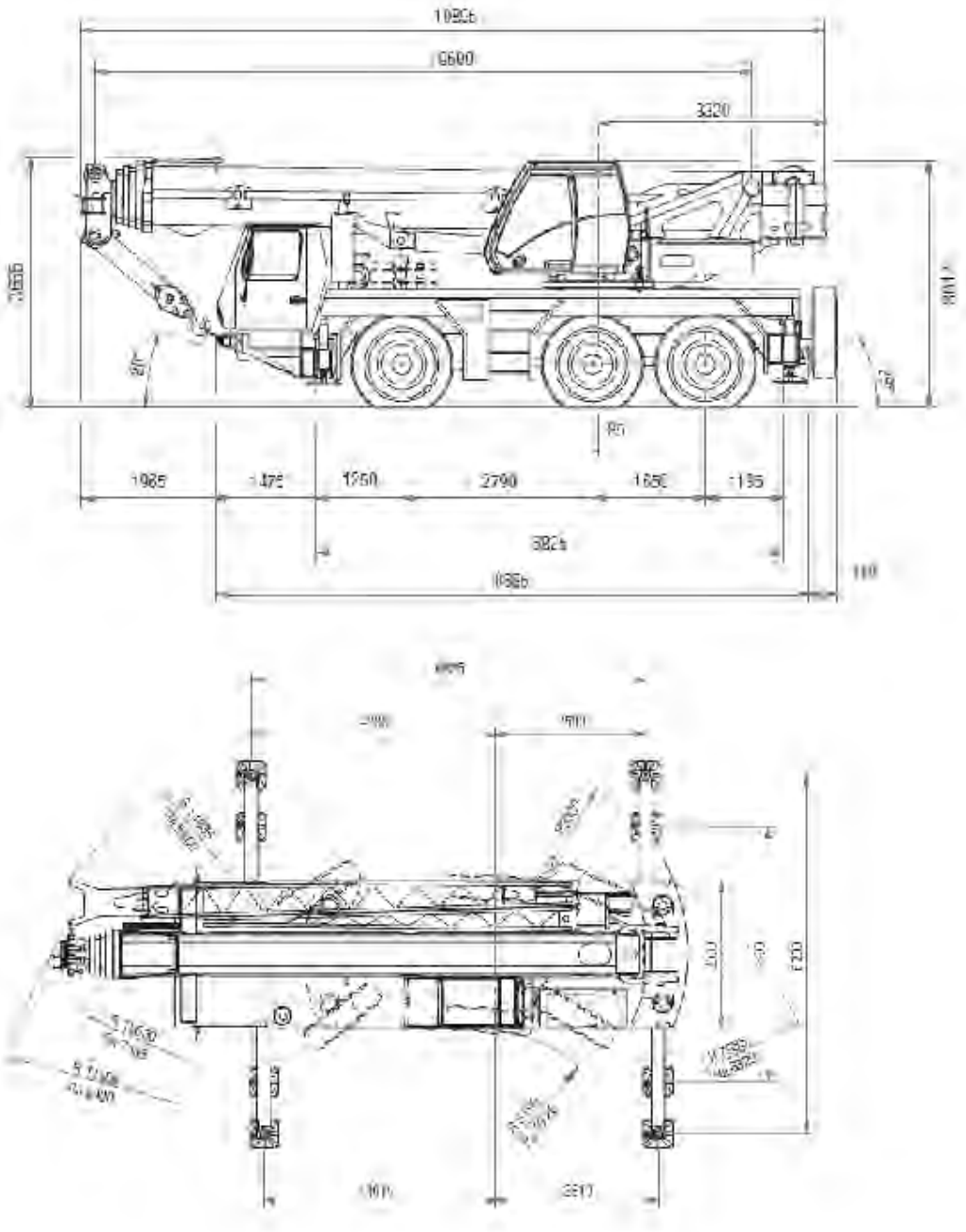

Figure 6.15: *36 tons mobile crane dimensions*

6.7.3 Field test equipment

The equipment used are two strain gauges, two LVDTs, an accelerometer and a data acquisition system. The strain gauge and LVDT are transducers and need to be calibrated before they are

used. This is because the measured values are in terms of voltage and need to be translated to strain, displacement and accelerations.

Transducers are used with lead lengths and these tend to affect signal quality due to their resistance and capacitance variation. Transducers also pick up noise which tends to affect the quality of the measured data. Unfortunately, this cannot be prevented in practice.

Strain gauge

The SLB700A strain transducer has been manufactured by Dehnungsaufnehmer and was used to measure static and dynamic strains when fixed to the beam upon which the mobile crane is travelling. The strain gauge is de-mountable and is calibrated using the four-wire technology whereby:

Blue- excitation voltage (+); Black- Excitation voltage (-); White- Measurement signal (+); Red- Measurement signal (-)

The main specifications of the strain gauge are: (1) Nominal strain of 500μm/m, (2) Nominal sensitivity of 1.5±0.15 mV/V, (3) Restoring force of 3110 N and (3) Input resistance of 1000Ω.

Figure 6.16: *Strain gauge*

LVDT

Linear Variable Differential Tranformers (LVDT) was used to the measure linear displacement of the bridge in response to the impact caused by the mobile crane. The LVDTs used have the following characteristics: (1) Sensitivity of 34.14 mV/V/mm with 5V (RMS) 5kHz, (2) Uncertainty of calibration of 13microns.

Figure 6.17: *LVDT manufactured by RDP*

Accelerometer

A Piezotronic accelerometer having a sensitivity 0.1107 V/m/s² was used for the tests to measure the accelerations of the bridge.

Figure 6.18: *Piezotronic accelerometer*

Data acquisition system

The data acquisition system consisted of the following: (1) A computer having the National Instrument Lab VIEW software installed, (2) A signal conditioner to capture the accelerations, (3) National Instruments input module to record measurements from the strain gauge and LVDT.

Figure 6.19: *Data acquisition system*

Figure 6.20: *National Instrument input module hardware*

The NISCX1-1540 card is an 8-channel linear-voltage transformer module which has been used to capture signals from the LVDT.

Strains measurements have been recorded using the NISCXI-1520 card which also has 8 input channels.

Figure 6.21: *Kistler Signal Conditioner*

All measurements were taken by a data acquisition system hardware manufactured by National Instruments and using the National instrument Lab VIEW software. Lab VIEW Signal Express optimizes virtual instrumentation by providing interactive measurements that require no programming. It has been used to acquire, generate, analyse and compare data samples before exporting them into ASCII files in Universal File Format.

6.7.4 Experimental procedure

The dynamic testing was performed on 5th October 2011. Two holes were drilled under on the 2nd beam at mid-span and quarter span respectively. Glue was applied to both strain gauges before they were tightly screwed to the beam.

The two LVDTs were each mounted on an adjustable aluminium rod which was fixed to a heavy steel stand to prevent them from swaying. The rods were extended until the LVDT slightly displaces by touching the beam. One of the LVDT was placed at mid-span and the other one at quarter span. Mid-span was chosen because this is usually where bridges displace the most. Deflection is zero at the support and maximum in the middle of the span.

The two strain gauges were then connected to the 1st and 2nd channel of the NISCXI-1520 card. The LVDTs were connected to the channels of the NISCX1-1540 card . Both cards were then plugged in the National Instrument hardware.

The accelerometer was connected to the Kistler Signal Conditioner and placed at mid-span on the side of the bridge. The Signal Conditioner and the National Instrument hardware were then

connected to the computer which had the Lab VIEW software installed. The channels to which the strain gauges and LVDTs were connected were then added to Lab VIEW. These devices were then calibrated. 512 samples were recorded at a sample rate of 64Hz for both devices.

The strain gauge resistance was set to 1000Ω to match the resistors used in the NISCXI-1520 card. A full bridge system was used to capture the strains. The low pass filter frequency was set at 10Hz. The LVDTs were calibrated to the sensitivity which was prescribed by the manufacturer.

The whole bridge was closed to traffic during the duration of the test. This was done so that the maximum response caused by the mobile crane alone could be measured. The mobile crane driver was instructed to travel along a straight line so that its left wheels are straight above the instrumented beam. By doing this, the maximum impact on that particular beam could be recorded. The mobile crane travelled on the bridge at the following speed: crawl speed (5km/hr), 10, 20, 40, 60 and 75km/hr. 75km/hr was the maximum speed at which the mobile crane could travel.

Figure 6.22: *Mobile crane and bridge interaction*

In order to model a severely deteriorated road surface condition, three planks each having a thickness of 18mm were stacked on top of each other and placed in the middle of the span. The 36 tonnes mobile craned travelled over planks at a speed of 40km/hr.

Figure 6.23: *Planks used to model road surface deterioration*

The accelerometer was left on the bridge for about five minutes after the tests to measure the accelerations of the bridge under normal traffic conditions.

Measurements of all the scenarios were recorded in separate files. The Run function was used to activate the signals and the Stop function to stop Lab VIEW from recording.

6.8 Data processing

ME'scope VES software was used to process the field data. The software has a Fast Fourier Transform (FFT) and Inverse FFT option that is useful to analyse signals. Noise level and irrelevant measurements captured during the test were be filtered out using this software.

After the filtering process, the strain measurement and displacement were obtained for the period at which the mobile crane crossed the bridge. The natural frequency and damping of the bridge were also obtained. The software was also used to perform statistical analysis of the signals.

6.9 Data validation

The experimental results were then compared to the Finite element Model representing the interaction between the 36 tonnes mobile crane and the 28m span bridge. The bridge was modeled as being simply supported and having 56 elements of 0.5m each. The mobile crane was modeled using three moving point loads of 12 tonnes each. The speed mentioned in section 7.7.4 was modeled by varying the load arrival time.

The comparison of the experimental results to the theoretical results will be discussed in Chapter 7.

6.10 Chapter Summary

This chapter gives a detail explanation of the experimental and FE study done to measure the dynamic response of a bridge under a moving mobile crane. A critical step of this thesis was to produce a finite element model of the vehicle-bridge interaction. The model had to simulate static response and dynamic response in order to calculate the impact factors.

The main challenge in the modeling process has been simulating the spring rate and damping of the hydraupheumatic suspension system. This is because this type of suspension system adjusts itself depending on the road condition. The experimental work has modeled a deteriorated road condition by getting the vehicle to travel on a pile of planks thereby causing an impact on the bridge.

The field tests involved measuring strains and displacement of the bridge at mid-span and quarter span using strain gauges and LVDTs respectively. Experimental data were recorded using Lab VIEW software and analysed using ME'scope VES. The next chapter discusses the results of the experimental and FE model.

7. DISCUSSION OF RESULTS

7.1 Introduction

This chapter presents and discusses the results obtained from the field measurements and the Finite Element model.

The dynamic response of the Berg River Bridge was measured and analysed using the procedure explained in Chapter 7 using Lab VIEW and ME'scope VES. The parameters which were measured are deflection and strains.

The strain gauge which was fixed at mid-span did not respond during the test. The measurements obtained from this device were not considered for further analysis.

Field measurements have been used to calibrate the stiffness and damping of the mobile crane suspension system for the finite element model. The dynamic response for the FE model of the Berg River Bridge was then compared to field measurement.

Once the model calibration was done, it was used to analyse the impact caused by different vehicle weights travelling at different speeds on various span lengths.

7.2 Bridge natural frequency

The response of the bridge was measured using two LVDTs which were positioned at quarter and mid span and a strain gauge which was fixed at quarter span. Five hundred and twelve response readings were recorded at 64 Hz for each scenario. An accelerometer was also placed on the bridge deck to measure the bridge accelerations under normal traffic load. The response signal from the accelerometer with respect to time is shown in Figure 7.1.

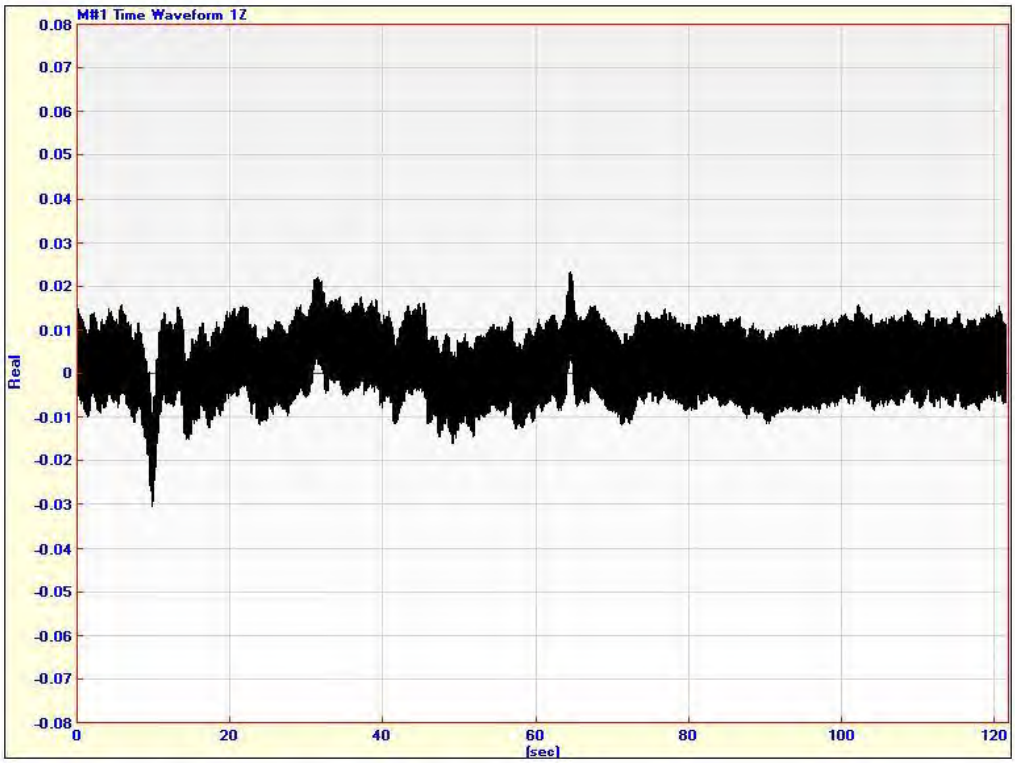

Figure 7.1: *Response time waveform signal*

The response under normal traffic load was measured for about two minutes. Direct current (DC) was removed from the measurement in ME'scope VES to offset the data to the zero axes. An automatic spectra analysis was then performed to obtain the natural vibration frequency of the bridge.

The measured natural frequency of the bridge is about 4.22 Hz. The first dominant frequency of the traffic loading during the test period is about 4.35 Hz. During the test period, the bridge was used by heavy abnormal vehicles and a few light vehicles. Most of these vehicles were travelling at a speed higher than 40 Km/hr. Both lanes were also opened to traffic. The Berg River Bridge is therefore not safe under normal traffic load since the natural frequency of the bridge is almost equal to the frequency of the bridge under the influence of traffic. This frequency matching leads to an important amplification of the dynamic response of the structure.

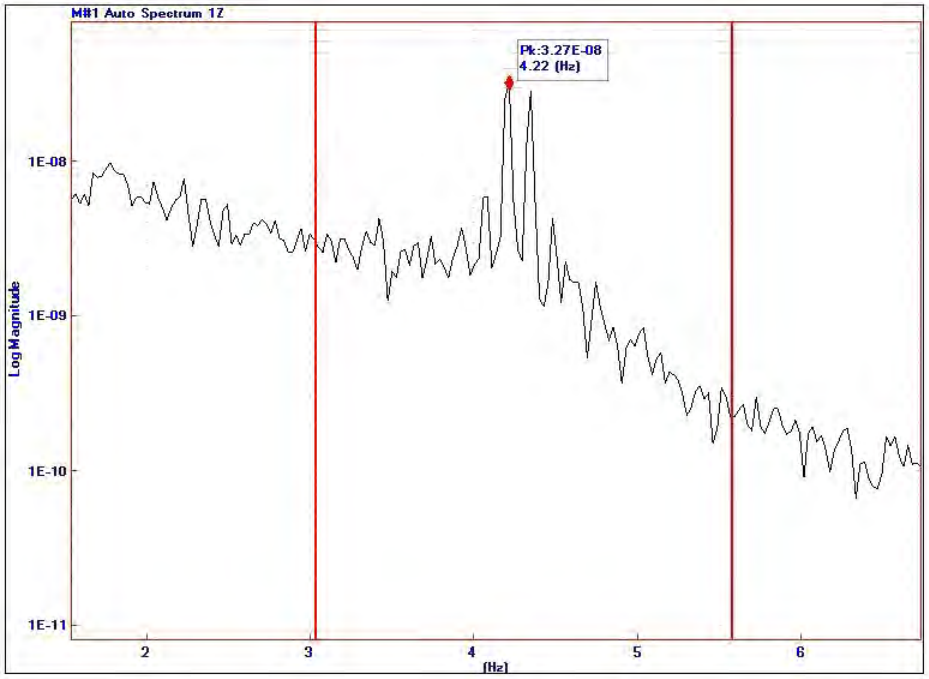

Figure 7.2: *Natural frequency of the Berg River Bridge measured from accelerometer*

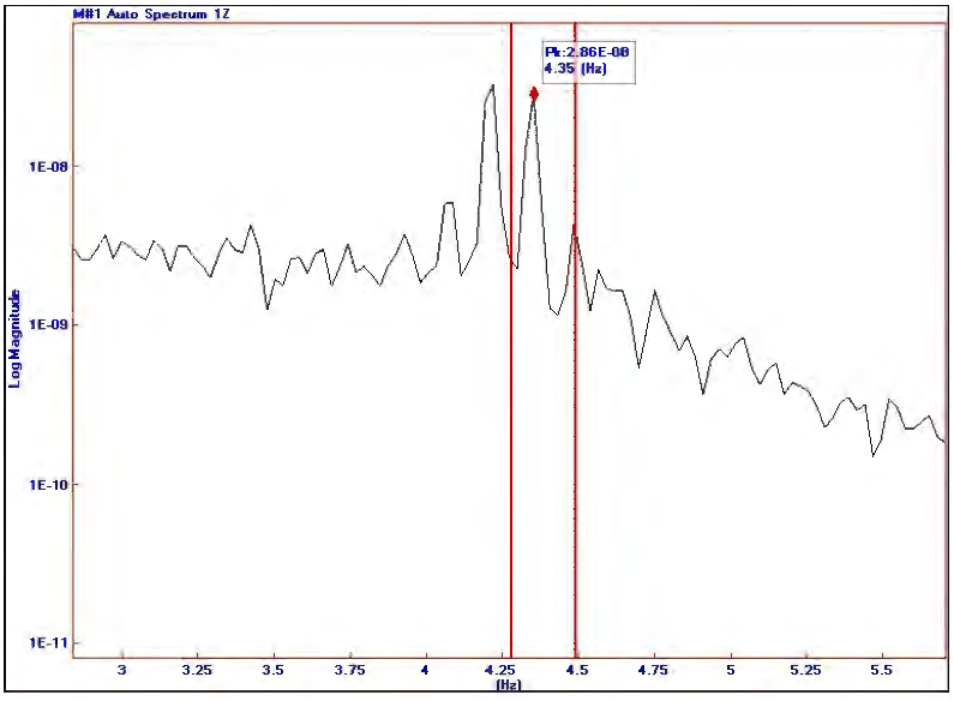

Figure 7.3*: First dominant frequency of normal traffic load*

The natural frequency for the bridge under the moving 36 tonnes mobile crane was measured using the LVDTs and strain gauge. The measurements obtained were analysed using ME'scope VES by carrying out a spectra analysis. The spectrum block size used is 237 with a number of averages of 14.

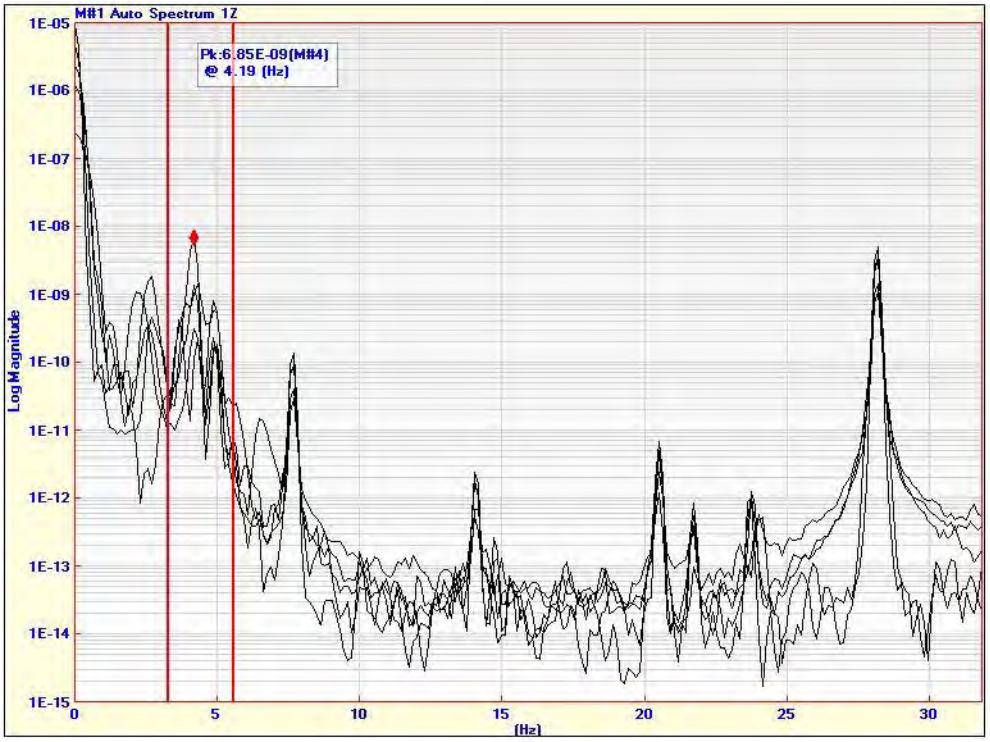

Figure 7.4: *Overlaid traces for speed 5, 10, 20, 40, 60, 75 km/hr at quarter span*

Figure 8.4 shows that the natural frequency of the Berg River Bridge is about 4.19 Hz. The frequency of the bridge under the moving load for speed between 5 Km/hr and 60Km/hr is about 2.7 Hz. This indicates that the 36 tonnes crane can travel safely on the bridge for speeds below 60 Km/hr.

From Chapter 5, it was found that heavy commercial vehicles exhibit two vibration modes: body-bounce vibrations at frequencies ranging from 2-5 Hz and wheel-hop vibrations at frequencies which are greater than 7 Hz. From Figure 7.4 it is clear that when the mobile crane was travelling at speeds between 5 and 60 Km/hr, it was causing body-bounce vibrations to the bridge since the first dominant frequency occurs at about 2.7 Hz.

The frequency of the bridge at 75 Km/hr is about 3.3 Hz. The amplitude of vibration is higher at that speed. This causes to fatigue of the structure and leads to structural damage. This is the reason why speed limits are applied for bridges and heavy vehicles.

Figure 7.5 shows the dynamic vibrations caused when the mobile crane is travelling on a poor road surface which has been modeled by placing planks on the bridge. The frequency of the bridge under moving load is 4.87 Hz which higher than the fundamental frequency of the bridge. As a result, this frequency matching leads to an important amplification of the dynamic response. Consequently, this can lead to fatigue and deterioration of the bridge.

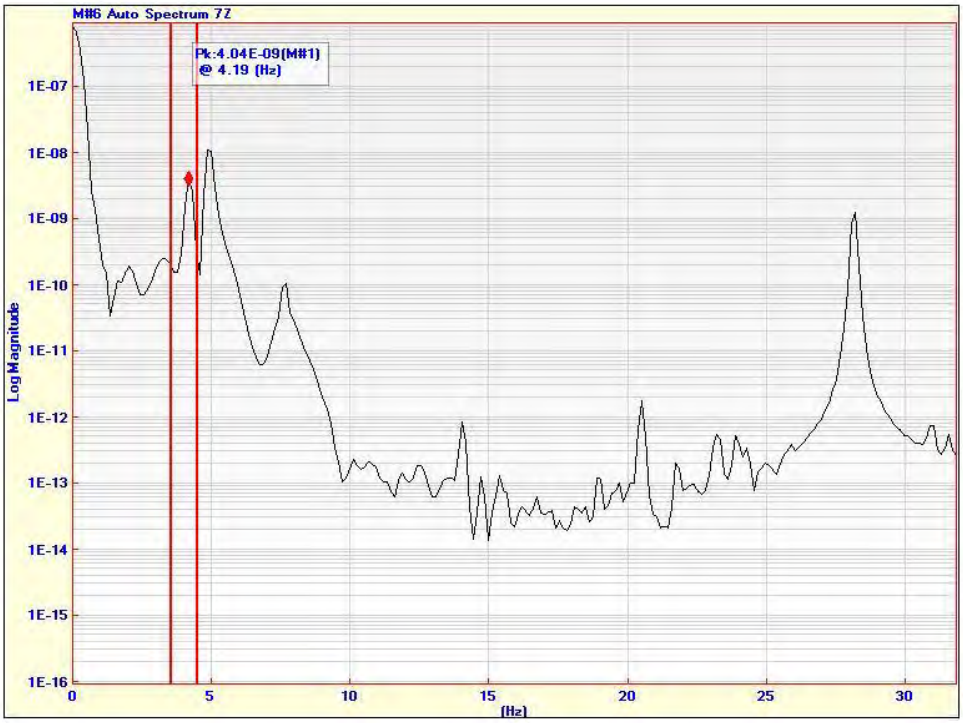

Figure 7.5: *Motion of mobile crane on a plank*

The natural vibration frequency of the bridge is calculated from equation 5.1 which has been explained in Chapter 5. For the 28m span length, the natural frequency of the Berg River Bridge is 4.08 Hz.

$$f^0 = 82Lmax^{-0.9} \quad (5.1)$$

The fundamental frequency obtained from the field measurements (4,22 from the accelerometer and 4.19 from the LVDT) is very close to the theoretical frequency which of 4.08 Hz. This confirms that the instrumentation was responding well during the experiment.

The frequency analysis shows that the safest speed that light vehicles can use the Berg River Bridge is about 50 Km/hr. For vehicle between 30 to 40 tonnes, a safe speed would be 20 Km/hr. For mobile cranes heavier than 55 tonnes, crawl speed would be the safest speed. The bridge should also be closed to normal traffic when abnormal loads are using the bridge.

7.3 Data Processing

7.3.1 Dynamic analysis

Signals were captured and saved from the strain gauge and LVDTs for each scenario using the LabVIEW software. The raw data was imported to ME'scope VES to be cleaned and analysed. Figure 7.6 shows measurements taken for a period of 70 seconds. The mobile crane arrived on the instrumented span after 45 seconds. Measurements recorded before that time is discarded as they do not affect the final result. Measurements triggered after 50 seconds are also neglected for the same reason.

The results are then offset to the zero axes. Figure 7.7 shows the dynamic response of the bridge and a clear indication of the noise level.

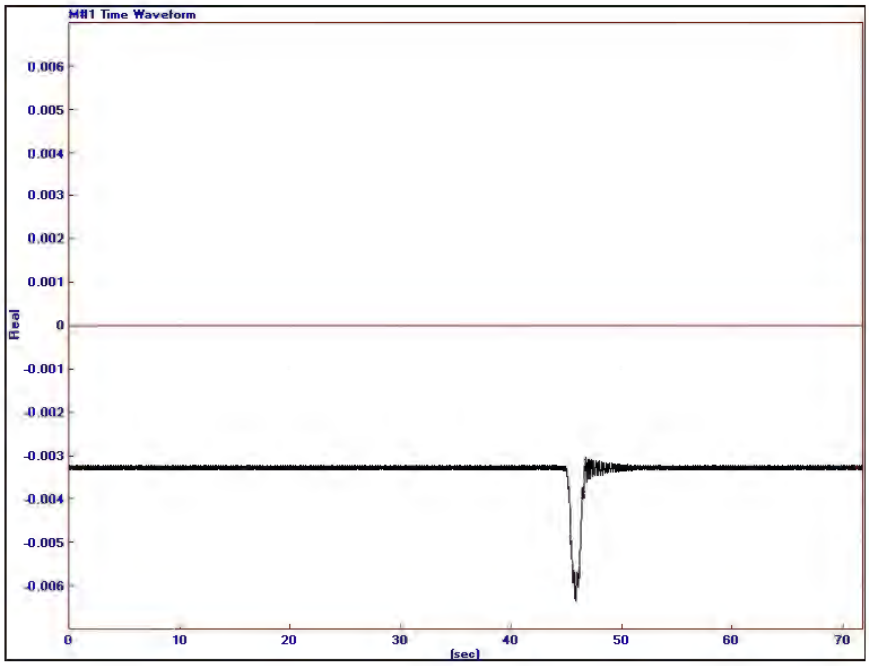

Figure 7.6: *Raw data from LVDT for 75 Km/hr scenario*

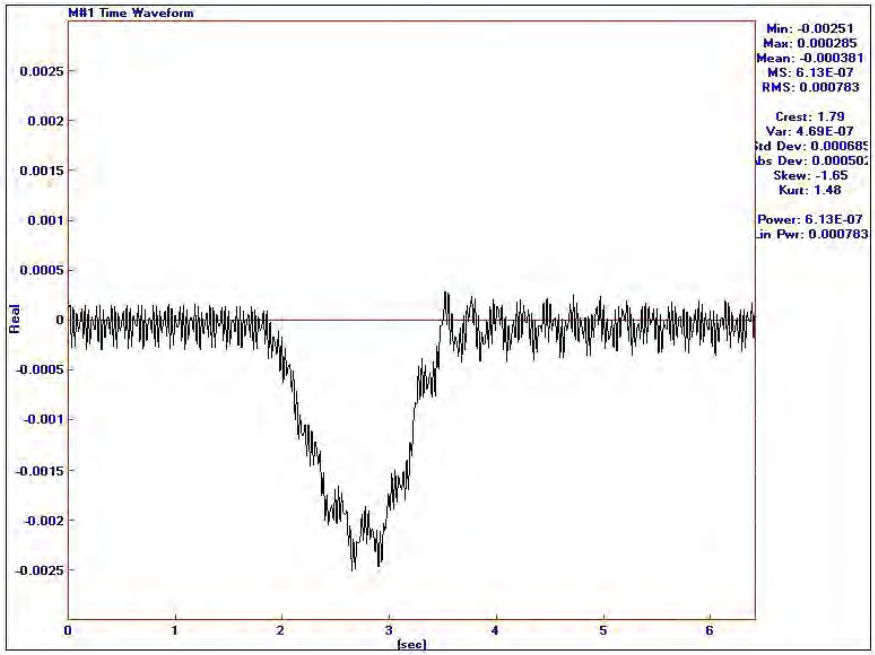

Figure 7.7: *Processed data from LVDT for 75 Km/hr scenario with noise*

The data is further processed by applying an FFT to remove all the noise. A notch is applied just after the fundamental frequency of the bridge for each scenario. All other dominant frequencies

which occur after the natural frequency are discarded. An inverse FFT is then done to get the graph in Figure 7.8.

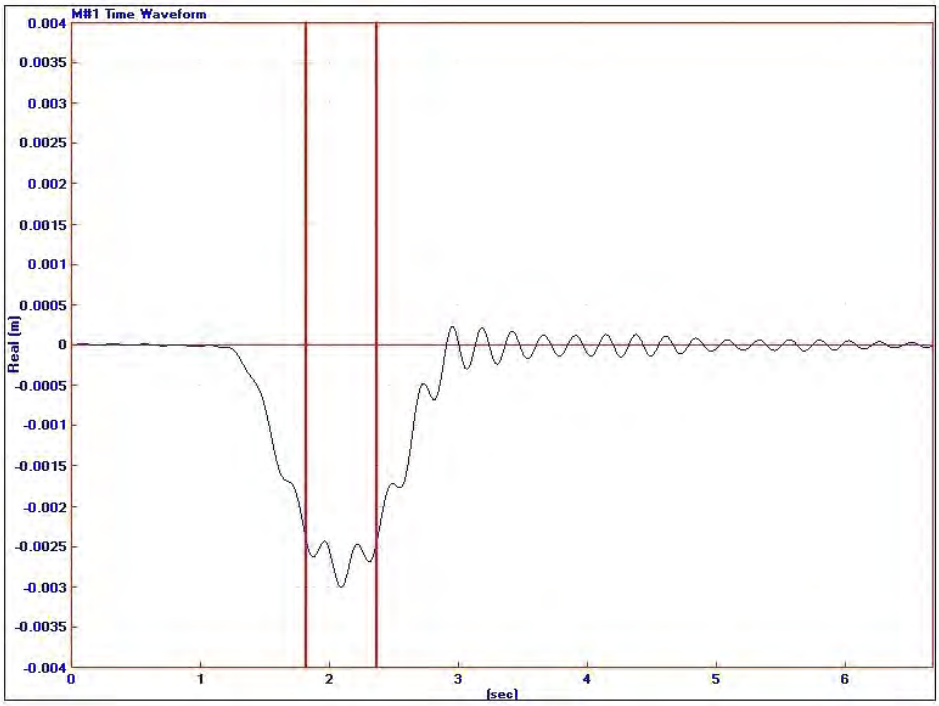

Figure 7.8: *Dynamic response from the LVDT for bridge at 75 Km/hr*

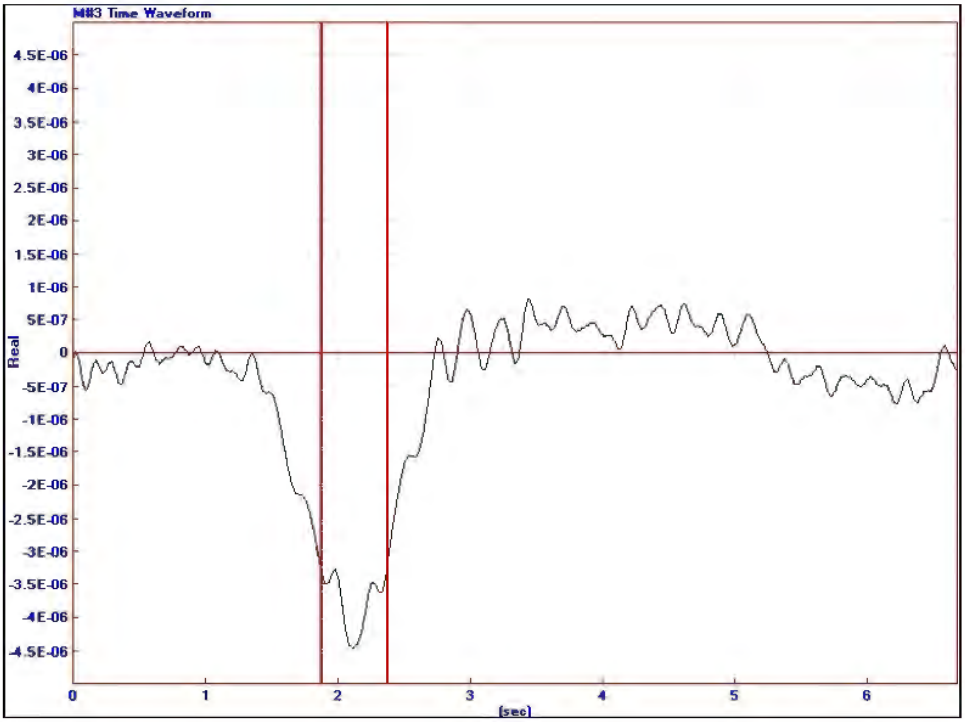

Figure 7.9: *Dynamic response from the Strain gauge for bridge at 75 Km/hr*

Figure 7.8 shows that the mobile crane arrives on the tested span at time = 1 sec and leaves the bridge at time = 2.9 sec. After the vehicle leaves the bridge, the structure undergoes damping and this is shown by the decreasing amplitude of the signal. The Berg River Bridge gets back to its normal state after about 7 seconds. For this scenario, the impact on the bridge happens between the two red vertical lines. The maximum dynamic displacement during the vehicle-bridge interaction is 3mm.

The damping ratio of the bridge is calculated using formula 8.1

$$\zeta = (x_n - x_{n+1})/2\pi x_{n+1} \tag{7.1}$$

Where $x_n = 2.79$ and $x_{n+1} = 2.18$ are the two consecutive displacement obtained from Figure 7.7 when the vehicle has left the bridge. The calculated damping ratio for the bridge is 0.044. This value is in the range of prescribed by Table 1 in the Bridge dynamics and dynamic amplification factors journal (Paultre, Chaallal, & Proulx, 1992).

7.3.2 Static analysis

The static analysis of the field measurement has been done using ME'scope VES. An FFT was applied to the results obtained from the dynamic analysis. A notch is applied at a frequency which is about twice the frequency obtained from Equation 8.2. This frequency is usually where the first peak occurs. It should be noted that this peak is not the dominant peak.

$$f = \frac{1}{t} \tag{7.2}$$

$$t = \frac{s}{v} \tag{7.3}$$

Where S= Span length of 28m and V= Speed of approach of the mobile crane

Table 7.1: *Frequency about which notch is applied*

V (km/hr)	f (Hz)	Notch f (Hz)
5	0.05	0.10
10	0.10	0.20
20	0.20	0.40
40	0.40	0.79
60	0.60	1.19
75	0.74	1.49

Figure 7.10: *Notched frequency for 75 Km/hr scenario*

An inverse FFT is then applied to Figure 7.10 to get the static displacement and strain measurements.

The static analysis produces a graph which does not include the dynamic impacts. The graph is smooth and its peak displacement is less than the peak obtained from the dynamic analysis. Figure 7.11 and 7.12 shows the static displacement and strain obtained after further processing the dynamic results for when the crane was travelling at 75 Km/hr. As expected, there is no damping for the static displacement. This is because the analysis only considers the effect of the vehicle when it is static, i.e. not in motion, on the bridge.

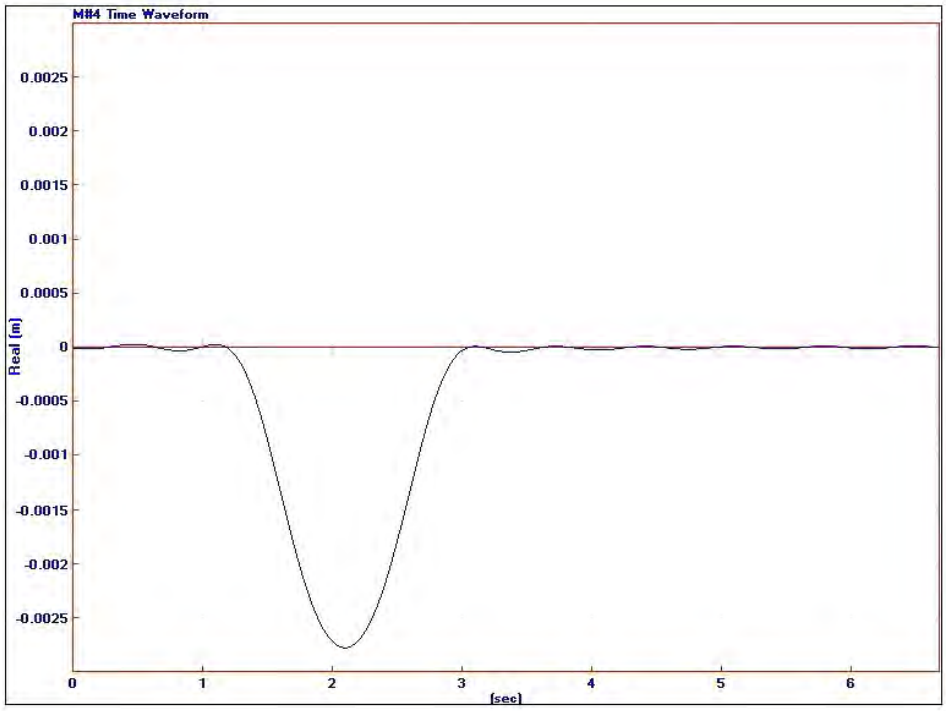

Figure 7.11: *Static displacement at mid-span*

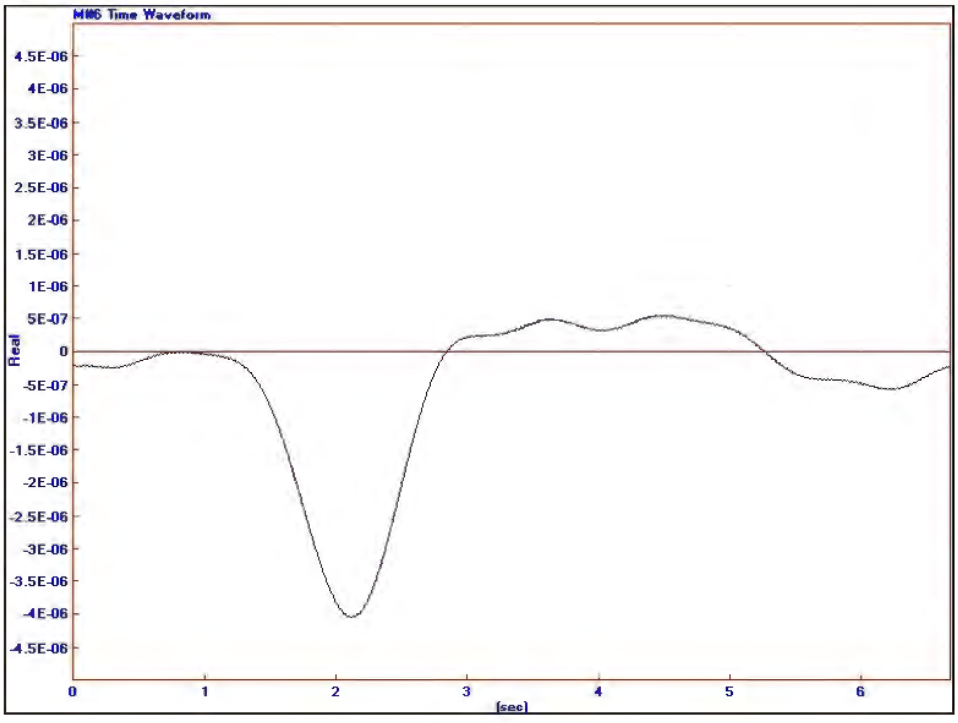

Figure 7.12: *Static strain at mid-span*

7.4 Impact factors

The impact that the 36 tonnes mobile crane cause on the bridge is measured using the formula 6.4 discussed in Chapter 6.6.

$$Im = \frac{R_D - R_S}{Rs}$$

Where Im = Dynamic amplification factor; R_D = dynamic response; and R_s = static response

In ME'scope VES, the dynamic and static traces for each speed scenario were imported to the same file and overlaid. The impact was measured by taking the peak difference between the two graphs and dividing this difference by the peak static value.

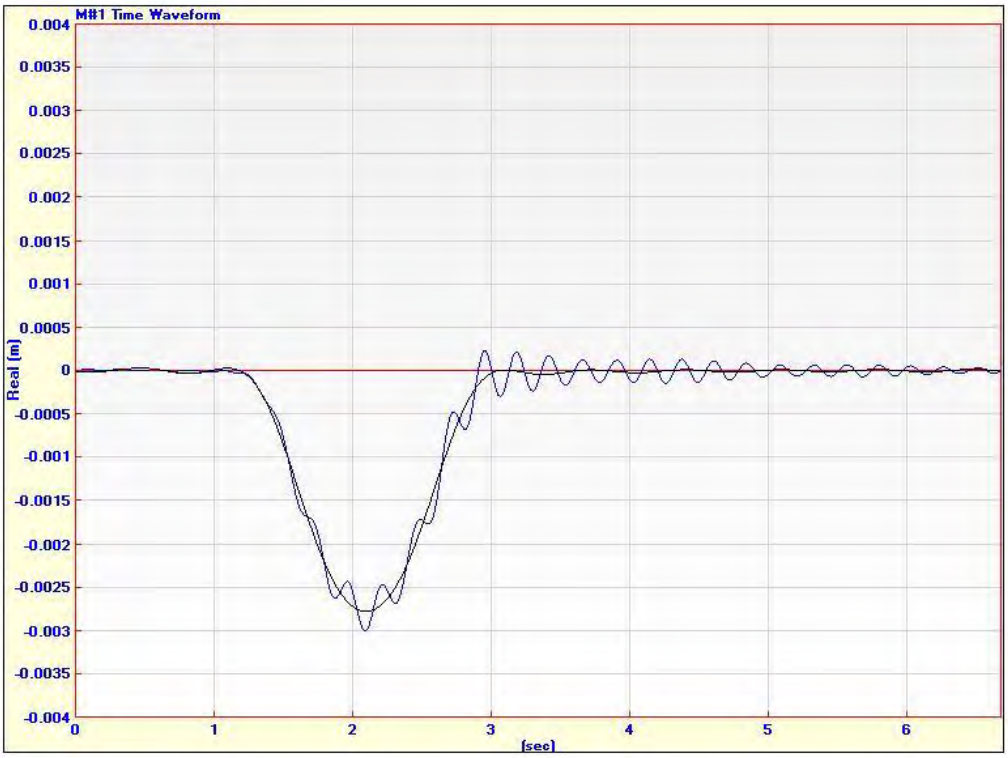

Figure 7.13: *Overlaid traces for displacement at 75 Km/hr*

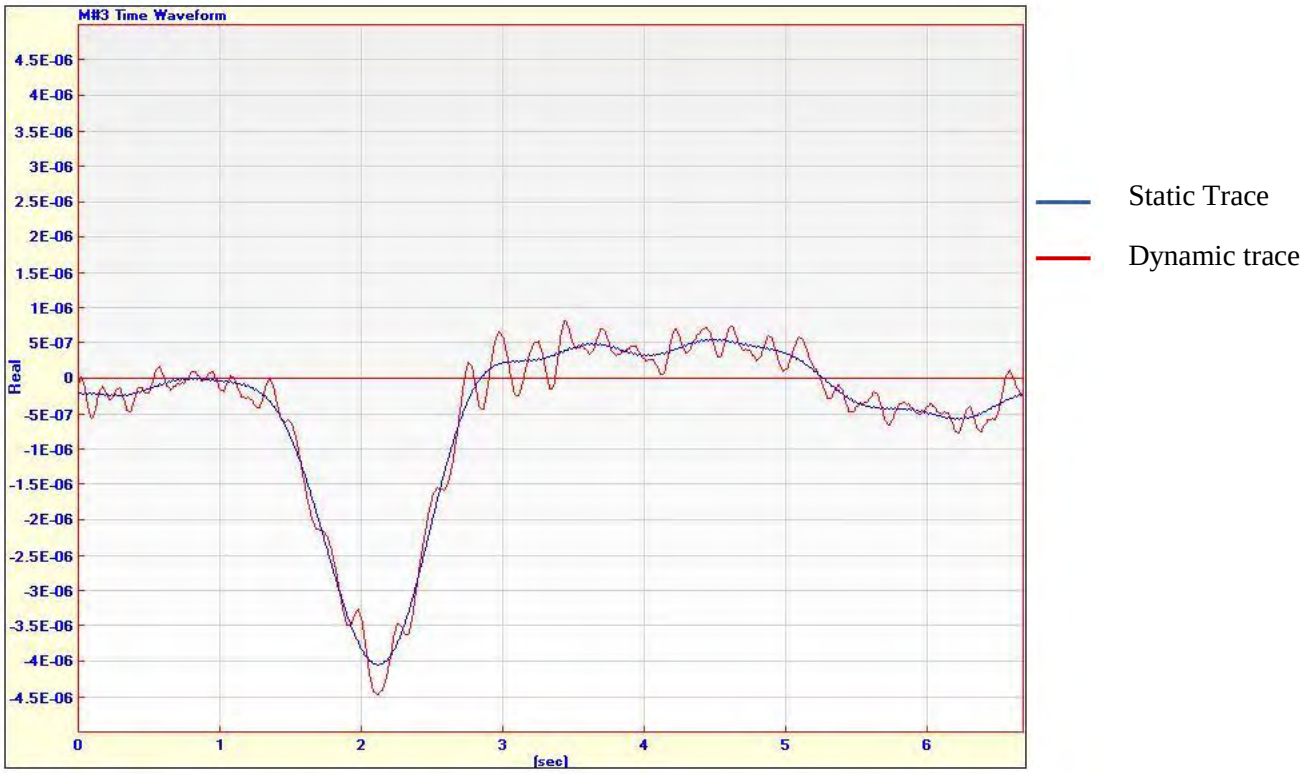

Figure 7.14: *Overlaid traces for strain at 75 Km/hr*

Tables 7.2 to 7.4 give the dynamic and static displacements and strains measured by the strain gauge and two LVDTs. The dynamic amplification factor is generally written as$(1 + Im)$. The mid-span of the Berg River Bridge is at 14m and the quarter span at 7m.

Table 7.2: *Impact factor obtained from measured static and dynamic readings at quarter span*

Speed (Km/hr)	**Dynamic** $(\times \mathbf{10^{-6}})$	**Static** $(\times \mathbf{10^{-6}})$	**Impact Factor** $(\mathbf{1 + Im})$
5	2.41	2.35	1.01
10	4.18	4.17	1.01
20	5.04	4.83	1.04
40	3.62	3.22	1.12
60	3.47	2.99	1.16
75	4.48	3.93	1.14
40-Plank	5.06	3.65	1.39

Table 7.3: *Displacement Impact factor calculated from measured Dynamic and Static readings at quarter span*

Speed (Km/hr)	Dynamic (mm)	Static (mm)	Impact Factor ($1 + Im$)
5	2.29	2.27	1.01
10	2.27	2.24	1.01
20	2.26	2.23	1.01
40	2.35	2.24	1.05
60	2.3	2.26	1.02
75	2.29	2.16	1.06
40-Plank	2.86	2.23	1.28

Table 7.4: *Displacement Impact factor calculated from measured Dynamic and Static readings at mid span*

Speed (Km/hr)	Dynamic (mm)	Static (mm)	Impact Factor ($1 + Im$)
5	2.97	2.95	1.01
10	2.9	2.87	1.01
20	2.9	2.87	1.01
40	2.99	2.89	1.03
60	2.99	2.92	1.02
75	3.01	2.78	1.08
40-Plank	3.72	2.89	1.29

Figure 7.15 shows the relationship between speed and the dynamic displacement measured at mid and quarter span. As expected, the deflection at mid-span is greater than the deflection at quarter span. The average difference between the mid-span and the quarter span displacement is 0.69 mm.

The displacement of the bridge when the mobile crane was travelling at crawl speed (5 Km/hr) is slightly higher than the displacement at 10 and 20 Km/hr. This is because the bridge was accidently opened to the traffic before the crane managed to leave the bridge. For the other speed

scenarios, the bridge was closed until the crane had left the bridge. Figure 7.16 shows the vehicles which were present while the crane was on travelling on the instrumented span.

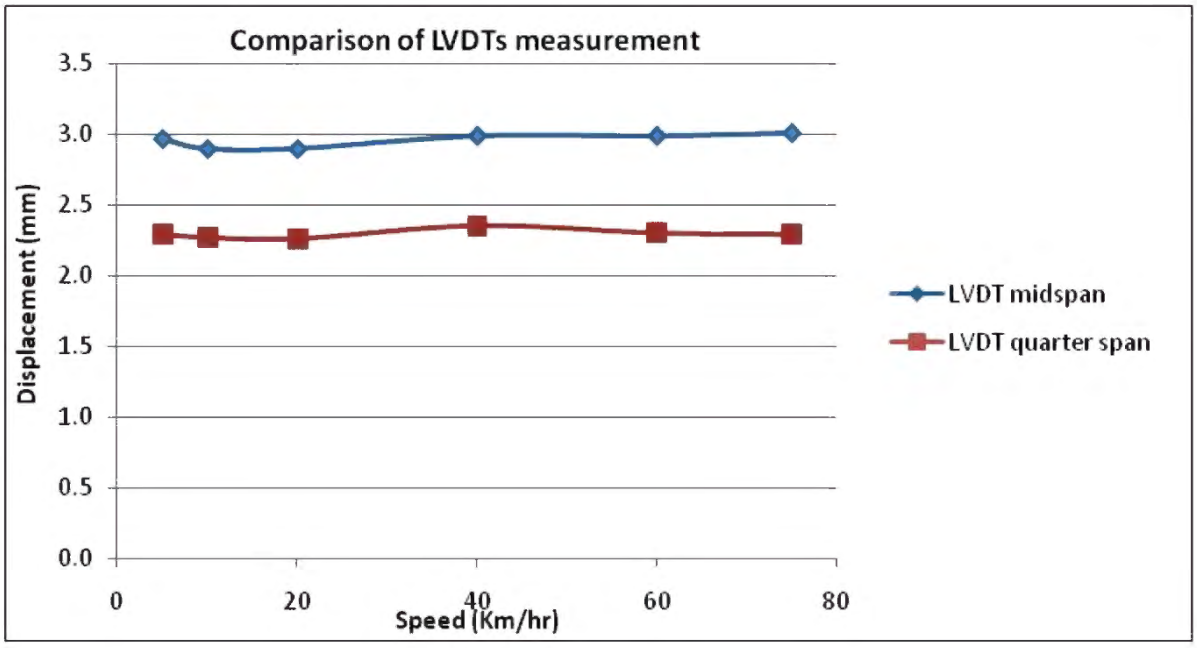

Figure 7.15: *Bridge deflection for the different speed scenario*

Figure 7.16: *Traffic influencing the dynamic effects*

The relationship between speed and the different Impact factors are represented in Figure 7.17. It is clear that as the mobile crane picks up speed, the impact caused to the Berg River Bridge increases. However, the relationship obtained is not linear. The strain impact factor is also higher than the displacement impact factor for speed greater than 10 Km/hr.

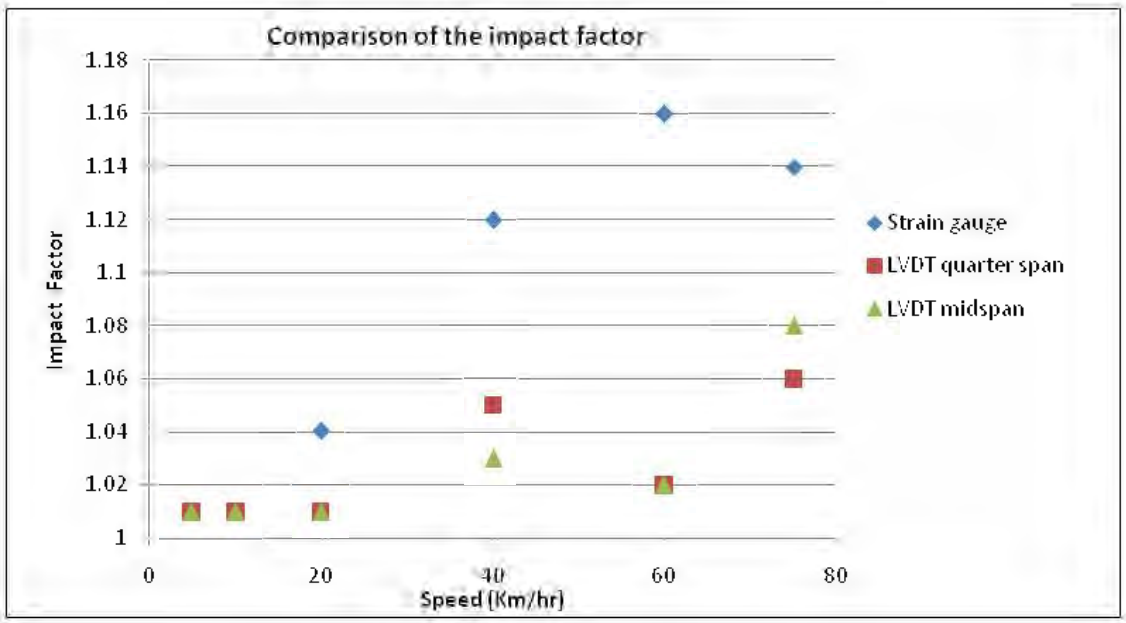

Figure 7.17: *Impact factor for the different speed scenario*

The different scenarios for which the crane travelled on the bridge are shown in Figure 7.18. For speeds of 5, 10, 40 and 75 Km/hr, the crane travelled from left to right i.e. it moved on all the eleven simply supported continuous spans before reaching the instrumented span. For speeds 20 and 40 Km/hr the vehicle travelled from the road surface onto the construction joint and onto the tested span.

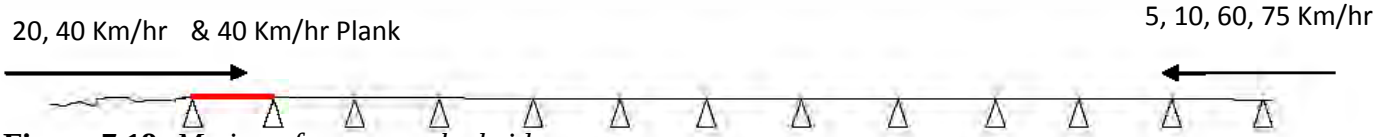

Figure 7.18: *Motion of crane on the bridge*

At high speed, it observed that the impact caused when the crane travels from right to left (i.e. from the road to the span in red) is bigger than the impact caused when the vehicle travels along the continuous span before reaching the red span. This additional impact occurs since the road surface is not continuous at the construction joint which links the road to the bridge. Therefore the vehicle bounces when it goes over the construction joint causing a higher impact to the

bridge. As speed increases, this impact also increases. This is why the dynamic amplification factor recorded by the strain gauge at quarter span is higher than the impact recorded at mid-span. The impact is lower when the vehicle travels from left to right since the slab lie on a simply supported continuous beam.

Figure 7.19 shows the impact factor when the mobile crane is travelling from left to right (i.e. for the speed of 5, 10, 40, 75 Km/hr). It is observed that the readings are more linear when compared Figure 7.17. The R^2 values are closer to 1 which implies that a linear relationship between Impact factor and Speed can be assumed.

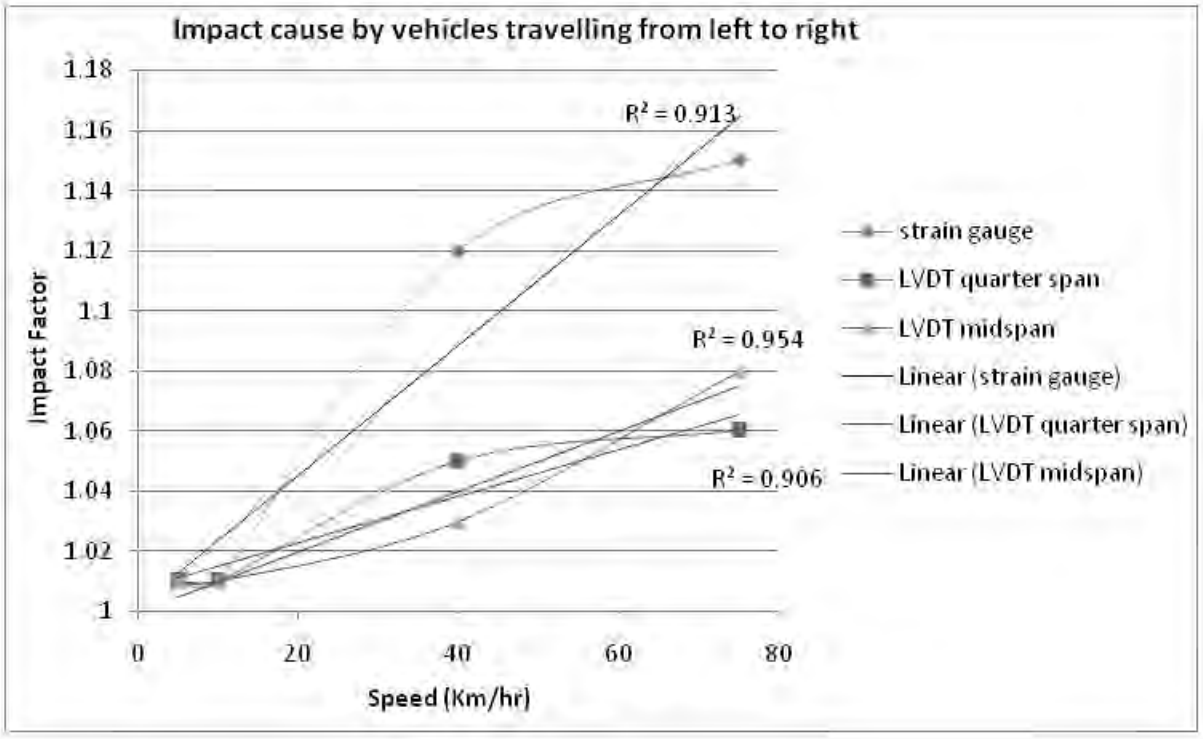

Figure 7.19: *Impact for 5, 10, 40, 75 Km/hr scenarios*

Due to the lack of data, the relationship for when the vehicle travels from the road surface onto the construction joint to the bridge could not be plotted. However, from the measurements obtained it is clear that the impact is higher.

In South Africa, the maximum permitted dynamic allowable factor is 1.5. This means that for design purposes, the dynamic effects of all vehicles on bridges are considered by multiplying the

static live loads by an Impact factor of 1.5. The relationship between dynamic impact factor and span length for various codes is given in Figure 7.20.

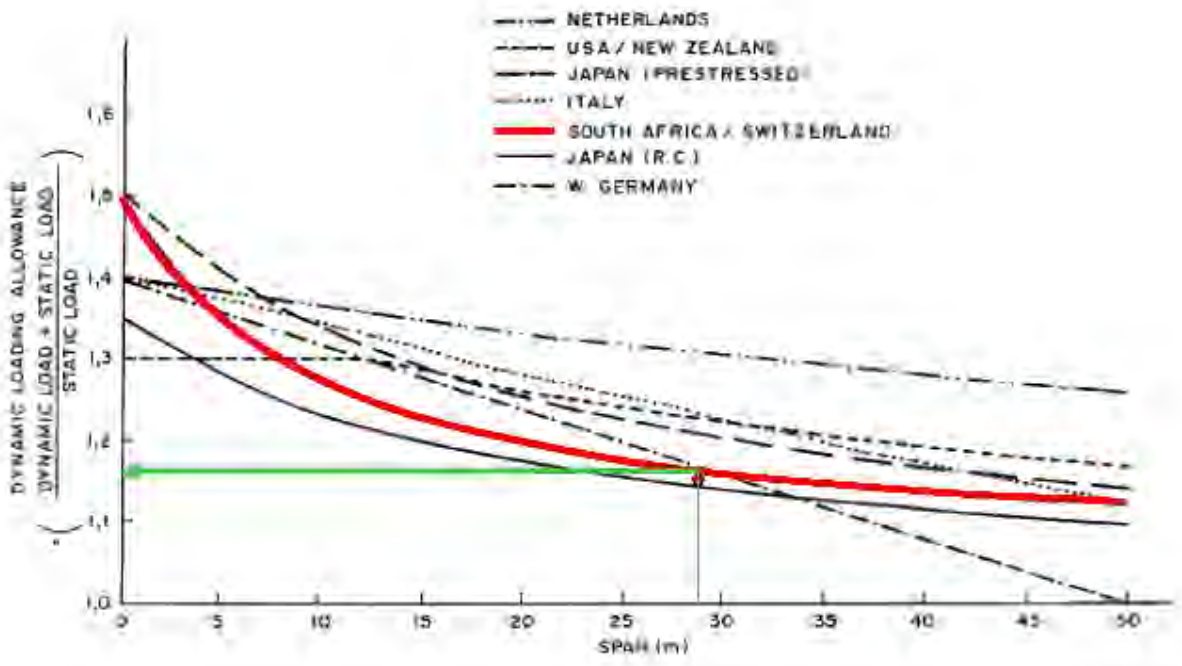

Figure 7.20: *Variation of dynamic loading allowance with span for different countries (CSIR, 1991)*

The highest impact factor obtained from the field experiment is 1.16. When plotted on Figure 7.20 (red dot), it is observed that the impact caused by the 36 tonnes vehicles is within the allowable range. From the codes, the maximum allowable impact factor for the 28m span is about 1.18. Therefore the presence of other vehicle on the bridge at the same time as the crane can render the structure unsafe as the impact factor will be exceeded. This confirms that the heavier the traffic load, the higher will be the impact on the bridge.

The dynamic load allowance of 1.18 for the Berg River Bridge would have been exceeded if the 36 tonnes crane travelled at a speed greater than 60 Km/hr. Therefore the safest speed at which the crane can use the bridge together with the normal traffic load is about 10 Km/hr. Normal traffic loading is up to 50 tonnes. The live load on the span should not exceed the 50 tonnes at any time and the light vehicles present must drive within the speed limit of 40 Km/hr.

Figure 7.21 shows the relationship between the natural frequencies and the dynamic load allowance for several codes. When plotted on the graph, the maximum Impact calculated from the field measurements falls within the safe range.

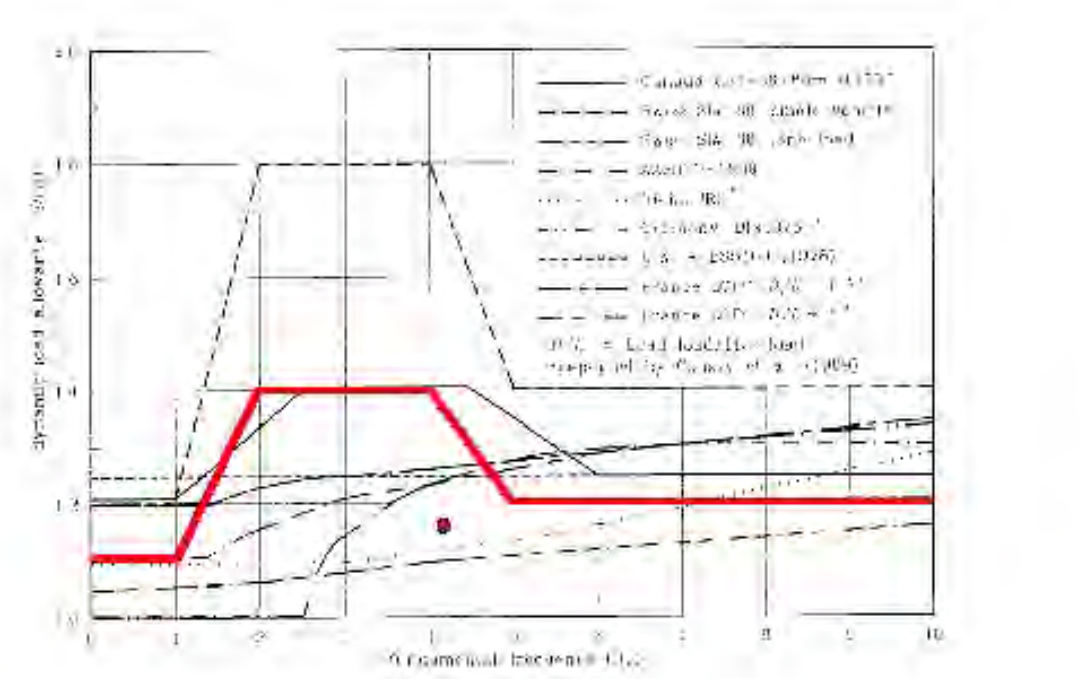

Figure 7.21: *Dynamic load allowance (DLA) versus fundamental frequency for different national codes (Paultre, Chaallal, & Proulx, 1992)*

7.5 Road roughness

The change road surface roughness was modeled by stacking three 18mm planks on top of each other at mid-span. In practice, the planks would represent a severely deteriorated road surface, which has been caused by a bridge approach depression, delaminations, potholes, or a threshold between the bridge approach and its deck (Kwasniewski et al, 2006).

The mobile crane drove on the planks at a speed of 40 Km/hr and significantly increased the dynamic interaction between the truck wheels and the bridge deck. The impact factors measured by the LVDTs at quarter and mid span is 1.28 and 1.29 respectively. The strain impact factor is 1.39 at quarter span. The dynamic and static displacements at mid-span and quarter span are shown in Figure 7.22.

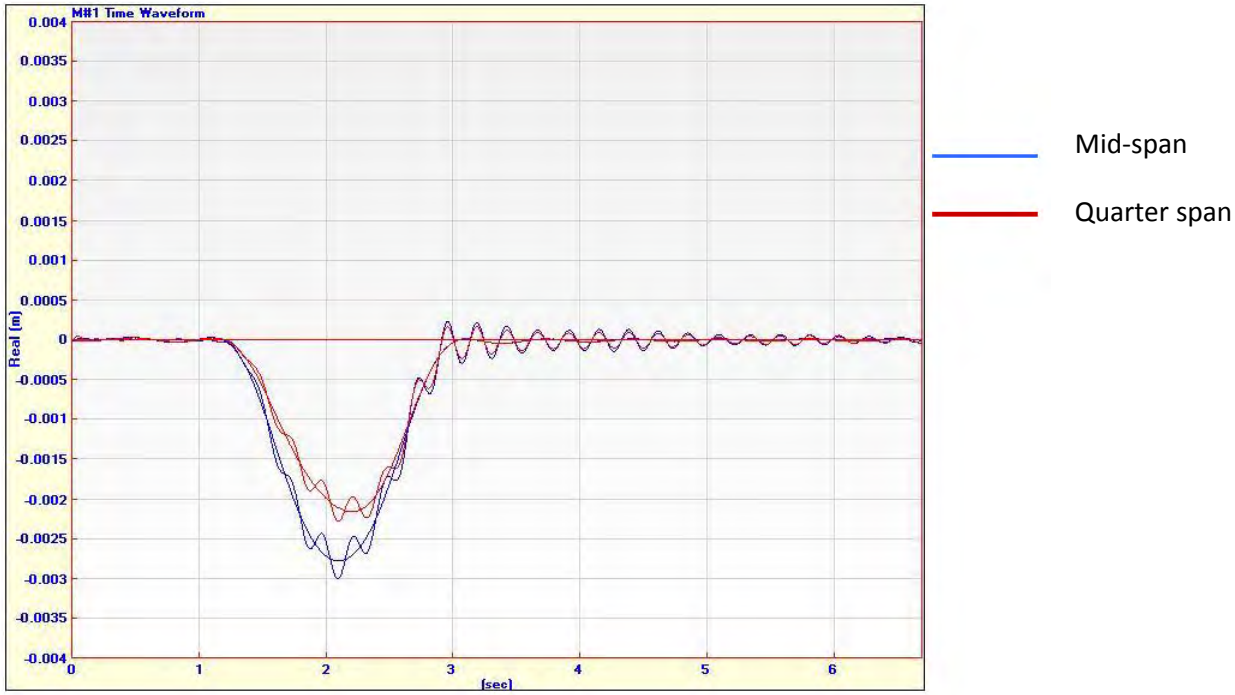

Figure 7.22: *Dynamic displacement at mid-span and quarter span*

Table 7.5 compares the impact factor for the plank and no plank scenarios at 40 Km/hr. The amplification of the impact is between 22-25% for the different measuring device. It is mainly caused by the bounce of the mobile crane wheels from the 48mm plank onto the road surface. This change in surface roughness causes the dynamic amplification factor to exceed the allowable impact factor suggested by the codes.

Table 7.5: *Impact factor at 40 Km/hr for Plank and No Plank scenarios*

		IF	% Increase
Strain gauge	No plank	1.12	24
	Plank	1.39	
LVDT 1/4 span	No plank	1.05	22
	Plank	1.28	
LVDT 1/2 span	No plank	1.03	25
	Plank	1.29	

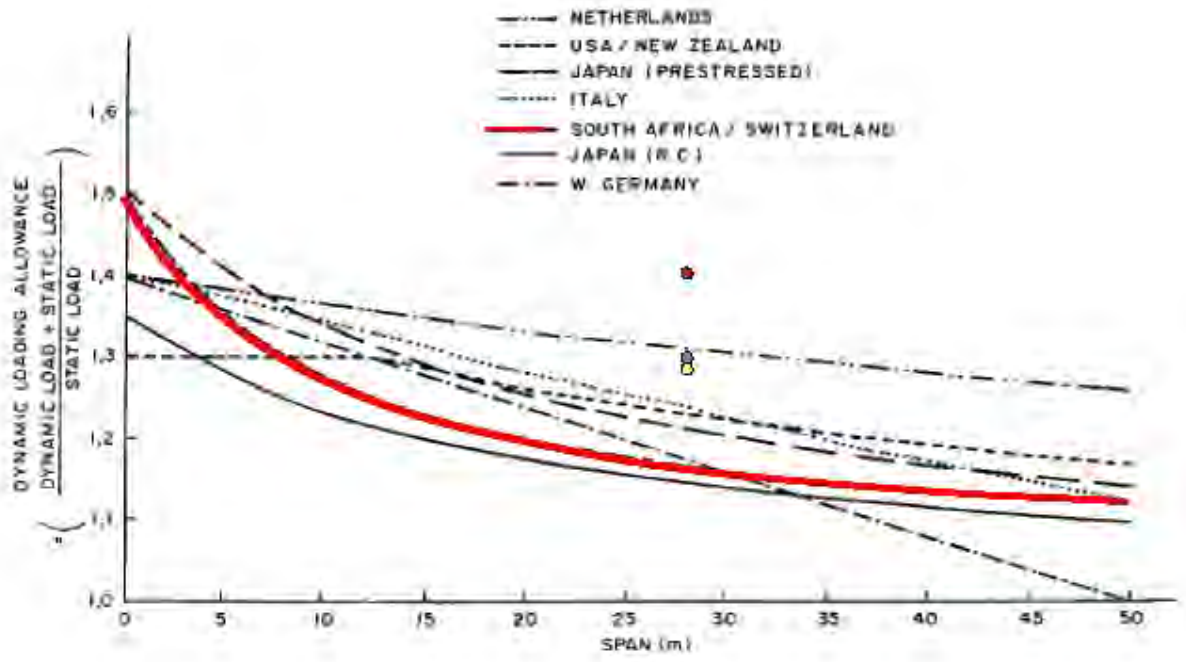

Figure 7.23: *Effect of road roughness simulated by a plank on the maximum dynamic amplification*

When plotted on the National codes graph, the plank impact factors listed in Table 7.5 lie above the curve representing the South African codes. For a 28m bridge, the design codes specify an impact factor of 1.18 which is about 17% less than the maximum impact factor measured during the experiment.

The 40 Km/hr plank scenario was modelled in Adina by varying the axle loads. In order to measure an impact of 1.29, the axle load of the vehicle would each have to be increased from 12 to 16 tonnes (48 tonnes vehicle). This model exceeds the permitted legal weight by 4 tonnes.

The presence of irregularities in the road surface makes the bridge unsafe causing fatigue of the structure thereby leading to structural damage. A proper maintenance of the bridge is therefore very important to minimize the effects of impact forces.

7.6 Finite Element Model

7.6.1 Berg River Bridge Model

The 28m instrumented span of the Berg River Bridge was modelled in Adina Finite Element Software. The modelling process is explained in Chapter 7. Each speed scenario was modelled

separately. The dynamic and static displacement obtained from the model was then compared to the field measurements.

Figure 7.24 and 7.25 shows the quarter span dynamic and static displacement of the bridge when the vehicle is driving at 60 Km/hr. Figure 7.24 shows that damping of the bridge occurs after the vehicle leaves the bridge after about 1.75sec. This is expected due to the impact caused by the moving vehicle. No damping occurs for the static analysis. The response is a smooth curve. The maximum displacement occurs at mid-span.

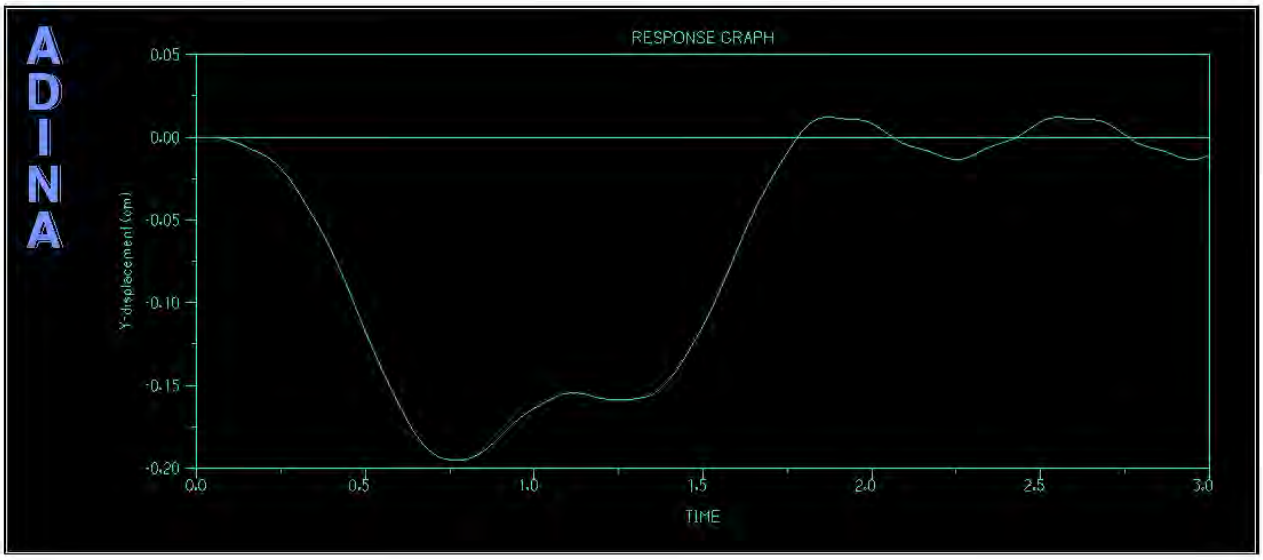

Figure 7.24: *Dynamic displacement at 75 Km/hr*

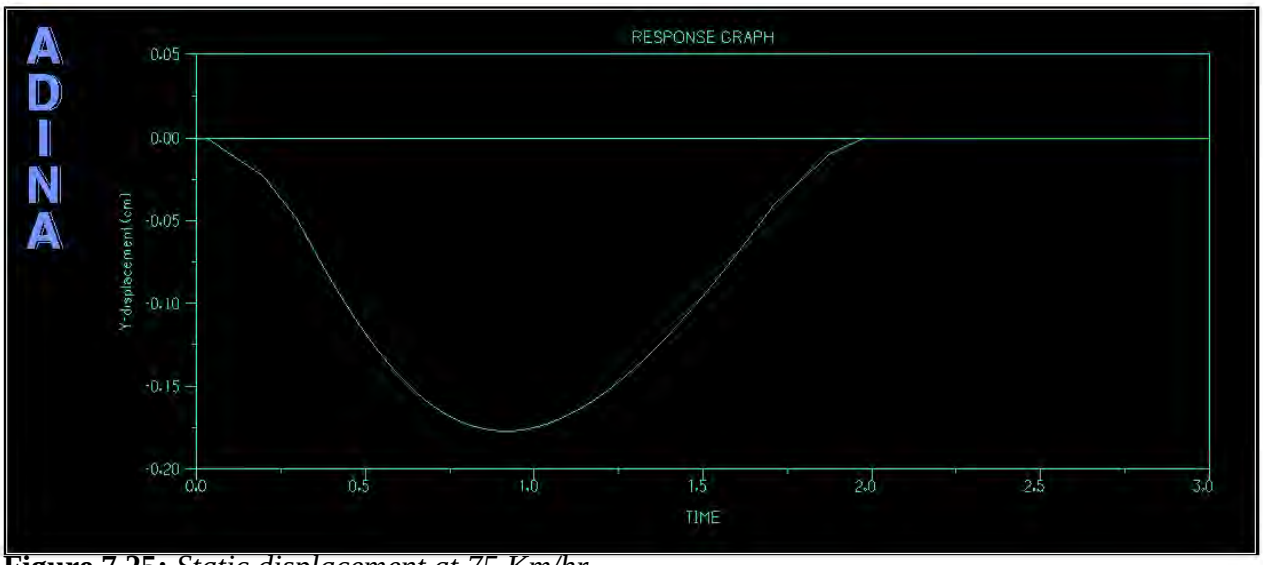

Figure 7.25: *Static displacement at 75 Km/hr*

The displacement impact factors at mid-span are almost similar for both the FE Model and the field experiment for speed between 5 and 60 Km/hr. However the FE Model gives a greater impact at a speed of 75 Km/hr. This may be because the FE Model does not consider the two cross beams which are at mid and quarter span respectively. Also in the FE model, the bridge has been modelled as one simply supported beam carrying the whole weight of the 36 tonnes crane whereas in reality, the weight of the vehicle is distributed to the 1st two beams since the distance between the two beams are 1.7m and the vehicle width is 2.55m. The experimental impact for the 75 Km/hr scenario would also have been bigger if the crane travelled on the construction joint to the bridge.

For the quarter span displacement, the FE Model gives higher impact factors than the field measurements. This is because only the instrumented span has been modelled and not the twelve continuous spans. Therefore the model assumes that the vehicle is going over the construction joint every time thereby amplifying the impact. The impact for the 75 Km/hr model is also higher than the field model compared to the field measurements for the same reason mentioned in the previous paragraph.

Table 7.6: *Displacement Impact factor at mid-span for different speed*

			FE Model	**Field Experiment**
Speed (Km/hr)	**Dynamic (mm)**	**Static (mm)**	**Impact Factor ($1 + Im$)**	**Impact Factor ($1 + Im$)**
10	2.9	2.87	1.01	1.01
20	2.91	2.87	1.01	1.01
40	2.92	2.79	1.05	1.03
60	2.78	2.68	1.04	1.02
75	3.23	2.65	1.22	1.08

Table 7.7: *Displacement Impact factor at quarter span for different speeds*

			FE Model	Field Experiment
Speed (Km/hr)	**Dynamic (mm)**	**Static (mm)**	**Impact Factor ($1 + Im$)**	**Impact Factor ($1 + Im$)**
10	2.04	2.0	1.02	1.01
20	2.09	2.01	1.03	1.01
40	1.95	1.77	1.10	1.05
60	2.06	1.88	1.10	1.02
75	2.21	1.75	1.26	1.06

The shear and moment impact factor have been obtained from the FE model using data obtained from the field experiment. The maximum shear occurs at the supports and the maximum bending moment take place at mid-span for all the scenarios. The maximum shear force is almost equal to the vehicle weight. For both cases, the impact factor is almost 1 for speed up to 60 Km/hr. At higher speed, bigger dynamic impact happens as the bounce between the construction joint and the bridge is amplified.

Table 7.8: *Dynamic and static shear and Shear Impact factor for varying speed*

Speed (Km/hr)	**Dynamic ($N \times 10^5$)**	**Static ($N \times 10^5$)**	**Impact Factor ($1 + Im$)**
10	3.54	3.54	1
20	3.54	3.47	1.02
40	3.45	3.39	1.02
60	3.31	3.20	1.03
75	3.76	3.27	1.15

Table 7.9: *Dynamic and Static moment and Moment Impact factor for different speed*

Speed (Km/hr)	Dynamic($N/m \times 10^6$)	Static ($N/m \times 10^6$)	Impact Factor ($1 + Im$)
10	2.47	2.44	1.01
20	2.48	2.44	1.02
40	2.48	2.37	1.05
60	2.33	2.28	1.03
75	2.68	2.25	1.19

Figure 7.26 compares the FE model Impact factors to the Experimental Impact factors. From the graph, it can be said that the safest speed for the 36 tonnes crane to travel on the bridge is 20Km/hr or less. This is because the impact caused to the structure is almost zero.

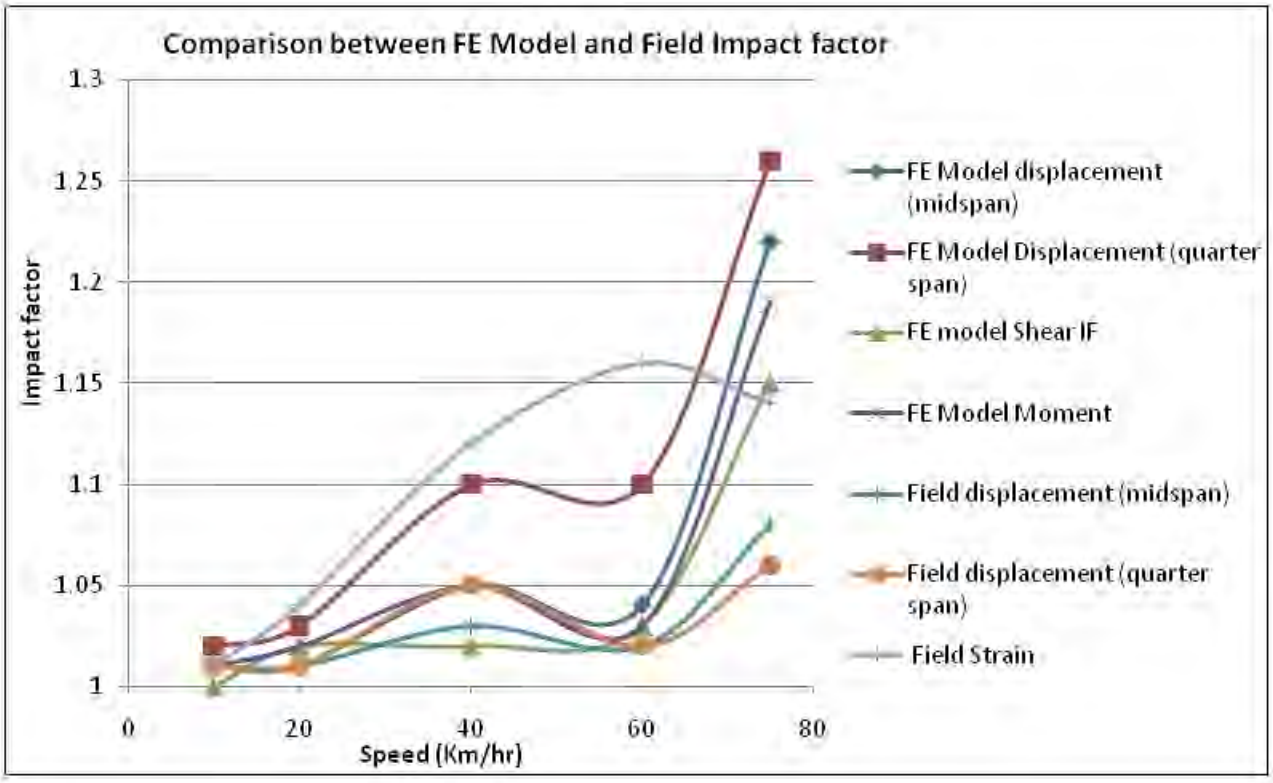

Figure 7.26: *Comparison of the different impact factors*

7.6.2 Effect of vehicle weight and span length on the impact factor

The mobile cranes discussed in Chapter 6.4.1 have been modelled in Adina travelling at a critical speed of 75 Km/hr on the 28 m Berg River Bridge. Table 7.9 gives the static and dynamic displacement for each model. Figure 7.26 shows the relationship between vehicle weight and

Impact factor. No linear relationship has been obtained but it is clear that as the vehicle weight increases, the impact factor decreases.

In theory, the dynamic impact factor should increase with increasing weight. However, mobile cranes are manufactured to limit impacts on highway structures. The Mobile cranes described in Chapter 6.4.1have different axle lengths, axle arrangements and vehicle length which helps mitigate impact provided that the vehicle is respecting the legal axle weight of 12 tonnes. The manufacturers also assume that the road surface is in good condition. A poor road surface will lead to severe amplification of the impact since the vehicles have more axles and hence more wheels being in contact with the deteriorated surface. Exceeding the 12 tonnes legal axle weight would also cause additional impact. In practice, the impact measured may be higher than the simulated model due to the number of wheels being in contact with the construction joint for a longer period. Further field experiment needs to be carried out involving heavier mobile crane to verify the above claim.

Table 7.10: *Dynamic and Static Displacement and Moment Impact factor for varying vehicle weight*

Vehicle weight (T)	**Number of axles**	**Dynamic Displacement (mm)**	**Static Displacement (mm)**	**Impact Factor** $(\mathbf{1} + \boldsymbol{Im})$
48	4	4.17	3.49	1.19
60	5	4.96	4.28	1.16
72	6	5.77	5.07	1.14
84	7	4.95	4.69	1.06
96	8	6.77	6.28	1.08
108	9	7.01	6.68	1.05

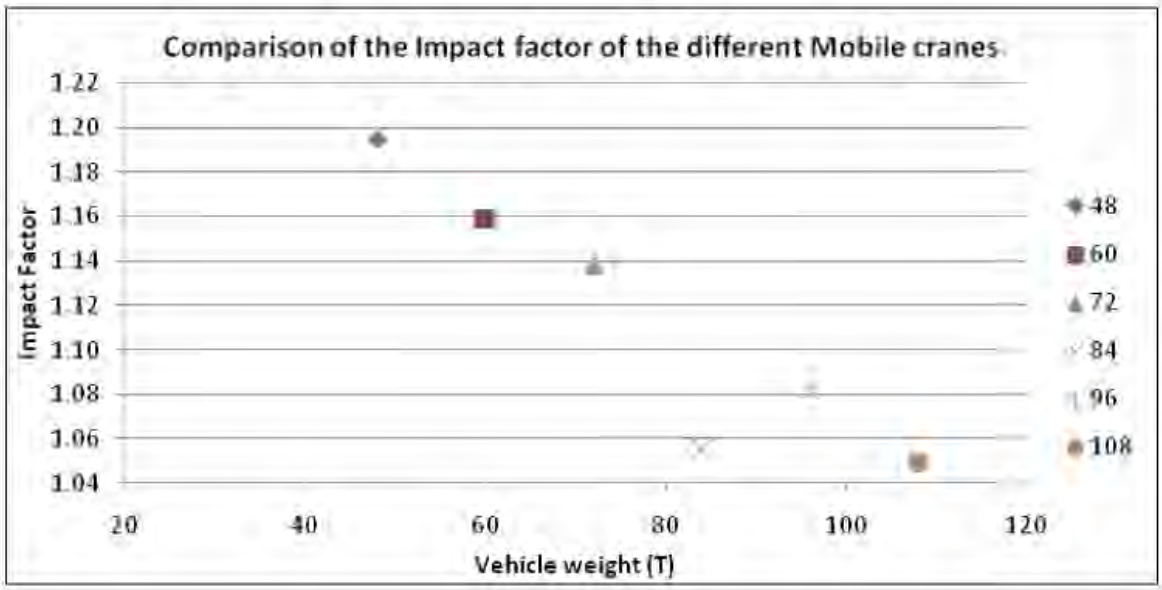

Figure 7.27: *Dynamic load factors for the different trucks*

Bridges having spans of 10m, 20m, 30m and 40m were modelled in Adina using the beam properties of the Berg River Bridge. The impacts caused by the six mobile cranes were simulated using the same software. Figure 7.27 and 7.30 clearly shows that the impact factor decreases with increasing vehicle weight. However this decrease is not caused by the decrease of dynamic deflection but an increase of the static deflection as shown in Figure 7.28 and 7.29.

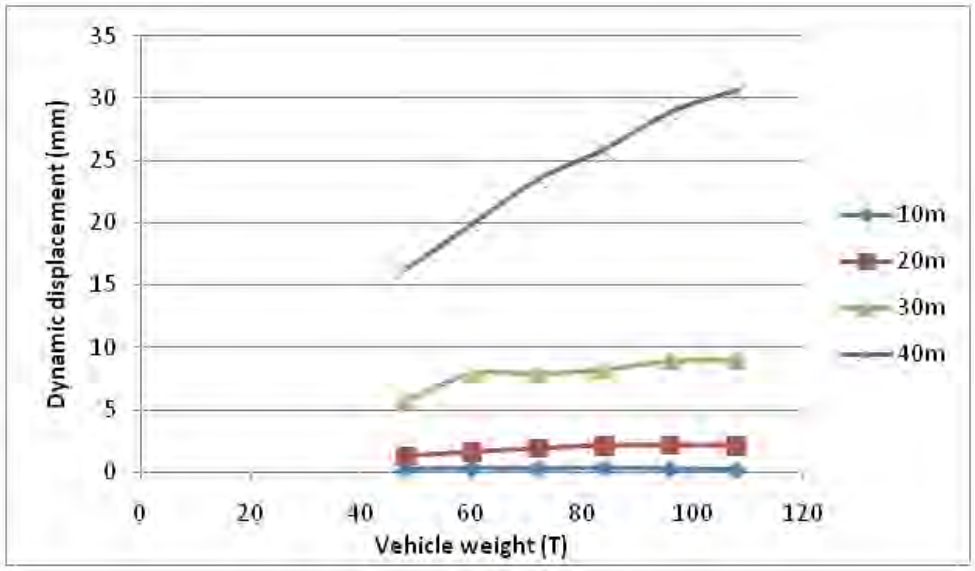

Figure 7.28: *Dynamic deflection versus gross vehicle weight for different span length*

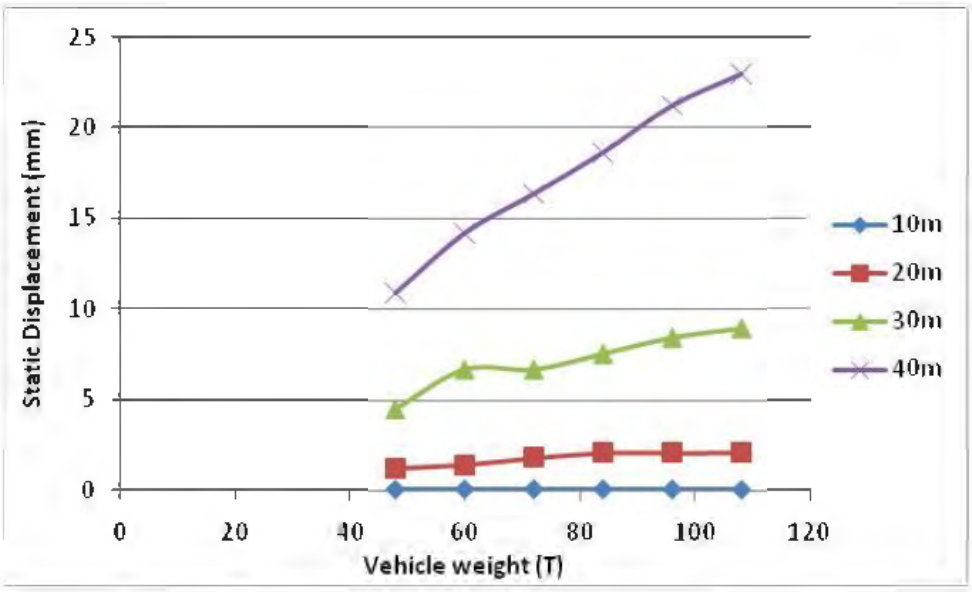

Figure 7.29: *Static deflection versus gross vehicle weight for different span length*

Figure 7.27 and 7.28 show that the maximum displacement at mid-span is almost constant regardless of the weight of the mobile crane for the spans of 10, 20 and 30m. Similar results have been obtained from a study done by Nowak on the "Simulation of Dynamic Load for Bridges".

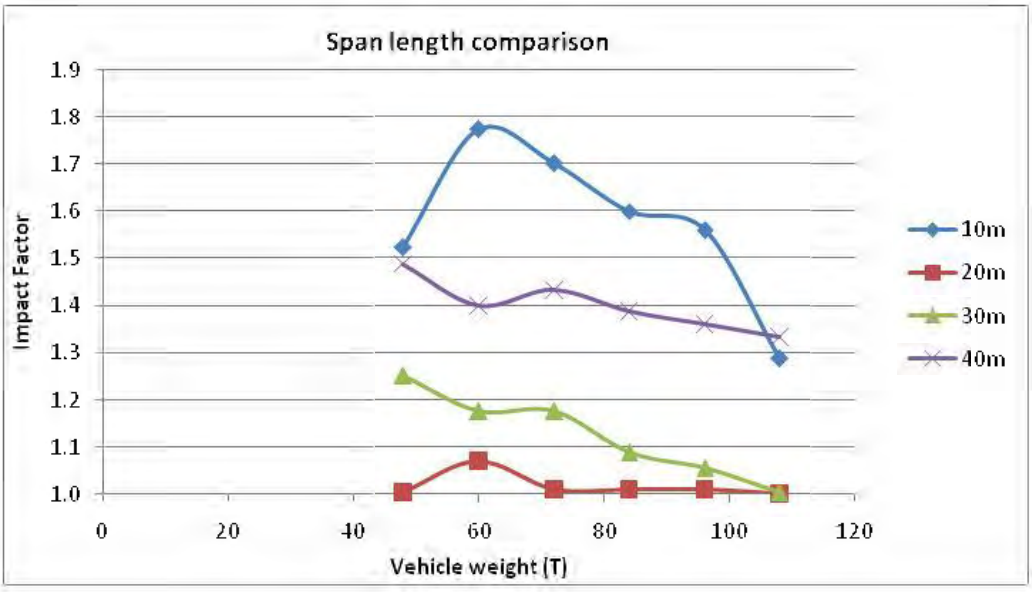

Figure 7.30: *Impact factor versus vehicle weight for different span length*

7.7 Chapter Summary

This chapter presents and discusses the experimental results obtained from the interaction between the 36 Tonnes mobile crane and the Berg River Bridge. The impact factor due to the various speeds and plank scenarios were calculated from readings obtained from the strain gauge and LVDT. They were then plotted on the impact graph which defines the allowable Impact in South Africa.

The natural frequency of the bridge was compared to the theoretical frequency. Both frequencies were found to be consistent with each other. The frequency of the structure under the moving load has also been measured and plotted on the graph representing South African guideline.

Validation of the results has been done by comparing the field results to those obtained by Finite Element model for the different scenarios. This Chapter has shown that there is a good correlation between the two sets of results.

A FE analysis of the Berg River Bridge gave the Moment and Shear Impact factor. The impact caused to the bridge under different loading conditions has also been measured. The effect of varying span length on the dynamic impact factor has been studied.

8 CONCLUSION AND RECOMMENDATIONS

8.1 Conclusions

Bridges are a key component of the transportation system and are one of the driving forces of the South African economy. They help connect people and are important in the transportation of goods across the country. There are more than 11 000 bridges in South Africa which have been built according to various design codes. More than 81% of these bridges have been designed using the MOT and BS5300 design code. However, the design loads considered in these codes are outdated since nowadays vehicles have more axles and are can carry higher loads. The code which is currently being used in South Africa is the TMH 7.

There are a growing number of damaged bridges due to ageing of the structures and increase in axle loads. Bridges are among the most expensive investment asset of any country's infrastructure and proper maintenance and load management system are required to extend their life span. The majority of bridges in South Africa are short to medium span bridges. The abnormal load management system used in South Africa is TRH 11 and the legal axle load is 12 tonnes.

The impact of mobile cranes on bridges has been investigated in this thesis. Even though mobile cranes fall in the category of abnormal vehicles, they have different axle configurations and suspension system. Their axles are closer and they use a hydro-pneumatic suspension which is capable of adjusting the suspension stiffness depending on the road conditions. Literature has shown that vehicles having hydro-pneumatic and air suspensions exhibit lower body bounce frequencies than those with steel suspensions. No research has previously been done on the impact of mobile crane on highway structures. All existing literatures are about the impact of heavy vehicles.

The main focus of this study has been to measure the impact of mobile cranes on short span bridges. Visual inspections and field experiments are still the most effective way of assessing the health of a bridge. However they are an expensive and tedious especially if there is limited access to the bridge. Adina Finite Element software has been used in this research to model the interaction between the mobile crane and the bridge. Field experiment was also performed to calibrate and validate the FE model.

The dynamic response of the Berg River Bridge under the influence of a 36 tonnes mobile crane was measured using LVDTs and strain gauge. These highly sensitive devices have been manufactured by National Instruments. The bridge was instrumented at mid-span and quarter span. The different vehicle-bridge interaction scenarios which were experimented were (1) mobile crane driving at crawl speed (2) 10 Km/hr (3) 20 Km/hr (4) 40 Km/hr (5) 60 Km/hr (6) 75 Km/hr and (7) vehicle driving on a plank at 40 Km/hr to model road roughness. The signals captured were cleaned and processed using ME' Scope Ves 5.0 to obtain the dynamic displacements and strains. Accelerations of the structure due to normal traffic loading were also recorded.

The experimental natural frequency of the Berg River Bridge is about 4.20 Hz. It is close to the theoretical frequency of 4.08 Hz. The frequency of the bridge under the moving load for speeds between 5 and 60 Km/hr is about 2.07 Hz. For speeds higher than 60 Km/hr, this frequency was closer to the fundamental frequency of the bridge thereby causing resonance and making the structure unsafe.

The bridge impact factor was measured by dividing the maximum dynamic response by the static response. This impact is the peak difference between the static and dynamic graph. Strain and displacement impact factors were obtained for quarter span and mid-span. This study has shown that for the speed scenarios below 20Km/hr, the impact caused to the bridge is almost nothing. Increasing speed causes high dynamic effects; hence reduction in speed is a viable option in an overweight permit process to ensure safety.

The South African codes allows for an impact factor of 1.18 for a 28m Bridge. The highest impact factor measured is 1.16 for a speed of 60 Km/hr. It implies that the impact caused by the 36 tonnes mobile crane is within the permitted range provided that the bridge is closed to traffic.

It has been observed that the impact is higher when the vehicle travels over the construction joint onto the bridge compared to when the crane drove on the continuous spans before reaching the instrumented span.

The effect of surface roughness has been simulated by stacking three planks at mid-span. The strain gauge at quarter span measured the highest impact for this scenario. The impact factor calculated was 1.39. It is higher than the allowable impact factor of 1.18 thereby causing to

structural damage to the bridge. Therefore it is not safe for the 36 tons crane to travel across a bridge which has a deteriorated surface.

A finite element model of the Berg River Bridge was done in Adina to model the different scenarios. There is a good correlation between the experimental and FE results. The shear and moment impact factor was obtained from the FE model. As expected, the maximum shear occurs at the supports and the maximum bending moment at mid-span.

The effect of vehicle weight on the displacement impact factors was investigated. The impact factor was found to decrease as vehicle weight increased. This decrease is not caused by a decrease in dynamic displacement but an increase in static displacement. Axle length, axle arrangements and vehicle length was also found to have an influence on the impact factor.

8.2 Recommendation

The research was restrained to only one field experiment due to financial and time constraints. More tests need to be done to validate the FE model. Bridges having span length between 10 and 40m should be selected.

Further tests on the Berg River Bridge involving heavier mobile cranes should be done to verify if the impact factors really decreases with increasing vehicle weight.

For future impact tests, the vehicle should move on the construction joint to the instrumented span instead of it moving along the continuous span. The experimental findings has shown that the most important impact forces occur at the bridge approach as the mobile crane crosses the joint irregularities that occur between bridge and the abutments.

As previously mentioned, abnormal vehicles have different axle configuration and suspension system when compared to mobile cranes. It will be interesting to compare the impact caused by the 36 tonnes mobile crane to a heavy vehicle of the same weight.

In order to get a more precise indication of the effect of the change in surface roughness, a bridge with a slightly deteriorated surface should be chosen. The strain gauge and LVDT should be fixed just below the deteriorated surface.

Finally, TRH 11 has to be modified since it considers all abnormal vehicles to be of the same class. The South African abnormal load management guideline needs to divide abnormal vehicles into different categories since mobile cranes are different to other abnormal vehicles. However more tests involving several types of abnormal vehicles with different axle configurations and suspension system need to be carried out before developing a new abnormal load management guideline.

BIBLIOGRAPHY

AASHTO. (1994). *LRFD bridge design specification.* Washington, D.c.

AASHTO. (2002). Standard specification for highway bridges. Washington, D.C.

and, M. o. (1976). Highway Bridge Design Brief. Auckland, New Zealand: Civil Division Publication.

Anderson, B. (2006). *Review of South Africa Live Load models for traffic loading on bridge and culvert structures using weight in motion data.* Cape Town: University of Cape Town.

Authorities, C. o. (2000). *Draft guidelines for granting of exemption permits for the conveyance of abnormal loads and for other events on public roads.* Bloemfountein, South Africa.

Board, C. o. (1991). *Summary report on a computerised system for the assessment of abnormal load vehicles on road bridges.* Pretoria, South Africa.

Chan, T. M. (2002). Bridge Live load models from WIM data. *Engineering Structures* , 1071-1084.

Chryssanthopoulos, M., & Micic, T. (1996). International symposium on the safety of bridges-Reliability evaluation of short span bridges. *Thomas Telford Conferences.* London.

D.R.Scheling, N. M. (1992). Evaluation of Impact Factors for Horizontally Curved Steel Box Bridges. *ASCE* , 3203-3221.

Directorate for Science, T. a. (1998). *DYNAMIC INTERACTION BETWEEN VEHICLES AND.* Paris.

Heywood, D. R. (1997). Hydro-Pneumatic crane and tractor semi trailers: A Comparative study of their dynamic effects on a short-span bridge. 51-72.

(1976). *Highway Bridge Design Brief.* Auckland: Civil Division Publication.

Hwang, E.-S., & Nowak, A. S. (1991). Simulation of dynamic Load for Bridges. *Journal os Structural Engineering* , 1413-1434.

Institutions, B. S. *British standard specification for girder bridges- Part 3: Load and stresses.* London, BSI.

James, R. W., & Zhang, H. (1991). Evaluation of Proposed Bridge Formula For Continuous Spans. *Journal of Civil Engineering* , 1144-1158.

James, R. W., Noel, J. S., Furr, H. L., & Bonilla, F. E. (1986). Proposed new truck weight limit formula. *Journal of structural Engineering* , 1589-1604.

Kwasniewski, L., Wekezer, J., Roufa, G., Li, H., Ducher, J., & Malachowski, J. (2006). Experimental Evaluation of Dynamic Effects for a Selected Highway Bridge. *Journal of Performance of Constructed Facilities* , 253-260.

Ministry of Public Works, I. (1962). *Norme Relative ai Carichi per il calcolodei Ponti Stradali.* Roma.

Nowak, A. S., & Szerszen, M. (1998). Bridge load and resistance model. *Engineering Structures* , 985-989.

Nowak, A., Kim, S., & Stankiewicz, P. (2000). Analysis and diagnostic testing of a bridge. *Compute Structures* , 91-100.

Page, J., & Ricketts, N. (1997). *Traffic data for highway bridge loading.* Crowthorne: TRL: Transport Research laboratory.

(1980). *Part 1-10, Steel, Concrete and composite bridges.* London: BSI: British Standard Institution BS 5400.

Partnership, F. a. (1996). *Probabilistic assessment of short span bridges.* Transport Research Laboratory Contractors Report CR 16. Unpublished project report for Highways agency.

Paultre, P., Chaallal, O., & Proulx, J. (1992). Bridge dynamics and dynamic amplification factor-a review of analytical and experimental findings. *Canadian Journal of Civil Engineering* , 260-278.

Report of the Joint Committee of Concrete Institute, I. o. (1918). *Loads on highway bridges.* London: the Concrete Institute.

Research, N. I. (1981). *Code of practice for the design of Higyway Bridges and Culverts in South Africa.* Pretoria.

Sennah, K. M., Zhang, X., & B., K. J. (2004). Impact factors for horizontally curved composite box girder bridges. *Journal of Bridge Engineering* , 512-520.

Setright L.J.K. (1974). MacPherson Strut: Legs to support cars. In *World of Automobiles* (p. 1235). London: Orbis.

Sowman, R., Poree, N., (2000), "Situation report on heavy freight vehicle overloading control in South Africa." *Automobile Association of South Africa*, Kyalami. Cited by: Ackerman, C.A. (2007), "A vibration based model that rates bridge structural deterioration in a bridge management system." *PhD thesis*. Tshwane University of Technology, Pretoria, South Africa. Available:http//:www.libserv5.tut.ac.za:7780/pls/eres/wpj_docload.download_file (17 January 2008)

Transport, M. o. (1922). *Report on the administration of the Road Fund for the year 1921-1922.* London: HMSO.

Wessels, L. (1990). *Road Traffic Act, 1989 (Act of 1989) and Regulations as amended.* Johannesburg.

Wickell, D. (2002). Pickup Truck Suspension Systems.

Wolfgang, B. (2010). *Hydropneumatic suspension system.*

X.Zhang, K. S. (2003). Evaluation of impact factors for composite concrete-steel cellular straight bridges. *Engineering Structures* , 313-321.